SKB

TECHNICAL REPORT 92-39

Characterization of crystalline rocks in deep boreholes. The Kola, Krivoy Rog and Tyrnauz boreholes

NEDRA – Scientific Industrial Company on Superdeep Drilling and Comprehensive Investigation of the Earth´s Interior

December 1992

SVENSK KÄRNBRÄNSLEHANTERING AB
SWEDISH NUCLEAR FUEL AND WASTE MANAGEMENT CO

BOX 5864 S-102 48 STOCKHOLM

TEL 08-665 28 00 TELEX 13108 SKB S
TELEFAX 08-661 57 19

CHARACTERIZATION OF CRYSTALLINE ROCKS IN DEEP BOREHOLES. THE KOLA, KRIVOY ROG AND TYRNAUZ BOREHOLES

NEDRA - Scientific Industrial Company on Superdeep Drilling and Comprehensive Investigation of the Earth's Interior

December 1992

CHARACTERIZATION OF CRYSTALLINE ROCKS IN DEEP BOREHOLES

THE KOLA, KRIVOY ROG AND TYRNAUZ BOREHOLES

NEDRA

Scientific Industrial Company on Superdeep Drilling and Comprehensive Investigation of the Earth's Interior

December 1992

Keywords: Deep boreholes, Crystalline rock, Salinity, Rock characterization

ABSTRACT

SKB studies, as one alternative, the feasibility of disposing of spent nuclear fuel in very deep boreholes. As a part of this work NEDRA has compiled geoscientific data from three superdeep boreholes within the former Soviet Union. The holes considered were: the Kola borehole, 12261 m deep and located on the Kola Peninsula, the Krivoy Rog borehole, 5000 m deep and located in Ukraine, and the Tyrnauz borehole, 4001 m deep and located between the Black Sea and the Caspian Sea. These boreholes all penetrate crystalline formations, but major differences are found when their tectonic environments are compared. Excluding the uppermost horizon affected by surface phenomena, data do not indicate any general correlation between depth and the state of rock fracturing, which is instead governed by site specific, lithological and tectonical factors. This applies also to fracture zones, which are found at similar frequencies at all depths. As opposed to the structural data, the hydrogeological and hydrochemical information reveals a vertical zonation, with clear similarities between the three boreholes. An upper zone with active circulation and fresh or slightly mineralized groundwaters reaches down 1000-2000 m. The interval from 1000-2000 m down to 4000-5000 m can be characterized as a transition zone with lower circulation rates and gradually increasing mineralisation. Below 4000-5000 m, strongly mineralized, stagnant, juvenile or metamorphogenic waters are found. Geothermal data verify the existence of this zonation.

ABSTRACT (SWEDISH)

SKB utreder, som ett av flera alternativ, möjligheterna att deponera radioaktivt avfall i mycket djupa borrhål. Till stöd för utredningsarbetet har NEDRA sammanställt geovetenskapliga data från tre befintliga super-djupa borrhål. Hålen återfinns i kristallin berggrund inom före detta Sovjetunionen, och har borrats inom ramen för ett omfattande geovetenskapligt forskningsprogram inriktat mot undersökningar på stora djup. Ett av borrhålen är beläget på Kolahalvön (12261 m djupt), ett utanför Krivoy Rog i Ukraina (5000 m) och ett i Tyrnauz mellan Svarta Havet och Kaspiska havet (4001 m). Studien visar att spricksituationen i berggrunden, med undantag av partier nära markytan, inte generellt kan korreleras med djupet. Vidare förekommer sprickzoner av olika storlek på alla djup. Inte heller sprickzonernas frekvens eller typ kan korreleras med djupet. Däremot uppvisar de hydrogeologiska och hydrokemiska förhållandena ett likartat djupberoende i de tre borrhålen. Man kan urskilja en zon med aktiv grundvattencirkulation och relativt låg mineraliseringsgrad på grundvattnet, som sträcker sig ner till 1000-2000 m. Därunder, och ner till 4000-5000 m djup återfinns en blandzon med väsentligt långsammare cirkulation och successivt ökande mineralhalter i grundvattnet. Under 4000-5000 m är cirkulationen närmast obefintlig, och vattnet juvenilt eller metamorft genererat med mycket höga salthalter. Denna skiktning av grundvattenrörelserna styrks av geotermiska data.

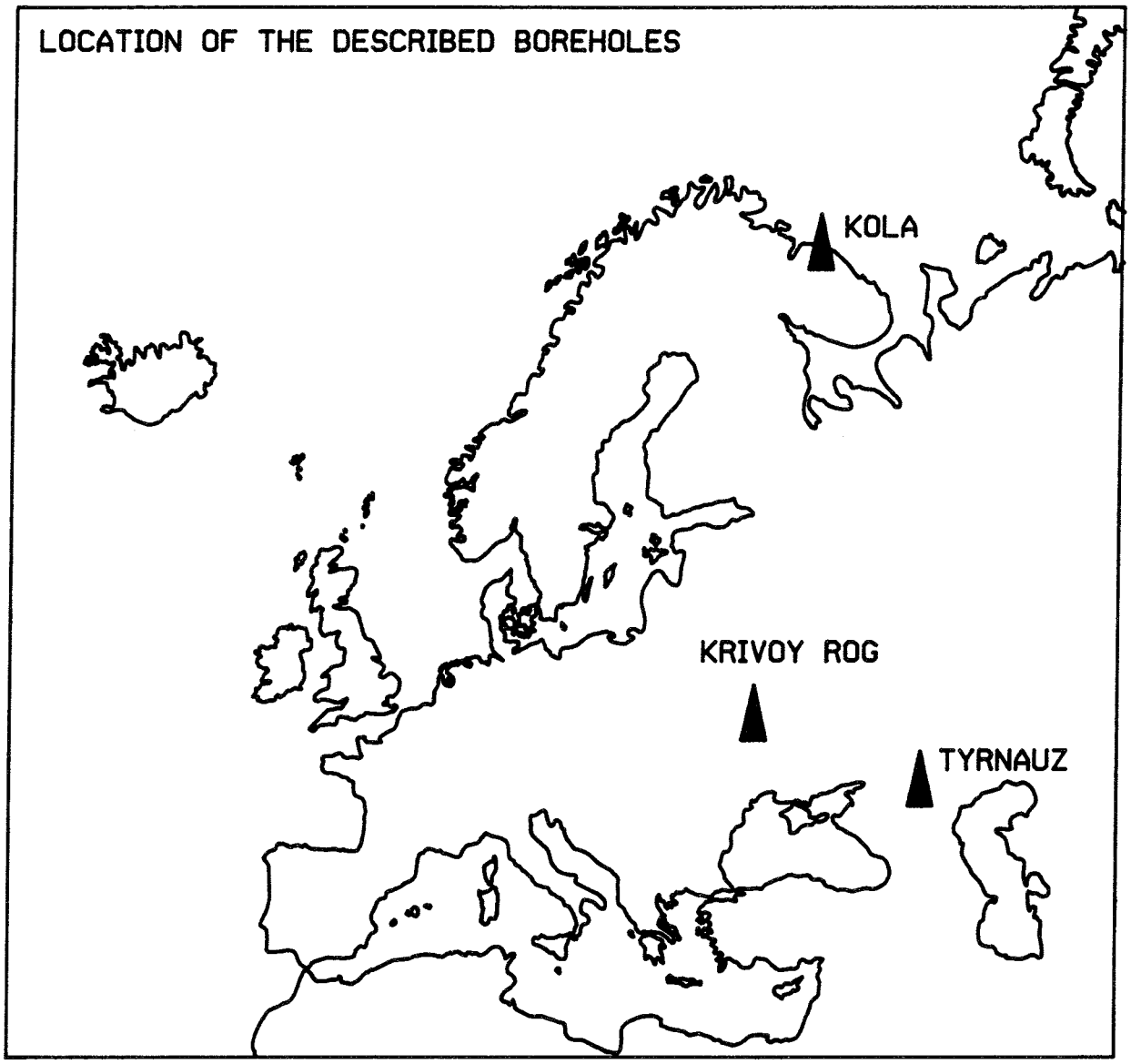

Fig. 1. Location of the Kola, Krivoy Rog and Tyrnauz deep boreholes

TABLE OF CONTENTS

PART 1

EXECUTIVE SUMMARY

1 BACKGROUND

The present report compiles results from investigations performed in deep boreholes by NEDRA. The report was produced by NEDRA scientists at the request of SKB.

The programme for investigation of deep boreholes has been in progress for the last 20 years and aims to characterize major geostructural elements such as shields, platforms and folded belts of different geological settings. Besides drilling 12 deep boreholes, an extensive field data collection programme was carried out, that included the following methods:

- Geological mapping
- Seismic investigations
- Magnetic and gravimetric mapping
- Electrical investigations
- Extensive geophysical borehole investigations
- Core analyses
- Geochemical analyses of rocks, fluids and gases

The report focuses on a description of the geological setting and characterization of the upper 5 km of the earth's crust on the basis of results from the Kola, Krivoy Rog and Tyrnauz boreholes (Fig.1), which represent different geological regimes.

2 THE KOLA BOREHOLE

General data

The Kola borehole is located on the Kola Peninsula in the northeastern part of the Baltic Shield at latitude 69°25'N and longitude 30°44'. The borehole was spudded in May 1970 and has today reached a depth of 12260 metres. Coring has given a core recovery of 3592 m (29.3%), down to 12260 m. Data from investigations below 5000 metres are not included in the report. Main characteristics of the borehole are summarized in Table 1.

Geological setting

The Kola borehole is located within the Pechenga Trough which constitute a part of the Pechenga-Imandra-Vargus zone. The zone is approximately 600 km long and 40-50 km wide and extends from Varanger Fjord to the White Sea.

Table 1. Main characteristics of the Kola borehole down to 5100 m.

Depth, m	**Rock types**	**Physical properties** -Density -Compr. strength -Acoustic velocity	**Faults and fractures**	**Hydrogeology and hydrogeochemistry**
9 - 1059	Tholeiitic and picritic basalt Prehnite-pumpellyite facies	2.74-3.24 g/cm^3 130-260 MPa 6300-6900 m/s	0-800 m: Exogenic fractures 0-150 m: Open fractures without mineralisation 150-200 m: Secondary mineralisation of fractures 200-800 m: Secondary leaching of fractures 800-1059 m: Tectonic faults and shear fractures	Fresh water with mineralisation 0.04-0.4 g/l. The groundwater is saturated with oxygen and nitrogen Carbonate-rich solutions Hydraulic cond:1.2 x 10^{-7} m/s Water-bearing sections: 0.1-10 m Calcium-carbonate-rich water Hydraulic cond:3.4 x 10^{-11} m/s
1059-2805	Alternating sequences of tuffaceous and sedimentary rocks Transition from a prehnite-pumpellyite to a greenschist facies	Heterogeneous interval 2.65-3.36 g/cm^3 80-260 MPa 5800-7000 m/s	Concordant tectonic faults and shear fractures mainly along rock type boundaries	Change to reducing alkaline waters Mineralisation 60 g/l (Ra, Sr, Br, B, K, Rb, Cu, Pb, As)
2805-4400	Tholeiitic vulcanite, metadiabase and minor amounts of tuffaceous rocks. Greenschist facies	Fairly homogeneous interval 3.02 g/cm^3 (average) up to 270 MPa 6400-7000 m/s	Minor fracturing	
4400-5100	Basic and ultrabasic volcanitic schist, calcareous sandstone, intrusive schist Greenschist to epidote-amphibolite facies	2.66-3.10 g/cm^3 20-200 MPa 5600-6000 m/s	The zone includes the major Luchlompolsky fault	Water-bearing zone between 4565 and 4925 m Chlorine-rich fluids (710 mg/l) pH 8.0-8,5 K > Br > Y > B > F > Pb

The Pechenga complex, which includes the Pechenga Trough, is composed of a succession of Proterozoic sedimentary and volcanic rocks overlying Archaean granites and gneisses. The complex was formed by subduction of the Archaean basement followed by volcanic activity and deposition of volcanoclastic and terriclastic sediments during Proterozoic time.

The up to 8-9 km thick Pechenga complex, dominated by basic igneous rocks (80%), exhibits a gradual transition from prehnite-pumpellyite to epidote-amphibolite metamorphic facies. The rocks are characterized by variations in their degree of isochemical metamorphism which increases from the central parts of the complex to the peripheral parts and with depth. There is also a significant variation of the metamorphism within separate rock-blocks. The prehnite-pumpellyite facies are found exclusively in the upper part of the borehole down to approximately 1400 metres depth. Greenschist facies are found in the interval between 1400 and 4800 metres depth, and at depths below 4800 m the rocks exhibit epidote-amphibolite facies.

Faults and fractures

The Kola borehole is located away from any major faults and tectonic disturbances. The Pechenga complex is, however, significantly affected by different types of fault which largely control the rock-block subdivision of the complex. Major subvertical faults extend down to depths of up to 25 km.

Longitudinal conformable fractures between rock boundaries are numerous in the succession of rocks penetrated. They are generally associated with slickensides and crushed and disturbed zones of rock (mylonites and breccias). The fractures are from 0.1 mm to several centimetres wide. The fracture filling minerals are dominated by chlorite, carbonate, quartz and sulphide.

The number of fractures is related more to the type of rock than the depth. Basic rocks are, in contrast to sedimentary rocks, found to have a relatively low number of fractures. The investigations also verified that the rock mass is characterized by brittle deformation down to a depth of 6000 m or more.

Physical properties

The Kola peninsula is generally characterized by extensive horizontal stresses, with ratios of horizontal - to vertical stress reaching a factor 4. In the Kola borehole, however, the ratio was only 0.7, thus indicating low horizontal stresses. Evaluation was based on analysis of borehole cross-sectional geometry. The maximum horizontal stress was found to have a NW (290-300°) orientation.

The compressive strength, determined from core samples, varies from 80-260 MPa, with some mechanical anisotropy caused by laminations in the sedimentary rocks.

The density of the rocks down to 5100 m is between 2.65 and 3.36 g/cm^3, the average acoustic velocity is 6100 m/s.

The total porosity down to 4500 m is generally below 1%. The porosity in fractured zones is 5-10 times higher. The permeability is less than 25 mD.

Numerous thermal anomalies occur in the borehole which correspond to lithological boundaries and fracture zones. The temperature at 5000 m is 70°C.

Geochemistry and hydrogeology

Based on results from the investigations of borehole fluids the penetrated section can be divided into three zones:

1 Subsurface zone (0-800 m) with fresh or slightly mineralized meteoric water
2 Transition zone (800-4000 m) with increasing mineralisation of the formation fluids
3 Deep water (below 4400 m) with highly mineralized metamorphogenic fluids

3 THE KRIVOY ROG BOREHOLE

General data

The Krivoy Rog borehole is located in the Ukrainian Shield, 15 km NW of the town of Krivoy Rog. The borehole was spudded in September 1984 and is planned to have a completed depth of 12000 m. The depth was approximately 5000 m in June 1991. Coring has given a core recovery of 2850 m (62 %). Investigations from mines and other boreholes in the area are also included in the geological description. Main characteristics of the borehole are summarized in Table 2.

Geological setting

The Ukrainian Shield was formed during Late Archaean to Early Proterozoic times (3600-1300 Ma). The Shield is divided into three mega-blocks bounded by tectonic zones. The Krivoy Rog borehole is located in the Central-Ukrainian mega-block which is subdivided by a number of faults into a group of smaller regional rock-blocks. The borehole is located within an asymmetrical depression (Krivoy Rog-Kremenchug structure) between two regional rock-blocks (Kirovogradsky and Predneprovsky). The depression formed during Late Proterozoic times (2400 Ma) is filled with rocks belonging to the Krivoy Rog series, i.e. different types of schist, iron-deposits, conglomerate, arkose, amphibolite, etc. The petrography is more or less affected by metamorphic processes (greenschist-eclogitic facies) which occurred 1800-2000 Ma ago. Subduction of separate rock-blocks led to fracturing and

intrusion of gabbros (1700 Ma) and diabase dykes (1200-1300 Ma). Metasomatic and anatectic granites were also formed as a result of faulting and fracturing in conjunction with subduction of the major rock-blocks.

Subduction of the separate Archaean rock-blocks led to high shear stresses, causing formation of symmetric thrust zones, dipping 60-90° down to a depth of 2 km where they change to a subhorizontal position. One of these thrust zones, the Tarapakovsky thrust zone, is located at a depth of approximately 5000 m in the Krivoy Rog borehole.

Faults and fractures

The occurrence of fractures and faults in the Krivoy Rog borehole is mainly related to thrust zones and movements of regional blocks. Current movement (vertical and horizontal) of the larger blocks is 2.5-5.1 mm/year. The number of fault zones in the borehole increases with increasing proximity to the Tarapakovsky thrust zone at a depth of approximately 5000 m. The major fault zones are between 20 and 70 m wide and dominated by shear fractures filled with quartz, carbonate, chlorite and hematite. Eleven major zones are found down to 4596 m. Mylonites and crushed rock are also commonly found in the fault zones. Repeated movements inside zones have resulted in the deformation of minerals and development of microfolds.

Physical properties

Rock stress measurements were not performed in the Krivoy Rog borehole. The following geomechanical information is, however, available:

- The region is influenced by continuous upwarping. The movements have an oblique orientation which causes shear deformations in conjunction with major thrust zones, e.g. the Tarapakovsky zone.

- Borehole deformations attributed to lateral rock stress has been observed below 3000 m depth.

- Significant discing of cores occurred in the interval 3620-3850 m.

- Caving occurred throughout the borehole. Below 3500 m caving became more intense.

- The rock exhibit a wide range of strength properties.

Analyses of the data showed that the current stress field is caused by two main components; the lithostatic pressure and dynamic tectonic forces. The Tarapakovsky thrust zone causes extreme horizontal stresses at depths below 3000 m which induce caving and peeling of the borehole walls.

The porosity of the rocks investigated was generally low (0.5-1.4%). Higher porosities, maximum 7.4%, were found in connection with tectonically disturbed zones. The permeability is 5-390 mD for monolithic rocks and 89-2300 mD for rocks within fracture zones. Maximum permeabilities and porosities were observed in two tectonic zones, at 3620-3700 and 3760-3850 m. Severe caving of the borehole occurred in these intervals. An explanation for the caving problems occurring at these depths could be that the lithostatic pressure exceeds the compressive strength of the rock at a depth of 3500-4000 m.

Table 2. *Main characteristics of the Krivoy Rog borehole down to 4596 m. Results are from the Krivoy Rog borehole, mines and other boreholes in the area.*

Depth, m	**Rock types**	**Physical properties** -Density -Porosity -Compr. strength -Tensile. strength -Acoustic velocity	**Faults and fractures**	**Hydrogeology and hydrogeochemistry**
0--1509	Alternating intervals of apoleurite, apopsammite, quartz-feldspar-biotite schist and metaconglomerates	2.75-2.78 g/cm^3 0.45-0.87% 129.5-164.0 MPa 3.77-6.55 MPa 5200-5660 m/s	Shear fractures and ruptures	pH 6.8-8.3 Mineralisations 0-500 m: 0.41-7.2 g/l 500-1000 m: 7.0-33.2 g/l 1000-1500: 27.1-69.0 g/l
1509-2351	Heterogeneous interval with apoaleurite, garnet-biotite schist, graphite schist, marble, cummingtonite schist, chlorite-talc schist, amphibolite and sandstone	2.77-3.20 g/cm^3 0.45-2.16% 30-140.2 MPa 3.38-6.10 MPa 4440-7100 m/s	Shear fractures, schistocity,	pH 6.9-8.2 Mineralisation >1500 m 98-142 g/l
2351-4596	Blastocataclasite and blastomylonites, plagio-granitoids, relicts of amphibolite. Trondhjemite 3800-4000 m.	2.67-2.72 g/cm^3 0.21-1.38% 100.1-132.1 MPa 3.30-5.60 MPa 6400-7000 m/s	Shear fractures, slicken sides, ruptures, peeling of rock in the borehole, discing and ruptures, mylonites	-"-

The density of the rocks down to 4596 m is between 2.67 and 3.20 g/cm^3, the acoustic velocity is 4400-7100 m/s.

Measurements of the borehole temperature give an average temperature gradient of 1.12° C/100 m. Anomalies in the temperature gradient correspond mainly to major tectonic zones.

Hydrogeology and geochemistry

The hydraulic conductivity of the rock in the Krivoy Rog borehole is strongly related to the porosity and number of fractures. Hydrogeologically, the formation can be characterized as a fractured medium. The transmissivity is between $6.9 \cdot 10^{-9}$ and $2.1 \cdot 10^{-5}$ m^2/s and the hydraulic conductivity between $2.3 \cdot 10^{-9}$ and $6.9 \cdot 10^{-9}$ m/s

The water mineralisation gradually increases from 0.41 to 142 g/l with depth and changes from hydrocarbonate-chloride-calcium-sodium to chloride-sodium-hydrocarbonate-rich waters. The formation water is found to differ from natural water basins by its high contents of cesium, rubidium and lithium. Furthermore, the water is aggressive to sulphate cements and metals.

4 THE TYRNAUZ BOREHOLE

General

The Tyrnauz borehole located between the Caspian and Black Seas was drilled within a geological regime that differs from those of the two previous holes. It was drilled during 1987-1989 and is 4001m deep. The borehole is located 1.5 km outside the town of Tyrnauz in a zone between the Cenozoic Caucasian fold belt and the ancient Skifsky-Turansky plate. Main characteristics of the borehole are summarized in Table 3.

Geological setting

The Caucasian region is composed of a complex system of folded structures formed during the Alpine orogeny. The borehole is located in the Pshekish-Tyrnauz zone which constitutes a thick deformed structure bordering the older Skifsky plate to the north. To the south it is bordered by schists and gneisses of the Proterozoic-Late Paleozoic age. To the east the zone is traced as an anticlinal structure extending to the Caspian Sea and to the west it converges with another marginal trough to the Skifsky plate.

The Pshekish-Tyrnauz zone is composed of tectonically deformed Mesozoic and Upper Paleozoic rocks. The main tectonic elements in the zone extend WNW. The Tyrnauz borehole was drilled within the Eldjurtinsky granite, which is the youngest intrusion in the area. The intrusion is 1.8-1.9 Ma old which corresponds to the Pleistocene age. The granite is stock shaped and extends 7 km (SE-NW) and is 2-2.3 km wide. The total volume of the massif is estimated at 90 km^3.

The granite is dominated by grey and pink biotite-rich porphyritic granites with variations in granulation and content of mineral inclusions. The granite is frequently penetrated by liparite, aplite dykes and heavily fractured crushed zones.

Faults and fractures

The Pshekish-Tyrnauz zone is bordered to the south and north by large subvertical regional faults which are at least 15 km long and have been traced to a depth of more than 2 km, in the Tyrnauz ore-field. In the zone there are several types of fractures, including wide extensive fault zones (up to 100 m wide), intrastructural, metre-wide and km-long faults of great amplitude (kilometres) and numerous lateral and oblique faults of minor amplitude and extension. The deformations are diverse, which gives a complex pattern of structural elements.

In the borehole there are heavily fractured crush zones with mylonite and cataclasite, and fracture zones with groups of tension fractures parallel to the Pshekish-Tyrnauz zone. Five different fracture sets were identified.

Physical properties

The granitic rocks penetrated are characterized by small variations in density (2.57-2.62 g/cm^3). The porosity of the granite varies between 1.29 and 2.58% and the permeability is 0.04-0.57 mD.

The stress field is mainly of an anisotropic and compressive type. The axis of maximum compression is oriented NE-SW. Results from strength determinations vary greatly, between 3.2 and 10.3 MPa (tensile strength) and 61.2-250 MPa (compressive strength). The vertical component of the stress field is 62 MPa and the horizontal 38-86 MPa, indicating a gravitational-tectonic type of stress field in the area.

The Tyrnauz borehole is located in a geothermally anomalous zone with a thermal gradient of 46° C/km, giving a bottom of hole temperature of 223° C. The thermal properties are homogeneous in the Eldjurtinsky massif, but two subzones (upper and lower) with somewhat different petrothermal properties were identified in the borehole.

Hydrogeology and geochemistry

The Eldjurtinsky granite forms a distinct hydrogeological massif surrounded by metamorphic host rock formations with different hydrogeological and geochemical characteristics. The water dynamics may be divided into a local subsurface flow, a regional subsurface run-off and a deep water circulation. The last system exists below a depth of several hundred metres and is dominated by relatively stable conditions.

The waters are dominated by mineralisations of calcium and magnesium in the upper part and by sodium hydrocarbonate at deeper levels. The mineralisation gradually increases with depth except in major fracture zones where a higher degree of

mineralisation was observed than that corresponding to the actual depth. This is probably caused by circulation of deeper water in the zones.

Table 3. Main characteristics of the Tyrnauz borehole

Depth, m	**Rock types**	**Physical properties** -Density -Porosity -Compr. strength -Tensile strength	**Hydrogeology and hydrogeochemistry**
0-260	Glaciofluvial sediments	-	-
260-715	Pink granite	2.60-2.61 g/cm^3 1.29-1.84% 130.3-154.0 MPa 6.8-8.6 MPa	Mineralisation: 0.1-0.4 g/l to 300-500 m, increases with depth
715-3835	Grey granite	2.59-2.62 g/cm^3 1.32-2.58% 85.6-146.6 MPa 4.4-9.4 MPa	Transition from active discharge to a zone of obstructed circulation. Excessive groundwater pressures. Mineralisation: 6-13 g/l Chlorine-hydrocarbonate-sulphate
3835-4001	Leucogranite	2.57 g/cm^3 2.13% 83.7 MPa 4.3 MPa	

6 CONCLUSIONS

The three boreholes, Kola, Krivoy Rog and Tyrnauz, presented in this study were drilled as a part of an investigation programme concerning characterization of the upper 5 km of the Earth's crust. The Kola (12261 m) and Krivoy Rog (4596 m) boreholes penetrate ancient volcanic, sedimentary and metasedimentary rocks of Early Proterozoic and Archaean age within the Baltic and Ukrainian shields. The Tyrnauz (4001 m) borehole penetrates granitic sequences in the Caucasian folded belt (Cenozoic).

The investigations provided information allowing development of a generalized model of the upper part of the crust. Even if there are numerous differences between the individual boreholes there are common features which may be summarized as follows:

- Fractures and fracture zones are to be found over the whole interval (0-5000 m). They are, however, more intense in the upper part, down to 1000 to 1500 m depth. The fracture zones are generally steep and of variable width (0.01-200 m)

- The porosity is generally less than 1.5% Slightly higher values are found in connection with fracture zones.

- The temperature gradient in the Kola and Krivoy Rog boreholes increases with depth: 1° C/100 m (0-1200 m), 1.0-1.5° C/100 m (1200-3000 m), 1.7° C/100m (3000-4500) and below 4500 m 2.0° C/100 m.

- There is distinct vertical hydrogeological and geochemical zonation in all boreholes. Three zones were identified:

  1) An upper zone down to approximately 2000 m which is characterized by free circulation of fresh to slightly mineralized (< 60 g/l/) meteoric waters.
  2 An intermediate zone between approximately 2000 and 4000 m characterized by mixing of deeper, heavily mineralized brines and overlying fresh meteoric waters.
  3) The zone below approximately 4000 m is characterized by heavily mineralized calcium-chloride-rich brines (up to 350 g/l).

- The boundary between the second and third zone is mainly controlled by the ratio between the lithostatic pressure and the rock strength.

ACKNOWLEDGEMENT

Special gratitude is expressed to SKB for their financial support for the production of this report. Thanks are also expressed to Bengt Leijon for valuable comments on the manuscript, Menachem Finkel for Russian translations, Mikael Erlström for the editorial work and compilation of the executive summary, and to David Bayne for linguistic assistance.

PART 2

CHARACTERIZATION OF CRYSTALLINE ROCKS IN DEEP BOREHOLES

THE KOLA, KRIVOY ROG AND TYRNAUZ BOREHOLES

NEDRA

Scientific Industrial Company on Superdeep Drilling and Comprehensive Investigation of the Earth's Interior

1 INTRODUCTION

1.1 OBJECTIVES AND SCOPE

This report has been prepared by the Scientific Industrial Company on Superdeep Drilling and Comprehensive Investigation of the Earth's Interior (NPO Nedra) on behalf of the Swedish Nuclear Fuel and Waste Management Company (SKB). The commission was specified by SKB in Contract No. 911630.

The objective of the work reported was to compile a generalized model of the geological environment in crystalline rocks, in order to substantiate a feasibility study on nuclear waste disposal in very deep boreholes, conducted by SKB.

The report draws on published information from geological, geophysical and hydrogeological investigations of crystalline formations in different regions of the former USSR (now the Commonwealth of Independent States - CIS). These investigations were conducted within the framework of the Programme for Investigation of Deep Structures of the Continental Crust of the Earth. This programme, which has been under way for a period of about 20 years, is devoted to the study of large geostructural elements (ancient shields, young and ancient platforms, folded belts of different ages and major sedimentary basins) by means of comprehensive investigations along geotraverses and superdeep drilling. It aims at advancing the geosciences and solving a broad spectrum of fundamental and applied problems, relating to properties and conditions at large depths. The scope of investigations includes methods for collecting data at large depths, fluid gas and geothermal regimes, characteristics of aquifers, chemical and isotopic composition of groundwater and gas, rock stress conditions, variations of natural and induced fields, etc., and the variation of relevant parameters with depth.

Twelve boreholes are being drilled at present. The locations of these holes are indicated in Fig. 1-1. Hole locations are intersected by geotraverses and comprehensive geological and geophysical investigations are conducted in the areas of the boreholes. Drilling is done with continuous coring and a wide range of borehole geophysical, hydrogeological and geochemical investigation methods are applied in the boreholes.

According to the agreement between NPO Nedra and SKB, the present compilation is based on results obtained from the investigations of the boreholes at Kola, Krivoy Rog and Tyrnauz, and their respective surroundings. In addition to published information, original data from these three boreholes have been used. General information about the Kola, Krivoy Rog and Tyrnauz boreholes is given in Table 1-1.

The report was prepared by the following NPO Nedra specialists: B.N. Khakhaev, L.A. Pevzner, V.I. Gorbachev, D.M.Guberman, V.S. Lanev, M.S. Rusanov, Yu.P. Smirnov, N.S. Kurlov, G.K. Budkov and E.S. Nikashin. Assistance was also

provided by O.L. Kuznetsov, N.D. Nartikoev (VNII Geoinformsystem) A.I. Zaritsky, V.V. Reshetnyak (State Committee of Geology of the Ukraine) and O.L. Kedrovsky (VNIPI Promtechnology).

SKB, represented by C. Svemar, R. Push, M. Finkel, K. Ahlbom and F. Karlsson, contributed actively in defining the scope of the report

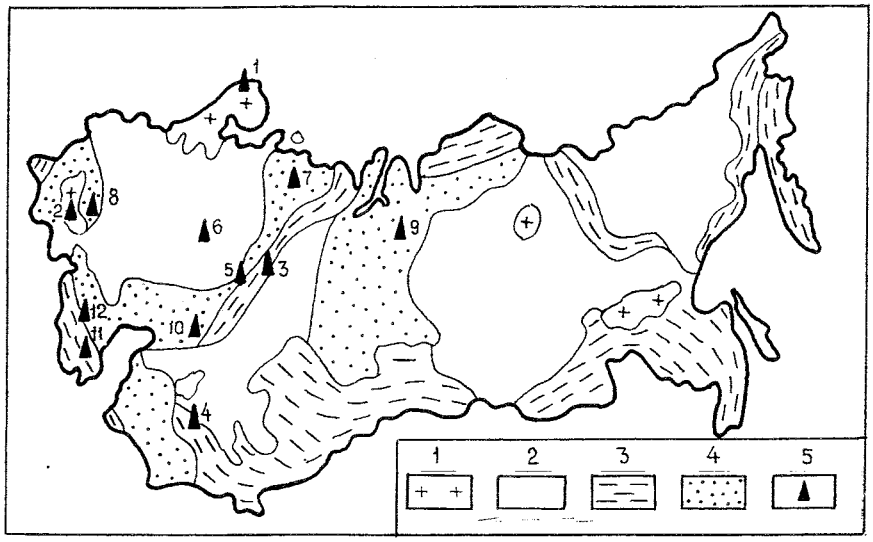

Age	DRILL HOLES 1	2	3	4	5	6	7	8	9	10	11	12
KZ												
MZ												
PZ_3												
PZ_2												
PZ_1												
PR_2												
PR_1												
AR_2												
AR_1												

Fig. 1-1. *Geotectonic location of superdeep boreholes and age-range of the investigated sections.*

1:	Kola	2:	Krivoy Rog	3:	Ural	4:	Muruntau
5:	Novo-Elkhov	6:	Vorotilov	7:	Timano-Pechora	8:	Dniper-Donetsk
9:	Tyumen	10:	Precaspian	11:	Saatly	12:	Tyrnauz

Legend

1:Shields 2: Platforms 3: Folded belts 4: Major sedimentary basins 5: Boreholes

Table 1-1. General information - Kola, Krivoy Rog and Tyrnauz boreholes.

No.	Borehole	Depth, m		Core recovery	Date		Design		Location	
		Target	Reached 910601	m/%	Spudding	Completion	Diameter (mm) and casing depth (m)	Nominal diameter (mm) of the open borehole	Geological	Geographic
1	Kola	15000	12261	3591.9/29.3	70.05.25		720/39 324/2000 245/8770	215	The NE part of the Baltic Shield, in the Pechenga synclinorium	10 km S of the town Zapolyarny
2	Krivoy Rog	12000	4596	2850.0/62.0	84.09.20		720/62 508/850 426/2800	215	Krivoy Rog-Kremenchug structure in the Ukranian Shield	15 km NW of the town Krivoy Rog
3	Tyrnauz	4000	4001	2683.0/67.0	87.11.18	89.11.01	530/12 324/290	215	The eastern part of the Pshekish-Tyrnauz zone in the Caucasian folded belt	1.5 km SW of the town Tyrnauz.

1.2 INVESTIGATION METHODS

As indicated above, the present report draws on data obtained using a comprehensive suite of geoscientific surface and borehole investigation methods.

The following surface investigation methods were applied:

- Detailed geological mapping, combined with drilling of shallow holes
- Seismics (deep seismic sounding - GSZ, methods of wave reflection - MOV, common deep point - MOGT, wave refraction - KMPV)
- Gravitational and magnetic surveys
- Electric surveys
- Hydrogeological investigations in shallow boreholes.

Borehole geophysical investigations included the following logging methods:

- Acoustic (broad range acoustic and borehole televiewer)
- Seismic (vertical seismic profiling - VSP)
- Radiometric (gamma-ray, spectral, neutron-gamma, gamma-gamma, neutron-neutron)
- Electric (lateral, lateral probing, induction, microlateral)
- Magnetic (including magnetic susceptibility)
- Thermometry
- Determination of borehole geometry (dipmeter and caliper).

Investigations of the drill core included:

- Lithological-stratigraphic
- Petrographic
- Geochemical
- Isotopic-geochronological
- Petrophysical
- Analyses of bitumen and carbonaceous matter, sampled gases and water.

Petrophysical parameters that were determined are shown in Table 1-2.

Table 1-2. Types of petrophysical investigation

TYPE OF INVESTIGATION	ACCURACY OF MEASUREMENTS
Mineralogical density	$\pm 5 \cdot 10^{-3}$ g/cm^3
Volume density	$\pm 2 \cdot 10^{-2}$ g/cm^3
Total porosity	±20%
Open porosity	±20%
Absolute gas permeability	±10%
ACOUSTIC PROPERTIES	
Propagation velocity of P-waves	±3-10%
Propagation velocity of S-waves	±6-12%
MECHANICAL PROPERTIES	
Tensile strength	±30%
Uniaxial compressive strength	
ELECTRIC PROPERTIES	
Electric resistivity	±30-40%
THERMAL PROPERTIES	
Thermal capacity	±10%
Thermal conductivity	±10%
MAGNETIC PROPERTIES	
Magnetic susceptibility	±6-8%

Hydrogeological investigations in superdeep boreholes (the Kola borehole) required development of special techniques in order to determine hydrochemical zonation of the penetrated section and to obtain hydraulic parameters. The following methods were used:

1) Monitoring of physical-chemical parameters of the drilling mud (OS). This method is widely used, and involves sampling the drilling mud at the well collar, followed by analyses of chemical composition and physical properties. Sampling was done at every 5 m of penetration. Sample analysis was made in an on-site laboratory, and comprised determination of cation-anion composition and some physical properties (density, pH, Eh and others). Control samples were analysed in laboratories and research institutes.

2) Fluid sampling by sampler from certain depth intervals, mostly in zones of anticipated water inflow.

3) Change of circulation regime (SRP-method) which allows approximate determination of formation pressure, permeability and hydraulic conductivity on the basis of recording drilling mud consumption as a function of applied drilling mud pressure.

4) Packer testing.

5) Hydraulic fracturing.

Methods 1) to 4) were used in the Kola borehole, methods 1) to 3) in the Krivoy Rog borehole, and methods 1) through 5) in the Tyrnauz borehole.

Geohydrological data from previous boreholes and excavations within the areas where the superdeep boreholes are drilled were collected and compiled. This information provided guidance as to the geohydrological testing programme for the superdeep holes and enabled development of geohydrological models of the areas considered.

Gas was sampled by degassing the drilling fluid and core samples recovered from the borehole. An automatic logging station provided continuous analysis of the gas constituent of the drilling fluid. Furthermore, gas samples for analysis were taken at every 5 m of drilling by thermal degassing of the drilling mud. The composition of gases in open and closed pores and gases of high sorption were studied on rock samples. The same methods were used in investigations of all boreholes. It is therefore possible to correlate bedrock properties to obtain the basic parameters for a generalized borehole model of crystalline rock.

2 FAULTS, FRACTURES AND FRACTURE ZONES

2.1 CLASSIFICATION

The rock mass may be dislocated by faulting and fracturing. Criteria for distinction between these two features are mainly based on parameters such as extension, relative displacement of adjacent points in the rock, geometrical structure and geological history.

The term "fault" refers, as a rule, to a relative movement of two formerly adjacent points in a rock mass. Faults (fault zones) are distinguished by the displacement, complex inner structure and long-term multistage geological evolution. Depending on extension, displacement and relation to other rock structures, faults can be classified into several orders.

The term "fracture" refers to ruptured disturbances, ranging in size from microscopic to in-plane extensions of hundreds of metres. The distinction between a large fracture and a small fault is to a certain degree arbitrary. Fractures are characterized by significant mutual displacement between the surfaces of separation.

Macrofractures can be observed with the naked eye, whilst the presence of microfractures has to be verified by microscopic investigations. Fractures can be categorized from several standpoints. Thus, we distinguish open fractures and "cicatrized" fractures (filled with the host rock particles or new mineral formations); shear fractures and extension (tension) fractures; conjugate, oblique and transverse fractures (according to the orientation with respect to bedding or stratification) and also fractures occurring in connection with rock volume changes. Practically all processes in the lithosphere are accompanied by fracturing. There are many systems for classifying fractures, based on different principles. The classification introduced by V.A. Nevsky [2:14] is generally used.

Fractures of tectonic origin are abundant in the borehole sections investigated. Weathering (exogenic) fractures prevail in the uppermost parts, down to depths of several metres or even hundreds of metres. Fractures related to thermal contraction, gravitational processes, etc. are subordinate. In deeper sections of the boreholes, distinct, subhorizontal fracture zones occur, which are related to processes at great depths.

The term "fracture zone" refers to a section of the rock mass where the intensity of fracturing is distinctly greater than that of its surrounding. The intensity of fracturing is classified according to the quantitative scale given in Table 2-1. Fracture zones may be formed by fractures of a certain type, or by assemblies of fractures of different genetic backgrounds. The following parameters were used in the investigation programme to distinguish and characterize fracture zones:

Table 2-1. Scale of fracturing intensity in rocks (V.A. Nevsky)

Fracture intensity	Fracture frequency
Very intense	33-20
Intense	20-7
Medium	7-3
Minor	3-1
Insignificant	<1

- Intensity of fracturing, i. e. fracture frequency (number per metre)
- Extent and width of zone
- Spatial orientation (azimuth and dip angle)
- Width (aperture) of fractures
- Intensity of secondary rock alteration.

The fact that the boreholes are located in different geological environments, however, necessitates a certain flexibility in the classification and description of fracture zones. Thus, fracture zones are identified and described on a more hole-specific basis, as found relevant throughout the report.

2.2 IDENTIFICATION METHODS

The identification and characterization of fracture zones and faults were based on the following categories of investigation methods:

- Surface geological and geophysical surveys
- Borehole geophysics
- Core analysis

The surface and geophysical investigations included seismic, gravity and magnetic surveys. Together with geological mapping, this allowed identification of faults of different orders, determination of their spatial positions and prediction of intersections with boreholes. Positions of fracture zones, as later recorded in the boreholes, were predicted with an accuracy of 200-400 m.

More detailed information about fracture zones was obtained from borehole geophysical investigation and core analyses. Data from the geophysical surveys made it possible to distinguish boundaries of fracture zones, to describe in detail their internal structure, and to determine structural elements in the near-borehole

environment. The most useful methods were borehole televiewer, acoustic log, vertical seismic profiling (VSP), formation inclinometry, radiometric log and magnetic surveys. Overall, the geophysical investigations were very important in describing the fracture zones. Analyses of the core material included detailed documentation at micro and macro level. A variety of petrophysical and geochemical investigations contributed significantly to the characterization of fracture zones and permitted characterization of individual fractures with respect to orientation, genetic history, secondary mineralization, aperture, etc. The applicability of core investigation methods was, however, restricted by limitations in core recovery. This included core losses over certain intervals and disturbances of core integrity attributable to stress relief with associated fracturing. The assessment of fracture zones was based on integrated interpretation of results obtained using the range of investigation methods indicated. This multidisciplinary interpretation enabled identification of fracture zones of all orders.

3 THE KOLA SUPERDEEP BOREHOLE

3.1 GEOLOGICAL AND TECTONIC SETTING

The Kola borehole (SG-3) is located in the north-eastern part of the Baltic Shield at latitude 69°25'N and longitude 30°44'E (Fig. 3-1). It is at present 12261 m deep. Down to a depth of 6800 m, the borehole penetrates rocks belonging to the Pechenga complex, which forms the Pechenga trough in the north-western part of the Kola Peninsula. The Pechenga trough constitutes a major part of the Pechenga-Imandra-Varzug synclinorium zone, which extends 600 km from the Varanger Fjord to the White Sea and reaches a maximum width of 40-50 km. The Pechenga complex is a unique geological formation characterized by:

- A complete succession of sedimentary and volcanogenic strata

- Metamorphic zonation from prehnite-pumpellyite facies, which correspond to transition of a cenotypal rock into a paleotypal one, to epidote-amphibolite facies characteristic of Precambrian formations

- Extensive sulphide copper-nickel ore deposits (prospecting included numerous multi-scale surveys such as electromagnetic, gravimetric and various seismic investigations).

The rocks within the complex outcrop fairly well, especially in the central part of the Pechenga trough.

Figs. 3-2 and 3-3 show the geological setting of the Kola borehole area. The geological investigations of the Pechenga complex significantly improved understanding of its genesis and structural characteristics. Thus, present knowledge shows that the Pechenga trough is a complex asymmetrical synclinorium, composed of metamorphic, volcanogenic and sedimentary rocks overlying a granite-gneissic basement [1:1-1:24]. The rocks dip towards the centre at an angle of 30-50° S and SE. The thickness of individual beds is uniform by both strike and dip. The maximum width of the synclinorium is 30 km and its length is 60 km. Judging from seismic data verified by results from borehole SG-3, the vertical extent of the Pechenga complex is estimated to be 8-9 km.

The Pechenga complex has been formed in several evolutionary stages. The initial stage was associated with rifting and subduction of the rigid Archaean granite-gneissic basement. This stage involved deposition of basal conglomerates (1st sedimentary suite), intrusion of magmatic rock bodies and eruption of non-differentiated andesite-basalt magma (1st volcanogenic suite). These events were succeeded by deposition of sandstones and limestones (2nd and 3rd sedimentary suites).

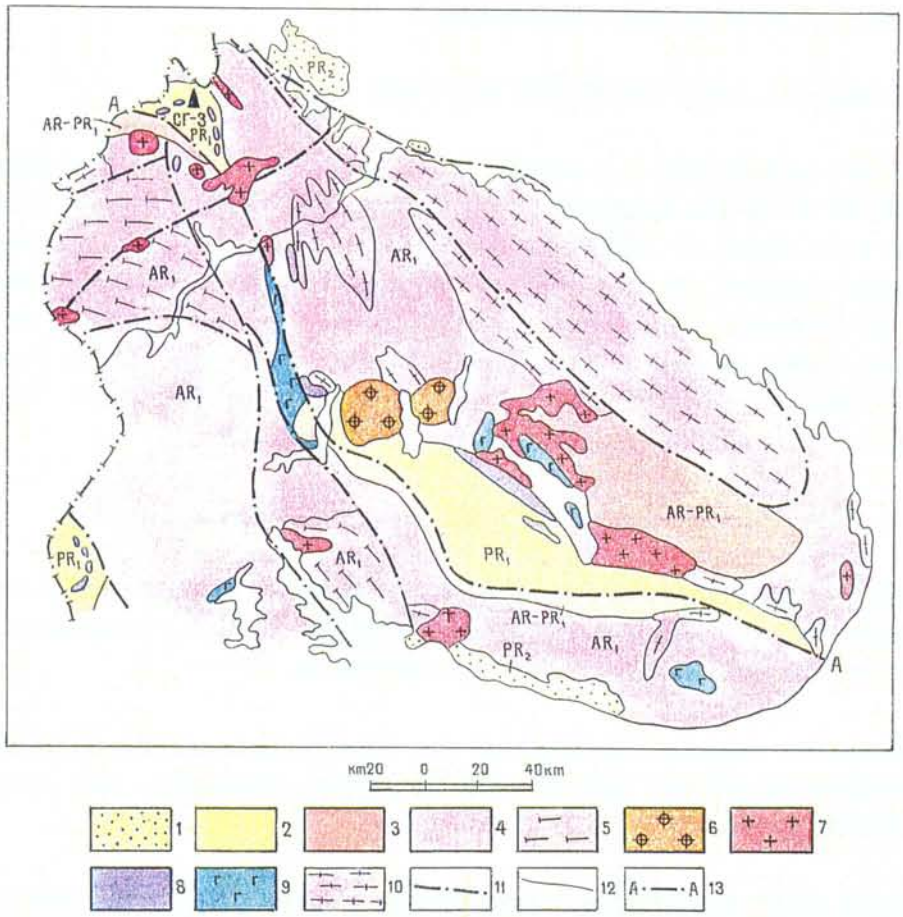

Fig. 3-1 *Geological map of the Kola Peninsula*

Legend.

1 *The Hyperborean complex* (PR_2) - sandstones, clay shale and dolomites

2 *The Pechenga (I),Imandra-Varzug(II) and Kuolayarvin (III) complexes* (PR_1) - basic, intermediate ultrabasic lava, subordinate phyillite, aleurolite, sandstone, dolomite

3 *The Tundra and Keyvskaya series* ($AR\text{-}PR_1$)- clay and micaceous shale and another shale and amphibolite

4 *The Kola series* (AR_1) - double-mica and biotite gneisses

5 *Granulite complex* (AR_1)- garnet--pyroxene-biotite gneisses and amphibolite

6 Complex of alkali nepheline syenite (PZ)

7 Granite, granitoid (PR_1)

8 Gabbro-norite, hyperbasite (PR_1)

9 Metagabbro (PR_1)

10 Gneiss-granite (AR_1)

11 Main tectonic unit

12 Geological boundaries

13 The Poritashsky regional deep fault

▲ The Kola borehole

Legend to Figs. 3.2 and 3.3.

Tundra series (AR-PR_1)

1 Schists upon andesite-metaporphyrite and tuffogenic-sedimentary rock

Pechenga complex (PR_1)

Nickel series

2 Matertinskaya suite (PR_1 mt), tholeiite lava with interlayers of picrite-basalt lava and basic and ultrabasic tuffes

3 Zhdanovskaya suite (PR_1 gd), alternation of phyllites, tuffites, aleurolites and sandstones with intrusions of gabbro-verlite and gabbro-diabase formation bodies

4 Zapolyarninskaya suite (PR_1 zp), tholeiite lava with little-thick interlayers of tuffogenic-sedimentary rocks in the middle part and the suite basement

5 Luchlompolskaya suite (PR lz), dolomites, arkosic sandstones, aleurolites, formation body of andesite-dacite porphyrites

Luostarinskaya series

6 Pirttiyarvinskaya suite (PR_1 pr), andesite-basalt lava and trachybasalt lava with dolomite, metasandstone and conglomerate interlayers and gabbro-diabase formation bodies

---

Kola complex (AR_1)

7 Gneisses, granite-gneisses

8 Tectonic disturbances
- A limited regional deep (Poritashsky fault)
- B intrastructural
- C longitudinal interbedding (Luchlompolsky fault)
- D lateral

9 Geological boundaries
- a complexes
- b suites
- c elementes of inner structure

10 Boundaries between metamorphic facies in the Pechenga compex:
- a prehnite-pumpellyte and greenschist;
- b greenscchist and epidote-amphibolite
- c epidote-amphibolite and amphibolite;

11 Contour line of geological section;

12 Position of the Kola superdeep borehole.

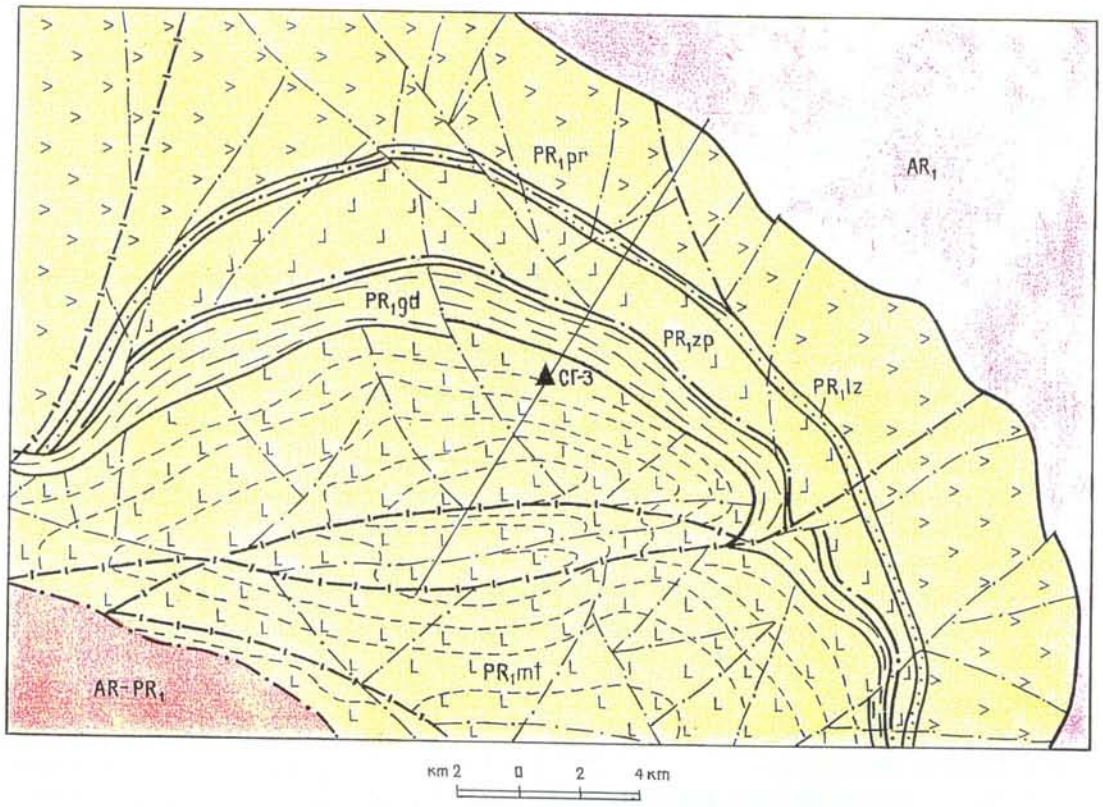

Fig. 3-2. *Geological and tectonic map of the Kola borehole area.*

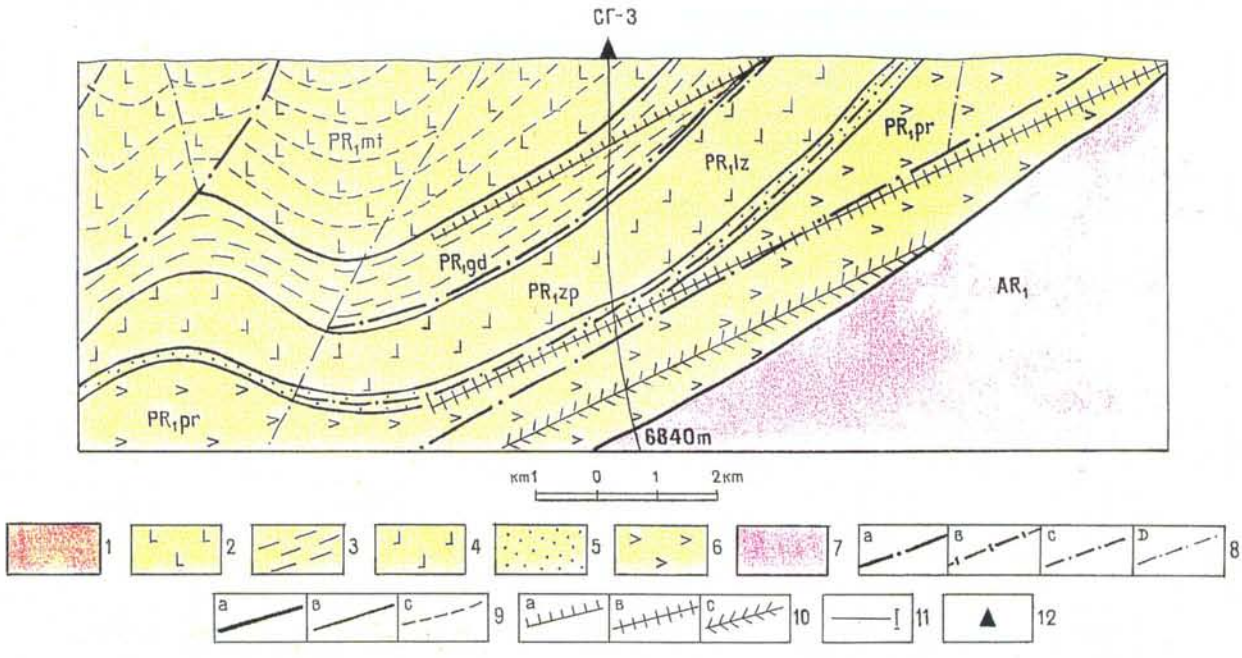

Fig. 3-3. *Geological section of the Kola borehole area.*

The magma was affected by alkaline and volatile components, followed by differentiation and eruptions of trachybasalt and trachyandesite volcanites (2nd volcanogenic suite). To some extent, the succession corresponds to the volcanic series of the continental rifts.

In the next stage of evolution, deeper parts of the magmatic centre were intruded. Eruptions of non-differentiated tholeiite (3rd volcanogenic suite) occurred and tuffaceous-flyschoid deposits were formed (4th sedimentary suite). During subsequent evolution of the magmatic centre, there was intrusion of comatiite magma with ultrabasic to basic and even acidic differentiates. It conditioned the eruption of tholeiite and comatiite (picrite-basalt) volcanites (4th volcanogenic suite) and intrusion of comagmatic rocks, especially nickel-bearing gabbro-verlite. Such a sequence is by composition close to the volcanic series of oceanic rifts, formation of mid-oceanic ridges, oceanic volcanic belts and "oceanization" zones of the Earth's crust.

The evolution of the Pechenga complex terminated with a phase of folding and progressive zonal metamorphism with successive faulting. The sedimentary and volcanogenic strata were stratigraphically classified into suites, forming two Lower Proterozoic, sedimentary-volcanogenic series [1:12], i.e. the Luostarinskaya and Nickelskaya series (Fig. 3-3). The rocks of the Pechenga complex are highly influenced by multistage metamorphic transformation. This is reflected by into zonations [1:7, 1:12], intersecting bedding at various angles (Fig. 3-3). The vertical variability of metamorphism is linked to the block structure. As a whole, the metamorphic degree increases from top to bottom and towards the periphery of the complex (from prehnite-pumpellyite to epidote-amphibolite facies).

Metamorphic transitions affect the properties of different rock types differently. For example, strength is found to increase with the degree of metamorphism for detrital (phyllite, aleurolite, sandstone, gravel) and acid magmatic rocks. For carbonatic and basic magmatic rocks, the strength increases from prehnite-pumpellyite to greenschist facies, after which a decrease is observed.

Basites account for more than 80% of the rocks of the Pechenga complex. Prehnite-pumpellyite facies are distinguished by the mineral paragenesis - magmatic monocline pyroxene with albited plagioclases and metamorphic prehnite and pumpellyite. In these facies the rock completely retains its original structure and texture. The prehnite-pumpellyite facies were found exclusively in the central part of the complex, and in borehole SG-3 down to a depth of 1400 m. The rock in these facies is brittle since its magmatic structure, including glassy appearance, has not been lost.

Greenschist facies in metabasite are characterized by paragenesis of actinolite with albite, where actinolite is usually formed pseudomorphously by pyroxene and albite - by magmatite plagioclase. The original texture is relic, but structures are fully

preserved. These facies occur mainly in the peripheral parts of the central blocks and are penetrated by borehole SG-3 at 2400-4800 m. The structure and mineral composition have been influenced by lithostatic and dynamic stresses, but no high degree of anisotropy has developed.

Epidote-amphibolite facies in the basic rock exhibit paragenesis, i.e. blue-green hornblende plagioclase (oligoclase-andesine). Relic original textures were rarely observed, but original structures are more or less present. Rocks of epidote-amphibolite facies are formed in marginal blocks, and observed in the lower part of borehole SG-3 (below 4800 m). The rock in these facies has been transformed into schist and schist amphibolite, exhibiting clear anisotropy in both mineral assemblage and structure.

In general, the metamorphism of the Pechenga complex is isochemical. This was verified by investigating separate sections of homogeneous tholeiite where successive changes of facies from prehnite-pumpellyite, over greenschist to epidote-amphibolite were observed along the strike [1:19].

The Kola borehole is located far from major faults, in a tectonically relatively undisturbed area. However, faults play a significant role in the structure of the Pechenga complex. They are classified as follows:

A *Marginal deep faults*: Ancient subvertical deep faults which delimit large geological structures.

B *Intrastructural faults*: Subvertical faults formed inside large geological structures that determine the subdivision of these structures into blocks.

C *Longitudinal faults*: Thrust faults inside large geological structures, which envelope the rock and rock boundaries.

D *Cross and diagonal faults*: A system of subvertical faults that intersect geological boundaries and show insignificant displacements.

The Poritashkaya zone, which extends over 600 km along the southwestern margin of the Pechenga-Imandra-Varzug synclinorium zone and limits it, is referred to as marginal deep faults (A). As interpreted from seismic data, the Poritashkaya zone has a subvertical dip and extends to a depth of 20-25 km. It is 10 km wide, and is composed of a sequence of parallel faults, with displacements of up to several kilometres.

Intrastructural faults (B) are important as delineators of the main blocks within the Pechenga trough. They have been identified by means of geological, geophysical and morphological methods. Total displacements of these subvertical faults are not yet known, but judging from observed horizontal movements they are of the order of

hundreds of metres.

Longitudinal faults (C) are frequent in the Pechenga trough. As a rule, they are encountered along boundaries between rock types with different properties. The Luchlompolsky fault (C1) belongs to this category. This fault is located along the interface between volcanic and sedimentary rocks, and was intersected by borehole SG-3. It is 400 m wide, and has been traced more than 40 km in the lateral direction.

The frequently occurring cross and diagonal faults (D) are generally steeply dipping (70-90°). They are characterized by displacements not exceeding 20-40 m, and widths less than a few tens of metres. Their extent on strike is usually limited to within the Pechenga complex.

High order faults, plicate within the Pechenga complex, are mainly located in sedimentary rocks.

3.2 RESULTS FROM BOREHOLE INVESTIGATIONS

3.2.1 **Rock types and fracturing**

The following section presents results from the investigations in borehole SG-3 and its immediate surroundings. Data refer to lithology, structural conditions, rock stresses and petrophysical properties, groundwater regime, hydrochemistry and thermal conditions. A geological section, comprising the vertical interval down to a depth of 5 km, was compiled on the basis of the data collected. Core recovery within the given interval was 60 %, and the geological compilation relies heavily on core investigations.

Table 3-1 presents basic rock properties, as determined for the different suites and rock types penetrated by borehole SG-3. Fig. 3-4 presents the geological column and a number of properties as a function of depth.

The SG-3 borehole was subdivided into sections exhibiting uniform fracturing, as indicated in the extreme right column in Fig. 3-4. The fracture frequency and relative core length composed of fractures and veins was then evaluated for each section (Fig. 3-4). Fracture frequency does not decrease with depth, and is still significant in the lowermost horizons penetrated (12000 m). On the basis of extensive investigations within the Pechenga complex, major rock types were ranked as follows, in order of ascending degree of fracturing: basite, tuff, hyperbasite and sedimentary rock.

Table 3-1. Geological, physical strength, thermal characteristics and gas saturation in different rock types in the Kola borehole.

Series	Nickelskaya											Luostarinska
Suite	Matertinskaya IV volcanogenic			Zhdanovskaya IV sedimentary			Zapolyarninskaya III volcanogenic			Luchlompolskaya III sedimentary		Pirttiyarvinskaya II volcanogenic
Facies of metamorphism	Prenite - pumpellite			Prenite-pumpellite-greenschist			Greenschist			Greenschist-epidote-amphibolite		Epidote - amphibolite
Interval, m	9 - 1059			1059-2805			2805-4673			4673-4884		4884-5642
Thickness, m	1050			1746			1868			211		758
Rock-type	Massive and globular tholeiite lava	Massive and globular picrite-basalt lava	Interlayers of basic and ultrabasic tuff	Interlayers of rhytmic coaly phillite, aleurolite, sandstone and conglomerates	Intrusive bodies of gabbro-diabase	Intrusive bodies of gabbro-verlite	Massive and globular tholeiite lava	A member of tuffaceous sedimentary rock in the central part of the suite	Basic and ultrabasic schist in the basal part of the suite	Interlayers of dolomite and arcosic sandstone, aleurolite	An intrusive body of andesite-dacite porphyr	Trachybasalt subalcalic (25) trachiandesitic-basalt (25) basalt (10) chyandesite (40) and trachyte lava
(% of total)	(77)	(4)	(19)	(60)	(30)	(10)	(90)	(3)	(7) (4400-4673)	(50)	(50)	
Rock properties												
Density (d), (g/cm^3)	2.74-3.24 * 3.02	2.82-3.24 3.02	2.61-3.07 2.92	2.65-3.36 2.90	2.63-3.20 2.98	2.72-3.20 2.88	2.70-3.22 3.02	2.70-2.96 2.88	2.85-2.99 2.93	2.66-3.10 2.78	2.69-3.04 2.82	2.72-3.15 2.92
Compressive strength (d_c) (MPa)	170-260 210			90-220 140	150-260 200	80-210 160	170-270 230	120-160 140	20-100 40	140-190 160	130-200 160	30-370 180
Tensile strength (d_p)(MPa)												
Parallell to bedding	30-55 35			25-50 35	30-45 35	20-50 30	20-50 35	30-60 45	8-20 10	20-40 25	10-20 15	30-50 40
Perpendicular to bedding				15-20 20				5-20 10	3-10 5	15-20 18	3-10 6	15-30 23
Coefficient of anisotropy by(d_p)				1.75				2.5	2.0	1.39	2.5	1.74
Tensile strength (d_i), (MPa) parallell to bedding	56-60 59			55-60 60	47	50	54-60 55					45

* *The given numbers correspond to min, max and average values*

Table 3-1. Continued.

Structural interval	V - Differentiated volcanite 9-1059 m			IV - Differentiated tuffaceous - sedimentary rocks with intrusions 1059 - 2805 m			III - Monolith volcanite 2805 - 4400 m		II - Luchlompolsky fault zone 4400 - 5100 m			I -Differentiated volcanite 5100 - 5600 m
Bending strength (d_i), (MPa)												
Perpendicular to bedding	54-60 57			35-40 38	45	48	45-55 50					37
Coefficient of anisotropy by (d_i)	1.03			1.58	1.04	1.04	1.07					1.21
Thermal conductivity (λ), W/(mK)	2.86-3.17 2.88	2.98-3.01 2.99	2.75-3.49 2.98	2.80-5.61 3.63	2.57-3.53 3.03	2.39-3.65 2.84	3.25-3.45 3.39	3.49-3.67 3.57	4.18-6.00 5.42	4.13-5.57 4.20	3.00-4.40 3.71	2.62-2.35 2.76
Thermal diffusivity W * 10^6, m^2/s	1.05-1.26 1.13	1.12-1.18 1.15	1.13-1.32 1.22	1.07-1.69 1.32	1.01-1.36 1.18	0.96-1.36 1.07	1.29-1.35 1.30	1.35-1.41 1.37	1.35-1.67 1.63	1.79-2.20 1.82	1.53-1.83 1.68	1.11-1.19 1.15
Specific thermal capacity (c) J/kgK	828-870 844	841-864 852	859-873 869	900-931 894	848-896 873	890-908 902	836-868 842	891-905 897	946-977 967	841-861 844	789-823 806	821-829 824
Average value of gas saturation of the drilling mud, cm^3/l												
He				0.0	0.0	0.0	0.0	0.0	0.17	0.17	0.07	0.36
H_2				6.72	2.40	1.20	43.90	7.90	459	74.3	152	357
CO_2				600	500	158	209	78	46	218	144	385
CH_4				14.7	6.3	1.88	1.73	1.79	1.69	3.39	3.11	9.44
C_2H_6				0.26	0.10	0.17	0.05	0.076	0.09	0.147	0.236	0.14
C_3H_8				0.062	0.067	0.003	0.019	0.029	0.026	0.047	0.076	0.03
C_2H_4				0.56	0.02	0.016	0.022	0.05	0.043	0.129	0.195	0.09
C_3H_6				0.048	0.03	0.002	0.016	0.017	0.023	0.065	0.11	0.01
C_4H_{10n}				0.04	0.037	0.0	0.007	0.0	0.001	0.008	0.015	0.001
C_4H_{10i}				0.06	0.003	0.0	0.007	0.0	0.009	0.023	0.039	0.02
Total				622	509	161	225	88	507	296	300	752

Legend to Fig. 3-4.

1 Age, stratigraphic index

---

2 Lithological column

The Pechenga complex

Tundra series AR-PR

1 Andesite metaporphyrite overlain by schist

2 Schist overlying tuffogenic-sedimentary rocks

Pechenga complex - PR (3-9); Nickel series (3-5)

3 Metamorphosed tholeiite-basalt

4 Tuff

5 Phyllite, tuffite, aleurolite, sandstone

Luostarinskaya series (6-7)

6 Metamorphosed andesite-basalt and trachybasalt

7 Dolomite, metasandstone, conglomerates

Intrusive rocks

8 Metagabbro-verlite

9 Metagabbro-diabase

---

3 Depth, km

4 Borehole diameter, cm

5 Fracture frequency (including veins), 1/m

6 Relative length of core composed of fractures and veins, cm/m

7 Propagation velocity of elastic waves from acoustic logging (Vp), km/s

8 Propagation velocity of elastic waves from VSP surveys (Vp), km/s

9 Rock density (core samples), g/cm^3

10 Propagation velocity of elastic waves in the rock core (Vp), km/s

11 Hardness of rock from stamp tests (P), kg/mm^2

12 Water-bearing (a) and water-resistant (b) horizons

13 Hydrogeological zones

- 1 Zone of regional subsurface runoff
  - a Subzone of open exogenous non-mineralized fracturing
  - b Subzone of secondary cementation of fractures
  - c Subzone of secondary leaching of fractures
- 2 Zone of transit and partial generation of water
- 3 Zone of deep water generation

14 Matter-structural layers of

- V Differentiated volcanites of the Matertinskaya suite
- IV Differentiated and intrusive tuffogenic-sedimentary rock of the Zhdanovskaya suite
- III Volcanite fracture blocks of theZapolyarninskaya suite
- II Schist, blastomylonite and blastocataclasite in the Luchlompolsky fault

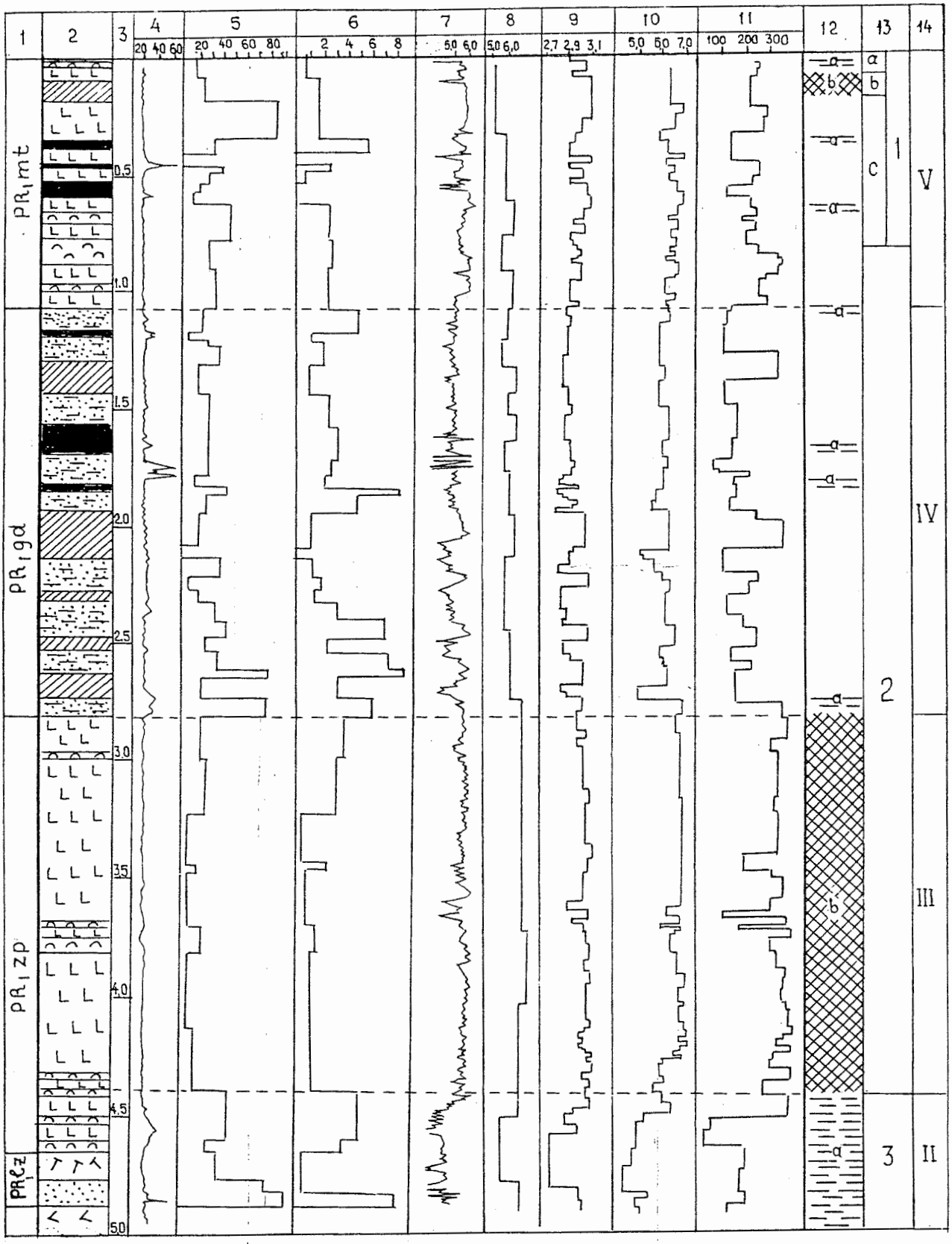

Fig. 3-4. *Geological column of the Kola borehole and rock properties.*

Classification of fractures with respect to tectonic origin was performed on the basis of more or less well oriented core sections. Four general categories of fracture were distinguished:

1) Fractures oriented parallel to the rock type boundaries,and dipping 30-60°

2) Fractures oriented almost perpendicular to bedding planes and rock boundaries, and dipping 60-80°

3) Usually vertical fractures, intersecting bedding planes and rock type boundaries at angles 30-60°.

4) Horizontal or gently dipping fractures intersecting rock boundaries and bedding planes.

Practically all fracture categories are represented in fault zones, but the type 1) prevails in thrust zones of the order C (see p. 18). Since the borehole is located far away from faults of the orders A and B, vertical fault displacements are moderate. They may be classified as being of the order D. These structures are accompanied by fracturing of all categories, but as a whole they do not significantly influence rock mass integrity.

Numerous longitudinal, conformal faults of the order C are observed, usually in connection with rock boundaries representing significant contrasts in composition and physical properties. Generally, the rock in these faults is fully exfoliated and crushed, with formation of blastomylonite and blastocataclasite.

Fracture filling (chlorite, carbonate, quartz, sulphide etc.) is common in tectonic fault zones. Fracture widths range from 0.1 mm up to several centimetres. The frequency, orientation and mineral paragenesis of mineralized fractures depend on rock composition, degree of metamorphic alteration, associated type of fault and bedding depth.

3.2.2 Stress conditions and physical rock properties

Rock stress conditions are controlled by lithostatic and tectonic factors. The Kola Peninsula is characterized by extremely high horizontal stresses - up to four times the vertical stress. This has been experimentally verified at a depth of 500-600 m in the Khibin and Lovozersk massifs. These excessive horizontal stresses in the upper part of the Earth's crust are generally the result of block upwarping. Investigations of the Baltic Shield [1:12] verified this finding.

However, the Pechenga massif, where the Kola borehole is located, lies within a zone of contemporary downwarping and low seismic activity. Stress determinations,

conducted by a stress relief method in deep mines of the Pechenga Nickel Company [1:21] show that the horizontal stresses in the area do not exceed 0.7 times the vertical stress.

The vertical stress component, σ_z, as a function of depth was estimated experimentally on the basis of P-wave velocities (Vp) obtained from broad-band acoustic logging, and from modelling using laboratory data from measurements of P-wave velocity on core samples under varying confining pressures (plot b in Fig. 3-5). Estimates were compared with results from analytical modelling, assuming elastic rock behavior and taking into account thickness, dip and mechanical properties of the rock (plot a in Fig. 3-5). The discrepancy observed between the experimental data and the modelling results does not exceed 30 % in the upper borehole interval. Below a depth of 4000 m, the discrepancy is up to 45 %. This is in agreement with modelling results, which indicate that σ_z decreases within the fault zone (4400-5100 m).

The horizontal stress conditions were evaluated by analysing borehole geometry data, obtained from caliper logging surveys (Fig 3-6). Local borehole breakouts occurred more or less immediately after drilling. Caving did not progress with time, except in fault zones subjected to high tectonic stresses. The caving produced elongated borehole cross-sections, and down to a depth of 5000 m the orientation of these elongations depended very little on the dip angle of the rock or structural/textural features. Instead, it was mainly controlled by the orientation of the major horizontal stress, which was perpendicular to the longitudinal axis of the borehole cross-sections [1:23], and primarily oriented to the north-west with an azimuth 290-300°. This is in accordance with results from analyses of focal plane mechanisms of earthquakes in the upper part of the Earth's crust [1:22], and from investigations in deep mines on the Kola Peninsula [1:21].

The compressive strength of the rock ranges from 80 MPa to 260 MPa, and the tensile strength values fall within the interval 10-50 MPa. This excludes schist deposited in the Luchlompolsky fault zone (depth 4563-4673 m), which has a compressive strength of 20-100 MPa and tensile strength values, taken parallel and perpendicular to the bedding plane, ranging between 8-20 MPa and 3-10 MPa respectively.

The mechanical anisotropy, as based on the rock strength data obtained in compression and bending (Table 3-1), indicates that the magmatic rock types are practically isotropic, whereas anisotropy is clearly manifested in the tuffaceous-sedimentary rocks. A high level of anisotropy was observed in connection with the Luchlompolsky fault zone.

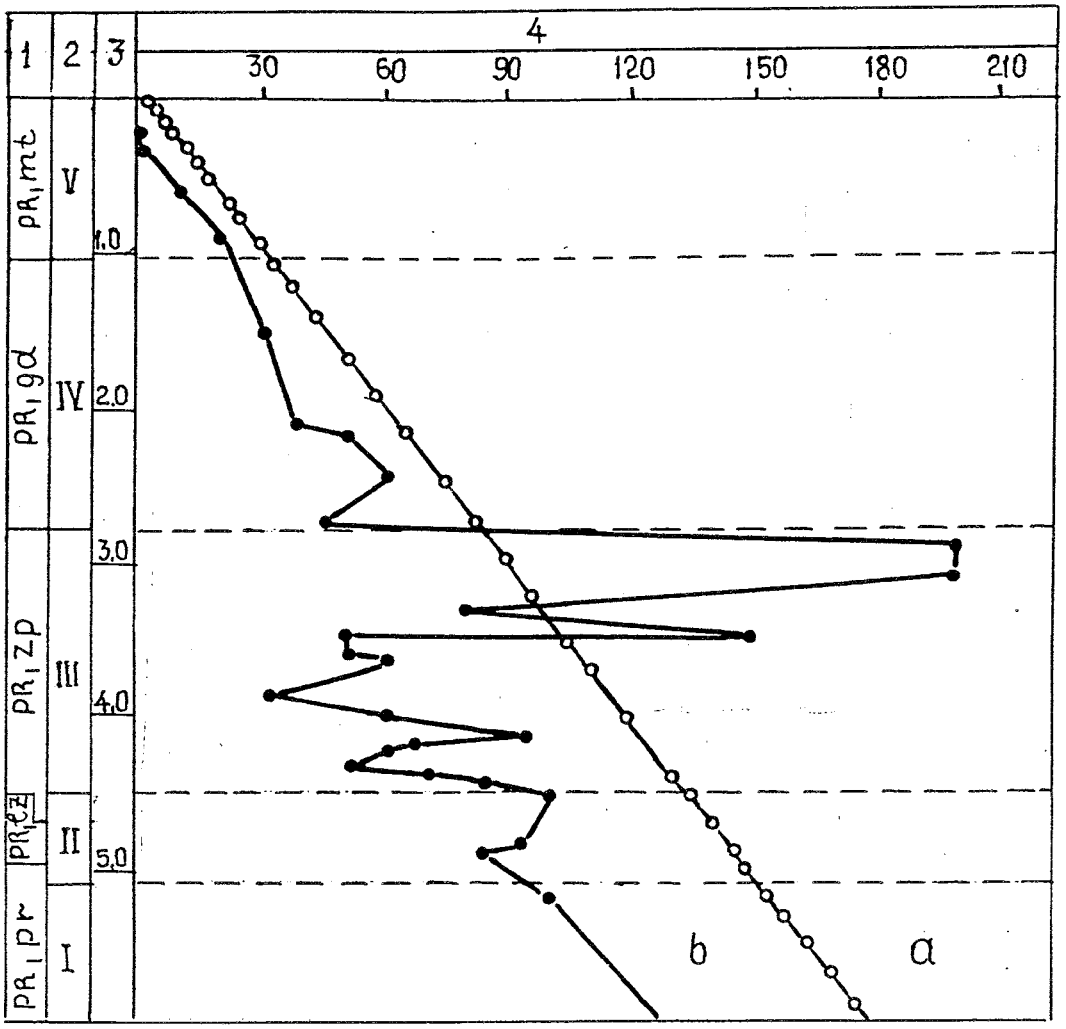

Fig. 3-5. *Vertical stress component in the Kola borehole.*

Legend

1 Age, stratigraphic index
2 Matter-structural layers (see Fig. 3-4; 14)
3 Depth, m
4 Stress (MPa)
  a Geostatic model
  b Experimental result obtained from elastic wave propagation data.

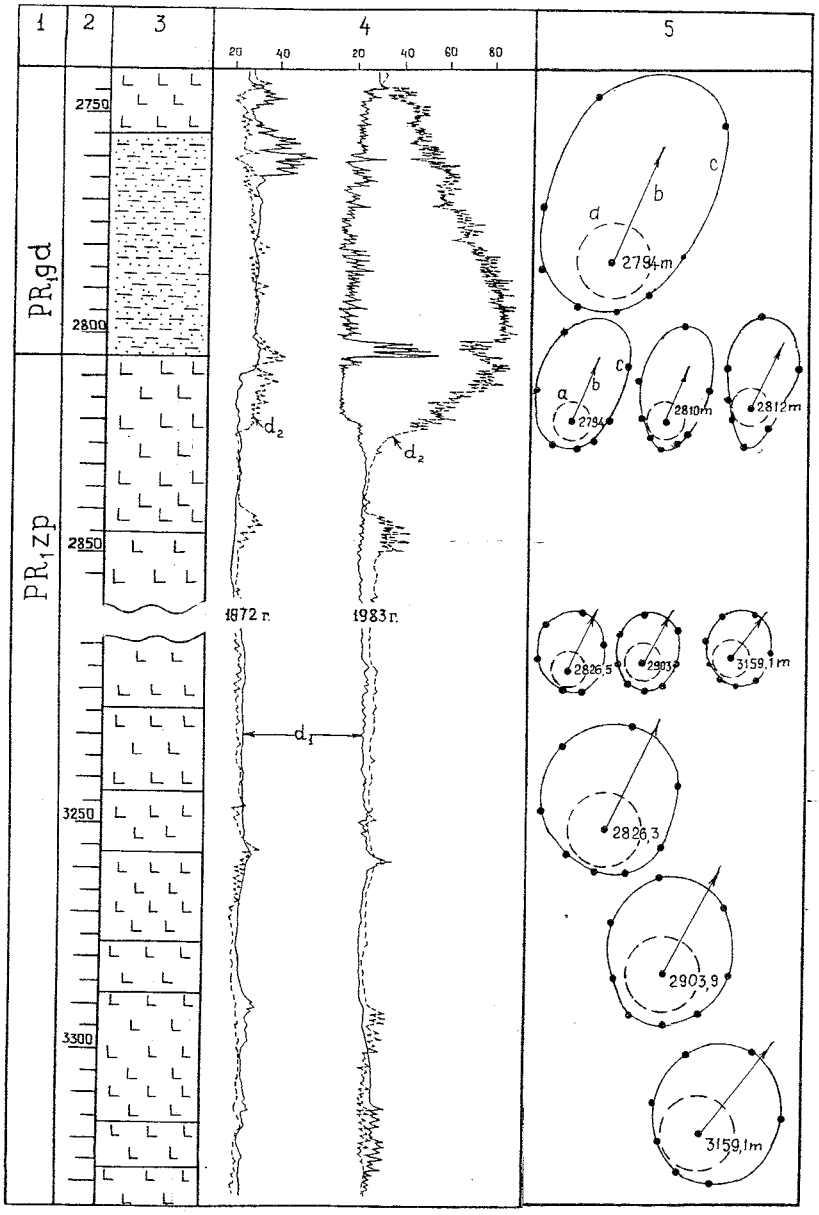

Fig. 3-6. Changes of borehole configuration with depth.

Legend

1 Age, stratigraphic index
2 Depth, km
3 Lithological column (legend in Fig. 3-4)
4 Borehole diameter, cm, in 1972 and in 1983
- d_1 By the first pair of caliper arms
- d_2 By the second pair of caliper arms

5 Lateral borehole cross-section obtained by measuring the diameter at different levels
- a Nominal diameter
- b Orientation of expansion
- c Actual size

Rock brittleness was determined from load-deformation curves, and under PT corresponding to thermobaric conditions in-situ. The brittleness factor was defined as the ratio between elastic deformation and total deformation at failure. The results are given in Table 3-2 and show that brittle deformation prevails to a depth of at least 6000 m.

The strength of filled fractures was determined and related to the dominant mineral composition of the fracture filling substance (Table 3-3). It was observed that the strength of fractures filled with hard minerals was often higher than the strength of the rock matrix itself. For example talc-chlorite schist showed low tensile strength values (8 MPa) compared with fractures filled with crystalline quartz and epidote. It was also found that mineralized fractures retain brittle deformation characteristics.

The effective porosity of the rock, as determined from core samples, averages 0.5 % down to a depth of 4500 m, the total porosity being on average 1 %, increases, however, up to 2.7 % within the Luchlompolsky fault zone. The relatively low porosity and essentially isolated pores yield low permeability. The value of the permeability coefficient of the fractured magmatic rock measured at UIPK-1 test stand is $25 \cdot 10^{-15}$ m^2 ($25 \cdot 10^{-3}$ D). This is 100-1000 times less than the normal range of values for fracture permeability.

Propagation velocities of elastic compression and shear waves (Vp and Vs) are high as a consequence of the high density and low porosity. Down to 5000 m depth, Vp averages 6100 m/s. Values recorded in the different geological suites were as follows: Matertinskaya - 6500 m/s; Zhdanovskaya - 6010m/s; Zapolyarninskaya - 6200 m/s and Luchlompolskaya - 4390m/s.

Table 3-2. Brittleness factor of rocks with depth

Rock type	Depth, m	Brittleness factor
Basic tuff	775.6	0.88
Diabase (lava)	1035.8	0.87
Gabbro-diabase (intrusion)	1990.5	0.88
Metadiabase (lava)	4005.8	0.94
Biotite-amphibole-plagioclase schist	4925.8	0.76

Table 3-3. Rock strength and relation to fracture filling material.

Fracture filling	Mohs' scale	Strength, MPa	
		Tension	Shear
Graphite, talc, chlorite, muscovite, biotite	1-2	1.0-4.0	2.0-5.0
Serpentine, calcite, baryte Chrysolite, asbestos, dolomite	3-5	4.0-12.0	6.0-12.0
Quartz, epidote, feldspar, garnet	6-8	12.0	15.0

3.2.3 Hydrogeology, groundwater chemistry and gases

The hydrogeological investigations in the Kola borehole and surrounding exploration boreholes were conducted by means of effective monitoring (EM) of the physical and chemical characteristics of the drilling fluid.

Mud temperature was measured at the well collar to an accuracy of ± 0.01 °C. Samples were taken at regular intervals (every 10 m) down to a depth of 4700 m. Below this depth, sampling was done at 5 m intervals. Each sample was analysed with respect to density, Eh and pH using an RN-340 potentiometer, providing an accuracy of ± 0.001 g/cm^3, ± 1 mV and ± 0.01 pH for the respective properties.

The hydraulic characteristics of the water-bearing sections were investigated using a special method of changing flushing regimes (SMF). Without involving any special instrumentation, this method permitted approximate evaluation of transmissivity coefficient, formation pressure and certain coefficients characteristic for the chemical composition of the groundwater.

The results from the hydrogeological investigations suggest that the Pechenga Proterozoic synclinorium zone is related to an ancient subartesian basin [1:12]. The upper 5000 m of the crust in the SG-3 area can be subdivided into three zones. The zones are distinguished by the type and degree of groundwater mineralization, gas chemistry, hydraulic characteristics and the type of fracture/vein reservoirs (Tables 3-4, 3-5 and 3-6; Fig. 3-4).

The three zones were defined as follows:

Zone 1	Regional subsurface run-off	Depth 0-800m
Zone 2	Transition and partial generation	Depth 800-4000 m
Zone 3	Generation of deep water	Depth > 4400 m

Table 3-4. *Groundwater chemistry in the area of the Kola borehole*

Borehole	Sputnik borehole			Borehole no: 1886				
Zone	1			1			2	
Depth, m	100	530	560	100	350	720	900	1200
	components,mg/l							
Na^+	49	983	1008	31	149	140	2368	6330
K^+	8.5	11	8	0.4	-	12	30	60
Ca^{2+}	35	385	372	56	148	-	5600	11800
Mg^{2+}	4	n.d.	n.d.	11	15	-	160	500
Cl^-	85	1790	1765	183	483	-	14644	31760
SO_4^{2-}	22	n.d.	n.d.	n.d.	4	-	4	4
HCO_3^-	71	86	357	70	81	-	451	306
CO_3^{2-}	6	429	402	n.d.	n.d.	-	n.d.	22
NO_3^-, NO_2^+	-	-	n.d.	-	-	-	-	n.d.
NH_4^+	-	-	n.d.	-	-	-	-	0.1
Br^-	-	17	-	4	7	-	128	272
J	-	n.d.	-	n.d.	1	-	3	8
F	0.2	n.d.	-	n.d.	n.d.	-	0.3	n.d.
B	2	0.9	-	-	n.d.	-	3	4
As	-	n.d.	-	n.d.	0.002	-	0.008	0.032
H_4SO_4	-	8	-	16	13	-	10	6
Fe^{2+}	-	0.4	0.5	0.2	n.d.	-	6	10
Fe^{3+}	-	n.d.	-	-	-	-	-	0.1
Fe(OH)	-	-	-	-	n.d.	-	3.8	0.5
Sr	-	7.35	-	0.3	4	92	208	1150
Rb	-	0.16	-	n.d.	0.01	0.01	0.10	0.15
Cs	-	0.01	-	n.d.	0.01	n.d.	0.02	0.04
Mn	-	0.05	-	n.d.	0.08	0.08	-	-
Al	-	0.5	-	-	-	0.35	-	-
Ti	-	n.d.	-	-	n.d.	-	n.d.	n.d.
Pb	-	0.2	-	0.065	0.064	0.15	0.093	0.13
Cu	-	0.03	0.024	0.02	-	n.d.	0.01	0.02
Ni	-	0.005	0.032	0.005	-	n.d.	-	-
Co	n.d.	n.d.	0.048	n.d.	n.d.	n.d.	n.d.	n.d.
Cd	-	0.03	-	0.55	0.007	0.0005	0.005	0.001
Mineral-ization	244	3591	3731	395	906	-	23960	51038
Dry residue	-	-	-	-	936	-	26904	55108

Table 3-5. *Chemistry of gas samples in the area of the SG-3 borehole.*

Zone	Bore-hole no:	Depth, m	Sampling method	Relative frequency, %				
				He	H_2	O_2	N_2	CH_4
1	2000	0	At the well head	0.1	-	5.5	49.0	45.1
	1886	100	Sampler	-	0.004	20.9	78.0	0.016
	1886	295	-"-	-	0.03	20.6	78.0	0.016
	Sputnik	530	-"-	1.42	0.09	6.8	52.4	36.7
	2244	556	-"-	0.36	0.006	6.1	34.0	56.6
	2286	720	-"-	-	0.16	20.0	78.0	0.033
2	2253	900	-"-	0.003	0.015	20.9	78.0	0.060
	1886	900	-"-	1.58	3.74	0.9	19.5	74.3
	SG-3	1160	During drilling	4.8	34.23	-	-	60.5
	1886	1166	Sampler	0.87	20.8	0.9	11.5	63.3
	1886	1200	-"-	0.35	3.13	7.7	18.3	64.3
	1886	1243	During drilling	-	6.27	-	63.5	16.8
	1886	1296	-"-	-	18.0	-	37.9	46.4
	1886	1323	-"-	-	14.6	-	36.6	38.9
	1886	1338	-"-	-	2.42	-	73.3	10.7
	1886	1339	-"-	-	21.8	-	31.4	47.9

Table 3-6. *Hydraulic parameters as function of depth in Sputnik and Verkhnee deposits in the area of the Kola borehole.*

Zone	Depth interval	Zone thick-ness	Sputnik deposit 1976		Verkhnee deposit 1986	
			Hydraulic conductivity m/day	Transmissivity m^2/day	Hydraulic conductivity m/day	Transmissivity m^2/day
1	0-160	160	0.0043	0.0900	0.0030	0.4800
	160-340	180	0.0033	0.5900	0.0015	0.2700
	340-580	240	0.0017	0.4100	0.0010	0.2400
	580-760	180	0.0010	0.1800	0.0006	0.1100
2	760-1240	480	0.00006	0.0300	0.00006	0.0300
	1240-1500	260	-	-	0.00003	0.0008

Analysis of gases in the SG-3 borehole was performed in conjunction with the hydrogeological investigations. This was done using an EM method with an automatic station for mudlogging and chromatography. This allowed continuous, qualitative and quantitative detection of hydrocarbon gases, helium, hydrogen and nitrogen to be performed (Table 3-1). It should be mentioned that drilling methods used down to a depth of 5369 m in SG-3 did not disturb gas assessment, since the drilling mud contained neither lubricants nor graphitic additives. Gas data from this interval were therefore highly informative. Besides borehole SG-3, sampling was also conducted in neighboring exploration wells (Table 3-5).

The results from gas analyses in SG-3 indicate that gas anomalies correlate with fracture zones in tectonic faults, occurring mainly along boundaries between magmatic and sedimentary rocks. These zones are also characterized by groundwater inflow (Fig. 3-4) along hydraulically conductive sections.

3.2.4 Thermal conditions

Temperature monitoring was performed at 500 m intervals in the Kola borehole. Results are given in Fig. 3-7. Delay times extended up to as much as 10 days. A maximum delay of 550 days occurred in connection with refurnishing work on the drill rig. Temperature readings were also taken in exploration holes, completed at least 9 months earlier. The accuracy attained in temperature measurements was ± 0.01 °C.

To estimate the heat flow, a total of 9000 measurements of thermal properties of core samples were made. The thermal conductivity (λ), thermal capacity (c) and thermal diffusivity were determined using a laser scanning method. The method involved scanning the surface of two consecutive standard samples and a series of test samples by a spot energy source and two thermal sensors. Measurement errors of thermal conductivity, thermal diffusivity and thermal capacity were $\pm 5\%$, $\pm 8\%$ and no more than $\pm 10\%$ respectively.

Processing of the thermal data down to 5000 m depth allowed the following thermal zones to be distinguished:

1)	Seasonal oscillations	from 0 m to 10-40 m
2)	No thermal gradients	from 10-40 m to 20-50 m
3)	Low gradients	from 20-50 m to 200-300 m
4)	Stable gradients	from 200-300 m to 800-850 m
5)	Intermediate gradients	from 800-850 m to 2800 m
6)	High gradients	below 2800 m.

The distributions of thermal conductivity, geothermal gradient and heat flow (Fig. 3-7, Table 3-1) show that the thermal field within the Pechenga structure is characterized by considerable thermal discontinuity with depth. Correlation with tectonic and hydrogeological data showed that the thermal anomalies are connected to fracture zones and lithological boundaries, which are also characterized by greater permeability than less disturbed intervals.

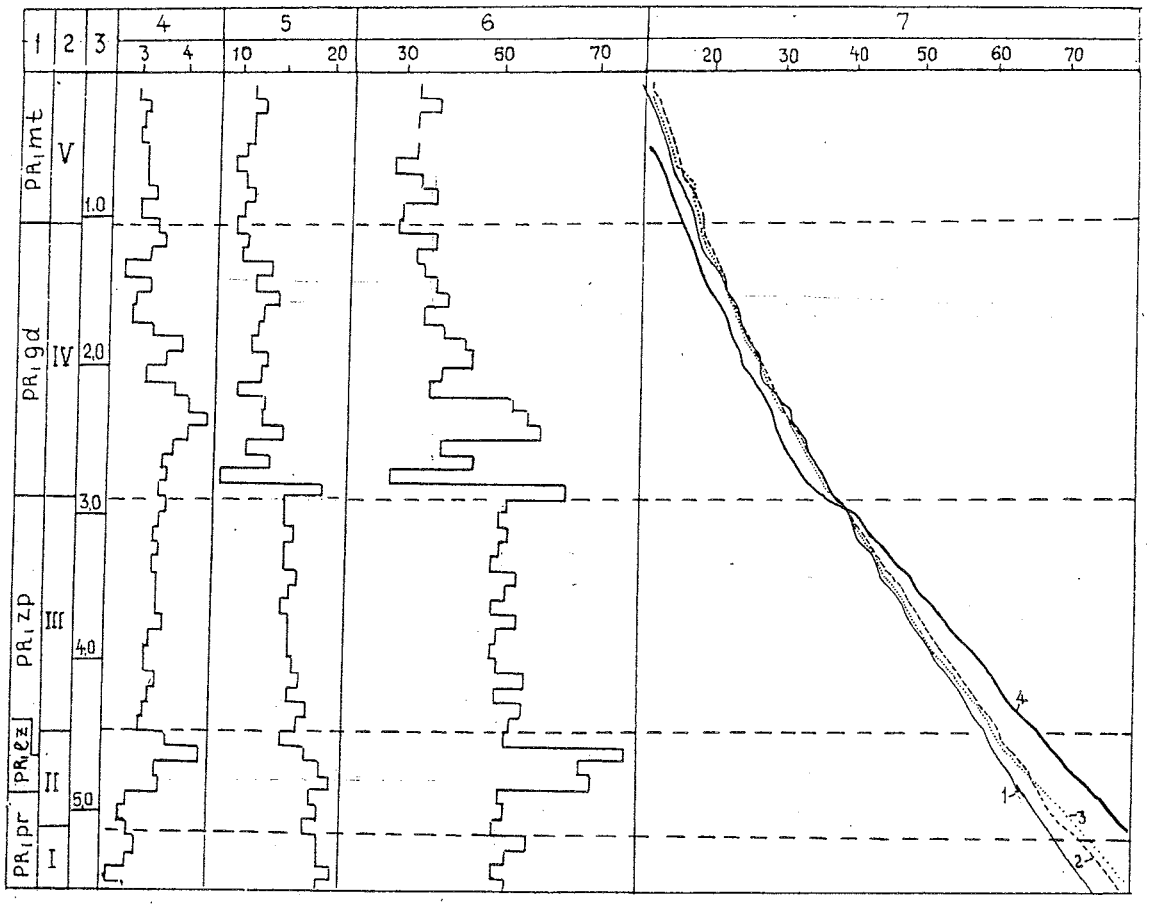

Fig. 3-7. Thermal properties and thermometry in the Kola borehole

Legend

1 Age, stratigraphic index
2 Matter-structural layers (see Fig. 3-4;14)
3 Depth, km
4 Thermal conductivity, W/Km
5 Geothermal gradient, K/km
6 Heat flow, mW/km^2
7 Thermometry (° C)

1	29.06.1972	122 hours of settling
2	04.10.1973	240 hours of settling
3	04.03.1974	216 hours of settling
4	02.10.1976	13344 hours of settling

3.3 GENERALIZED MODEL OF THE KOLA BOREHOLE

Below, the results from the upper 5000 m of the SG-3 borehole are presented in a generalized form. The presentation refers to the five major depth intervals (I-V) introduced earlier. These intervals corresponds more or less to individual stratigraphical suites (Table 3-1), excluding the Luchlompolsky fault zone, which is distinguished by its extent and overall unique characteristics.

Interval V, 9-1059 m

This interval is comprised of tholeiite and picrite-basalt volcanite of the Matertinskaya suite, which is metamorphosed into prehnite-pumpellyite facies. Heterogeneous composition and a high percentage of pyroclasites (about 20%) result in large variations in density (2.74-3.24 g/cm^3), P-wave velocity (6300-6900 m/s from acoustic log; 6240-6810 m/s from core samples) and compressive strength (130-260 MPa). Pyroclastic sections of the interval exhibit fracturing of the borehole walls, although the nominal borehole geometry is maintained and not altered by breakouts.

Exogenic fracturing is apparent down to a depth of 800 m. This coincides with an hydrogeological zone characterized by regional, subsurface run-off. A further subdivision of this zone from fracture mineralogical considerations yields:

Subzone A	Open exogenic, non-mineralized fractures	0-150 m
Subzone B	Secondary cementation of fractures	150-200 m
Subzone C	Secondary leaching of fractures	200-800 m

Subzone A is characterized by variable geothermal gradient, intense fracturing and a hydraulic conductivity of the order of $2 \cdot 10^{-6}$ to $6 \cdot 10^{-6}$ m/s. The groundwater is of fresh or ultrafresh character, and has a mineral content of 0.04-0.4 g/l (calcium hydrocarbonate composition). It is saturated with oxygen and nitrogen.

Subzone B is characterized by carbonate-filled fractures, a high geothermal gradient (5-10 K/km) and a decreasing hydraulic conductivity (from $1 \cdot 10^{-5}$-$1 \cdot 10^{-7}$ m/s).

Subzone C is characterized by partial leaching of the fractures, resulting in complete dissolution of carbonates. Quartz is transformed into an euhedral mass of crystals filling the cavities. The geothermal gradient is uniform over the interval (10.5-11.4 K/km) and the hydraulic conductivity is low ($4 \cdot 10^{-7}$-$1 \cdot 10^{-8}$ m/s). Water-bearing sections coincide with fracture zones. The width of these zones ranges from less than 1 m to 10 or occasionally 20 m.

Hydrochemically the zone is dominated by calcium carbonate. The total mineralization very rarely exceeds 0.5 g/l. Calcium sulphide (up to 2 g/l) and

calcium-sulphide-magnesium waters occur within intervals with sulphide mineralization. The lower part of the subzone contains calcium-sodium-hydrocarbonate-chloride water (up to 0.8-0.9 g/l) carrying methane. This indicates inflow of brines into the section.

Analyses of gas samples from the interval 800-900 m in exploration holes showed that this horizon is characterized by a predominance of nitrogen (34-78 rel. %), oxygen (6-30 rel.%) and, more seldom, methane (0.2-0.1; 30-50 rel. %) over other gases.

Below 800 m, the surface run-off groundwater regime is replaced by a transition zone with partial generation. Here, the hydraulic conductivity decreases to $3\text{-}6 \cdot 10^{-10}$ m/s. The water-bearing sections are concentrated to tectonic faults. The gas content is dominated by methane (15-75 rel. %), hydrogen (3-34 rel. %) and helium (up to 5 rel. %). Oxygen is practically absent. The geothermal gradient and heat flow increase (12.3-13.2 K/km and 1.2 mW/m^2 respectively).

Interval IV, 1059-2805 m

This interval corresponds to the tuffaceous-sedimentary Zhdanovskaya suite, which to 40 % consists of basite and basite-hyperbasite intrusions. There is a transition from a prehnite-pumpellyite to greenschist metamorphic facies. Sharp alterations in rock composition are reflected by considerable variation of rock properties. Density ranges from 2.65 g/cm^3 to 3.36 g/cm^3, compressive strength from 80 MPa to 260 MPa. P-wave velocities are 5800-7000 m/s as obtained from acoustic logging, and 5630-6670 in core samples.

Concordant tectonic faults are abundant. They tend to be located in the contacts between magmatic and tuffaceous rocks. The largest ones are found in the lower part of the interval, at the boundary between volcanogenic units, and also in the central part of a lower contact zone of a big basite-hyperbasite intrusion.

The interval is characterized by relatively extensive caving of the holes walls, resulting in an oversized and irregular cross section (Fig. 3-6). Progressive caving was observed in connection with fault zones. In these sections, the actual hydraulic pressure exceeds the hydrostatic pressure by 40%. The hydraulic conductivity is $2 \cdot 10^{-10}$ m/s. The interval is also characterized by a gradual increase in reducing conditions. The water composition is alkaline and dominated by calcium-sodium-chloride mineralizations. High contents of Ra, Sr, Br, B, K, Rb, Cu, Pb and As are also found. The total mineralization ranges up to 60 g/l. The largest gas anomalies (methane, hydrogen, helium) tend to be located to water-bearing sections.

The alterations in rock composition and the presence of tectonic zones with water-bearing sections reflects an extremely non-uniform and partly anomalous thermal

field. Anomalies are connected to water-bearing sections. Ranges of variation for thermal conductivity, geothermal gradient and heat flow are 2.53-4.55 W/mK, 8.8-19.5 K/km and 28-66 mW/m^2 respectively. At a depth of 2700-2800 m, a distinct minimum of the geothermal gradient (8.0 K/km) was observed. The interval between 2800 m and 2900 m represents a transition zone to more uniform thermal conditions at greater depths (Fig. 3-7).

Interval III, 2805-4400 m

This stratigraphic interval consists of tholeiite volcanics in greenschist metamorphic facies, transformed into metadiabase and minor portions (3%) of tuffaceous sedimentary rock. The massive and homogeneous metabasite exhibits compressive strength values up to 270 MPa. The density averages 3.02 g/cm^3. Ranges of the P-wave velocity, observed by acoustic logging and on core samples, were 6400-7000 m/s and 6150-6680 m/s respectively. These values are very similar to results obtained from VSP-surveys (Fig. 3-4).

Borehole walls do not tend to cave, and the cross-sectional hole geometry generally remains circular. The rock is not fractured, except in tuffaceous sections where minor fracturing was observed. As a consequence, the rock is more or less impermeable, which limits the downwards infiltration of surface water. In fracture-free sections, the coefficient of permeability is $25 \cdot 10^{-15}$ m^2, which is half or third the fracture permeability.

Thermal conditions are homogeneous over the interval. The thermal conductivity decreases gradually with depth, from 3.5 W/mK to 3.1 W/mK. A corresponding increase is observed in the geothermal gradient - from 15.0 to 17.6 K/km. The heat flow remains rather constant at 52 ± 2 mW/m^2. Thus, heat transfer in the rock is highly governed by conduction, which is proved by extremely little heat generation in the rock, about 0.12m W/m^3 [1:5]. Minor heat-flow anomalies, related to interlayers of tuffaceous rock, were observed in sections 3400-3500 m, 3700-3800 m and 4100-4200 m.

Interval II, 4400-5100 m

This interval combines ultrabasic volcanite schist from the base of the Zapolyarninsky suite, carbonate-sandstone rock of the Luchlompolsky suite, schist from the upper Pirttiyarvinsky suite and an intrusive body of andesite-dacite porphyrite in the contact between the Luchlompolsky- and Zapolyarninsky suites. The interval encompasses the Luchlompolsky fault zone, within which rock characteristics are highly influenced by the tectonic impact. Within the fault zone, almost all rock is transformed to different types of schist, blastocataclasite and blastomylonite. The greenschist metamorphic facies are replaced by epidote-amphibolite facies.

The density ranges from 2.66 g/cm^3 to 3.10 g/cm^3, and the compressive strength is 20-200 MPa. The total porosity attains values up to 2.7%, to be compared with 0.5% for the interval down to 4500 m. P-wave velocities are 4030-5380 m/s and 5600-6000 m/s, values representing core sample determinations and acoustic logging respectively.

In the uppermost part of the interval, the hydraulic zone characterized by transition and partial generation is replaced by a zone of generation of deep water, which persists to much larger depths. A water-bearing section, containing several small zones, is located at 4565-4925 m. It's conductivity is very low ($6 \cdot 10^{-11}$ m/s) and the hydraulic pressure exceeds the hydrostatic head by a factor of 1.5. Water inflow was observed when penetrating the section. Waters are characterized by chlorine concentrations up to 710 mg/l, and pH 8.0-8.5. Concentrations of other constituents found rank as follows: K > Br > Y > B > F > Pb. Helium occurs in significant amounts (0.007-0.023 cm^3/l).

Heat flow within the interval is as high as 73-79 mW/m^2, which is 1.5 times higher than in the overlying interval. In addition to hydrogeological factors, conductive heat inflow from deeper levels, facilitated by the high thermal conductivity within the interval, may contribute to the anomalously high heat flow. In comparison with its surroundings, the interval is also characterized by a higher thermal capacity, which promotes local heating and contributes to the heat transfer process.

The section of borehole SG-3 discussed above, i.e. the horizon down to 5100 m, is underlain by volcanogenic and sedimentary rocks belonging to the Luostarinsky series and granite-gneissic formations of the Kola series of the Pechenga complex. These rocks are altered into epidote-amphibolite facies (5100-6840 m). Characteristics are further discussed in a monograph on borehole SG-3 [1:12].

4 THE KRIVOY ROG SUPERDEEP BOREHOLE

4.1 GEOLOGICAL AND TECTONIC SETTING

A wide range of formations are present in the Ukrainian Shield, which was formed over a long period geological time, from the upper Archaean (3600 Ma) to the Lower Proterozoiceon (1200-1300 Ma), representing a variety of thermodynamic regimes. Most of the rocks are altered into greenschist to eclogitic facies.

Fig. 4-1 shows a tectonic map of the Ukrainian Shield. Three megablocks are found within the shield - the Volyno-Podolsky (Western) block, the Central-Ukrainian (Central) block and the Preazovsky (Eastern) block. These blocks are bordered by transregional tectonic zones - the Golovanevsky- and Orekhovo-Pavlogradsky zones. The Krivoy Rog borehole (SG-8) is located in the Central megablock. This block is subdivided by regional faults (The Vradievsky, Pervomaisky, Central and Tarapakovsky faults), delineating a group of smaller blocks - the Gaivoronsky, Bratsky, Kirovogradsky and Predneprovsky blocks (Figs. 4-2, 4-3).

The Krivoy Rog Kremenchug structure (Krivbass) was formed in the western flank of the Predneprovsky block, at the beginning of Upper Proterozoiceon (2400 Ma). The Krivoy Rog series were deposited in an asymmetric riftogenic depression. The series includes basic volcanitic, detrital clastic, ferruginous-siliceous, hydrocarbon, flyschoid and molassic formations, which have been metamorphosed (1800-2000 Ma) into amphibolites, polymict and oligomic metaconglomerates, arkoses, phyllites, magnetite schists, jaspilites, graphitic schists, apopsaminitic schists and polymictic metaconglomerates. Iron enrichment led to the formation of metamorphogenic iron ore deposits.

Subduction of the Predneprovsky and Kirovogradsky blocks induced fracturing and steep faulting, together with extensive formation of metasomatic and anatectic granites of the Kirovograd-Zhitomirsky complex (1800-2000 Ma). The process also involved penetration of intrusive bodies of gabbro and monzonite (1700 Ma) and diabase dykes (1200-1300 Ma). Shear stresses developing at the interface between the subducting Archaean blocks caused formation of almost symmetrical thrusts, accompanied by steeply dipping, secondary structures, shear fractures, cleavage zones and plication. The thrusts dip 60-90° down to 2000 m depth, and then flatten at greater depths. Krivbass is an underthrust-overthrust structure, formed in the zone of the Tarapakovsky deep thrust. Its underthrust part is represented by the Saksagan monocline, built up of rocks belonging to the Krivoy Rog series. The overthrust part is represented by the Annovsky syncline, which consists of formations of the Ingulo-Ingulets series. Archean plagiogranitoids constitute the basement for both structures.

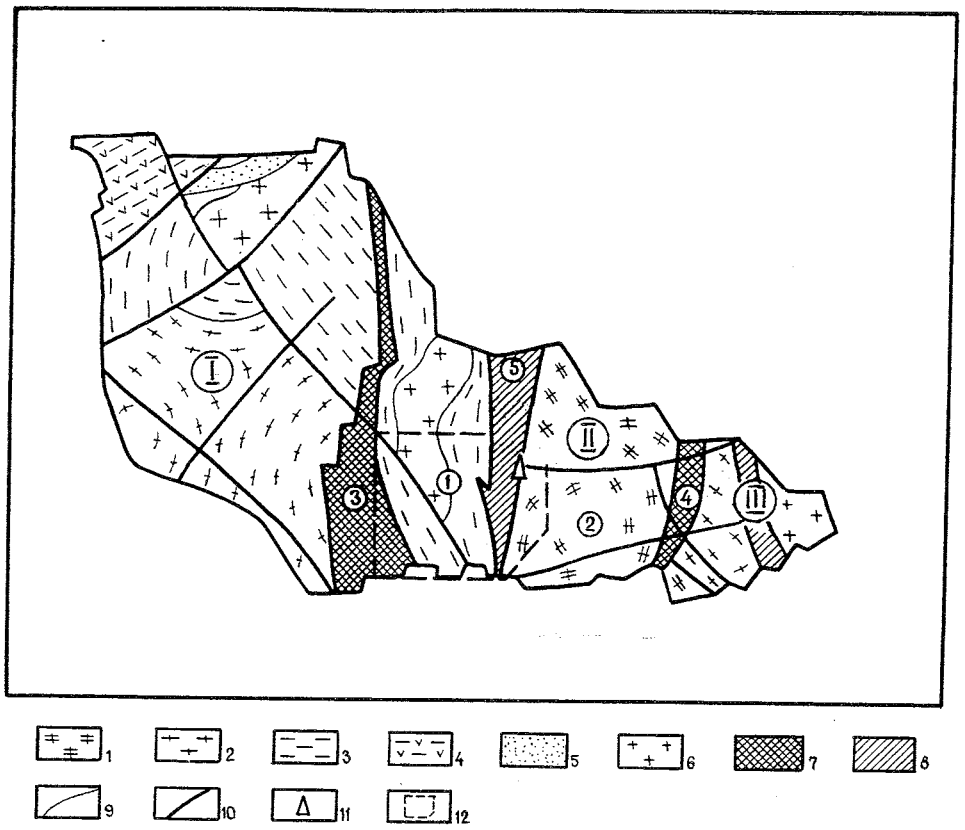

Fig. 4-1. Tectonic map of the Ukrainian Shield.

Legend

I The Volyno-Podolsky megablock (western part)
II The central Ukrainian megablock (central part)
- 1 The Kirovogradsky block
- 2 The Predneprovsky block
- 3 The Golovanev block
- 4 The Orekhov-Pavlograd sutural zone
- 5 The West-Ingulets sutural zone

III The Preazovsky megablock (eastern part)

---

1 Archean gneissic and granitic-gneissic rocks, partly altered in the lower Archean.
2 Archean gneissic, granitic-gneissic and granulitic rocks, altered during the Svecofennic-Karelian folding.
3 Upper Karelian metamorphosed sedimentary and volcanogenic series
4 Volyn (gothic) volcanogenic series
5 Platform rocks affected by Dalslandian deformations
6 Gothic granitoids
7 Zones dividing megablocks
8 Intrablock zones
9 Geological boundaries
10 Large faults
11 The Krivoy Rog borehole (SG-8)
12 Outline of detailed geological map cf. Fig. 4-2

Legend to Figs. 4-2 and 4-3.

Archaean (AR)

1 Dneprovsko-Bugskaya, Aulskaya and Konsko- Verkhovtsevskaya series, gneisses, quartzite, schist ultrabasite, amphibolite and iron formation.

2 Dnepropetrovsky and Sursko-Tokovsky complexes, plagiogranite and shadow plagiogranite, diorite, microcline-plagioclasic granites

Archaean-Lower Proterozoic ($AR\text{-}PR_1$)

3 Bugskaya series, gneisses interlayered by amphibolite

Lower Proterozoic (PR_1)

4 Krivoy Rog series (PR_1k), amphibolite, apoporphyrite, apoaleurite, apopsammite and graphite schist, marble, conglomerates and iron bearing formation.

5 Ingulo.Inguletskaya series (PR_1ii), amphibolite, magnetite quartzite, gneisses, marble.

6 Kirovogradsky-Zhitomirsky complex (PR_1kz), granite, monozonite

Korostyshevsky complex

7 Rapakivi granite

8 Gabbro, pyroxenite

Upper Proterozoic (PR_2)

9 Diabase dykes

10 Boundaries a. Geological units b: Lithosphere zones

11 Major overthrusts (1. Tarapakovsky, 2: Central, 3: Pervomaisky, 4: Vradievsky)

12 Tectonic disturbances

13 Tectonic blocks (1: Predneprovsky, 2: Kirovogradsky, 3: Volyno-Podolsky)

14 Estimated direction of rock block movement

15 The Krivoy Rog Borehole

16 Location of the "Granite" seismic profile

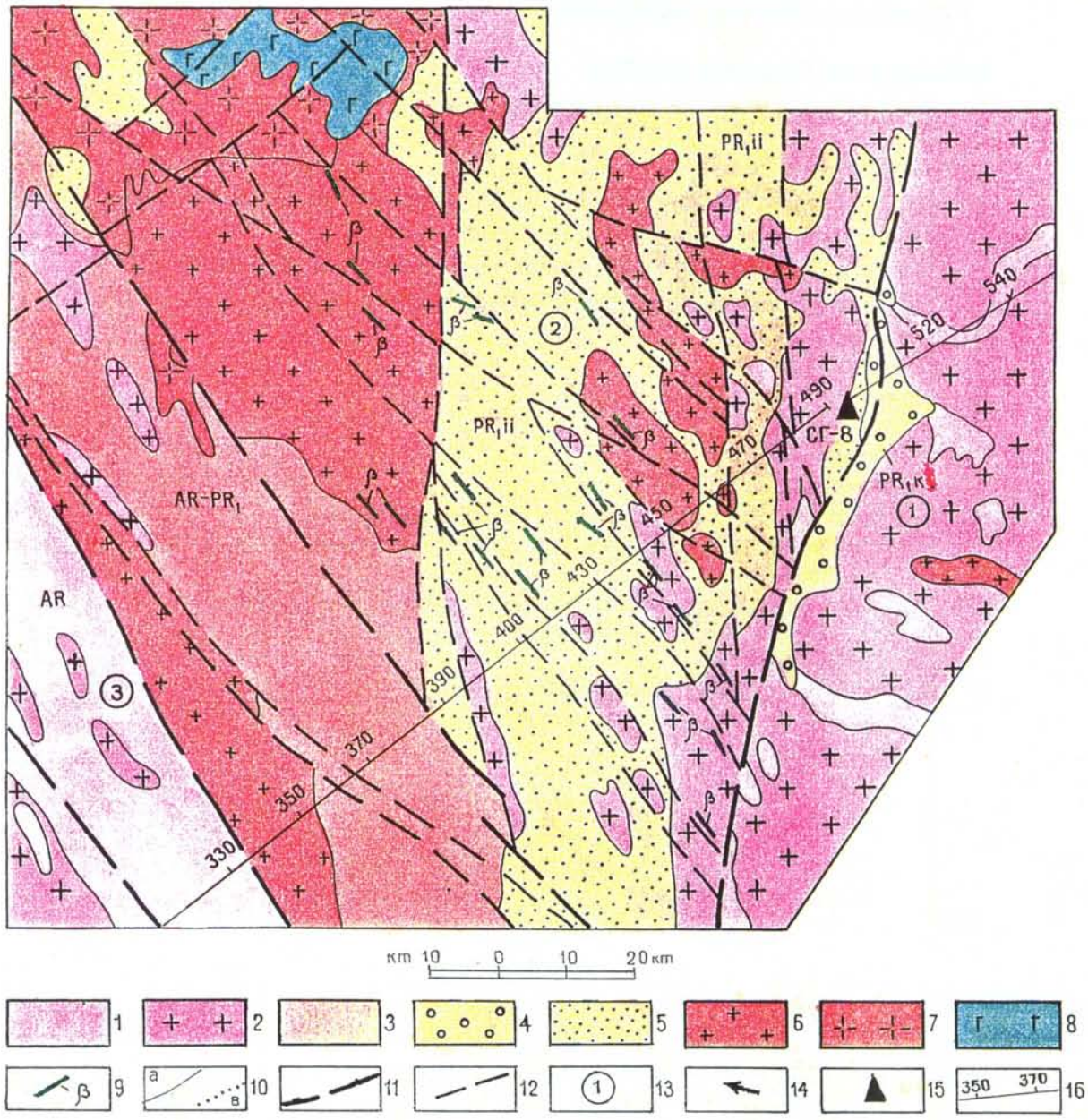

Fig. 4-2. *General geological map of the junction area between the Volyno-Podolsky, Kirovogradsky and Predneprovsky blocks of the Central part of the Ukrainian Shield.*

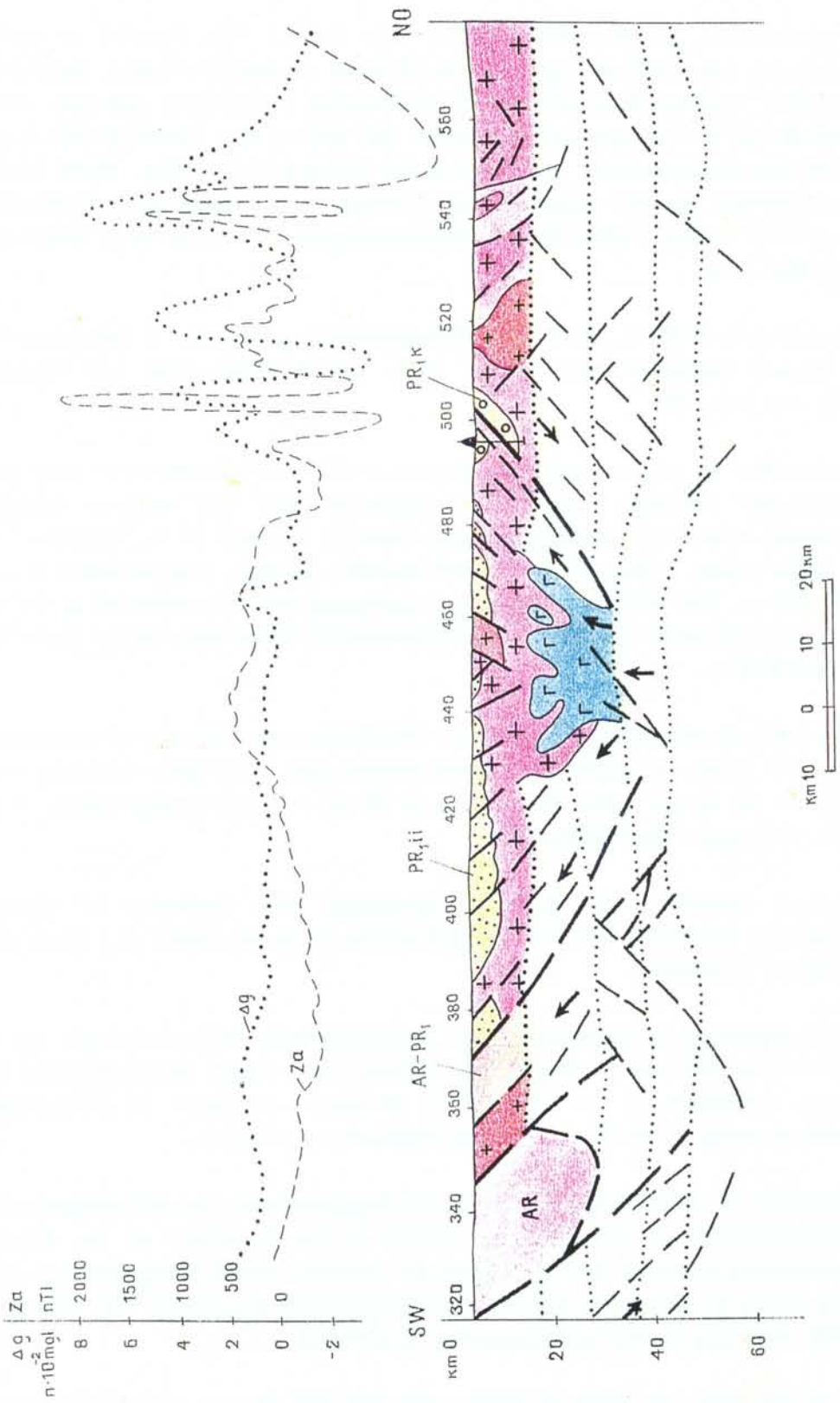

Fig. 4-3. *Geological and geophysical section along the Central part of the "Granite" geotraverse.*

Investigations, including the Krivbass hole (No 22 350, Fig.4-4) as well as other boreholes, identified the Saksagan and Eastern concordant thrusts, located along the boundary between hard and brittle iron-bearing formations, and very ductile talc-amphibolite and biotite-graphitic schist. The Krivoy Rog borehole (SG-8) penetrates numerous displacements, connected to the Tarapakovsky thrust. These structures are characterized by the formation of fracture zones, cataclase, mylonization and sections of intense plastic deformation accompanied by plication of metamorphic and granitoid rock.

To the north of SG-8, the Krivoy Rog-Kremenchug structure is intersected by a zone of closely spaced tectonic faults, with sublatitudinal strike and dipping 70-90° (Fig. 4-4 and 4-5).

If classified by origin, fractures observed in Krivbass fall into three main categories; weathering fractures, fractures in magmatic rock and tectonic fractures. The thickness of surficial weathering varies between 5 m and 30 m. The lower boundary of linear crusts, which coincides with tectonic faulting, extends down to a depth of 130-200 m. The influence of exogenic processes which is reflected in the formation of branch fractures and reduction of intermineral links, were traced down to a depth of 500-600 m.

Near-vertical, diabase dykes of Upper Proterozoic age intersect all metamorphic and granitoid rocks, and form a belt in the central part of the Kirovogradsky block. The width of the dykes varies from 0.3 m to 30-50 m. They contain sparse, 0.1-0-5 cm wide, carbonate-filled fractures.

Tectonic fractures and alteration, connected with formation of plicative and disjunctive structures, are predominant within the entire region as a result of its long history of evolution.

Initial fracturing of plagiogranite and plagiomigmatite with an isotopic age of 2800-3150 Ma is difficult to characterize, because these rocks suffered intense alteration during formation of the Proterozoic structures composed of metamorphic and granitoid rocks of the Kirovogradsky-Zhitomirsky complex.

Formation of 200-600 m wide zones of blastomylonite and blastocataclasite in the plagiogranitoids of the Ingulets massif at the boundary of the Krivoy Rog-Kremenchug structure (and penetrated by borehole SG-8) corresponds to one of the early stages of formation of the Upper Proterozoic structures. The isotopic age of blastic minerals (biotite and muscovite) is 1970 Ma.

Blastocataclasite and blastomylonite were probably formed under conditions of one-side compression, when the Kirovogradsky block was overthrusting the western part of the Predneprovsky block.

Legend to Figs. 4-4 and 4-5.

Lower Proterozoic (PR_1)

1 *Gleevatskaya suite* (PR_1-gl), polymict conglomerates, apopsammite, apoaleurite and amphibole-biotite schist.

2 The Ingulo-Inguletskaya series (PR_1-ii), gneisses, schist marble, calciphyre, quartzites, magnetite, amphibolite.

3 The Krivoy Rog series (PR_1-k), greenschist and silicate schist, marble, iron formation, jaspilite, iron ore, arkose, phyllite, amphibolite.

4 The Kirovogradsky-Zhitomirsky complex (PR_1-kz), granite, aplite pegmatite.

Upper Archean (AR_2)

5 The Sursko-Tokovsky complex (AR_2-st),Plagiogranite and plagiomigmatite

6 Geological boundaries (a: Between complexes, series and suites, b: Between different lithotypes within complexes, series and suites).

Ruptured tectonic disturbances

7 The Tarapakovsky regional overthrust zone (250-350 m thick)

8 Disturbed tectonic zones, >50 m wide

9 Disturbed tectonic zone, <50 m wide

10 Disturbances within the Predneprovsky block

11 Location of the Krivoy Rog borehole

12 Other boreholes in the area

13 A-B; seismic profile

14 Borehole intervals with <7 fractures/m

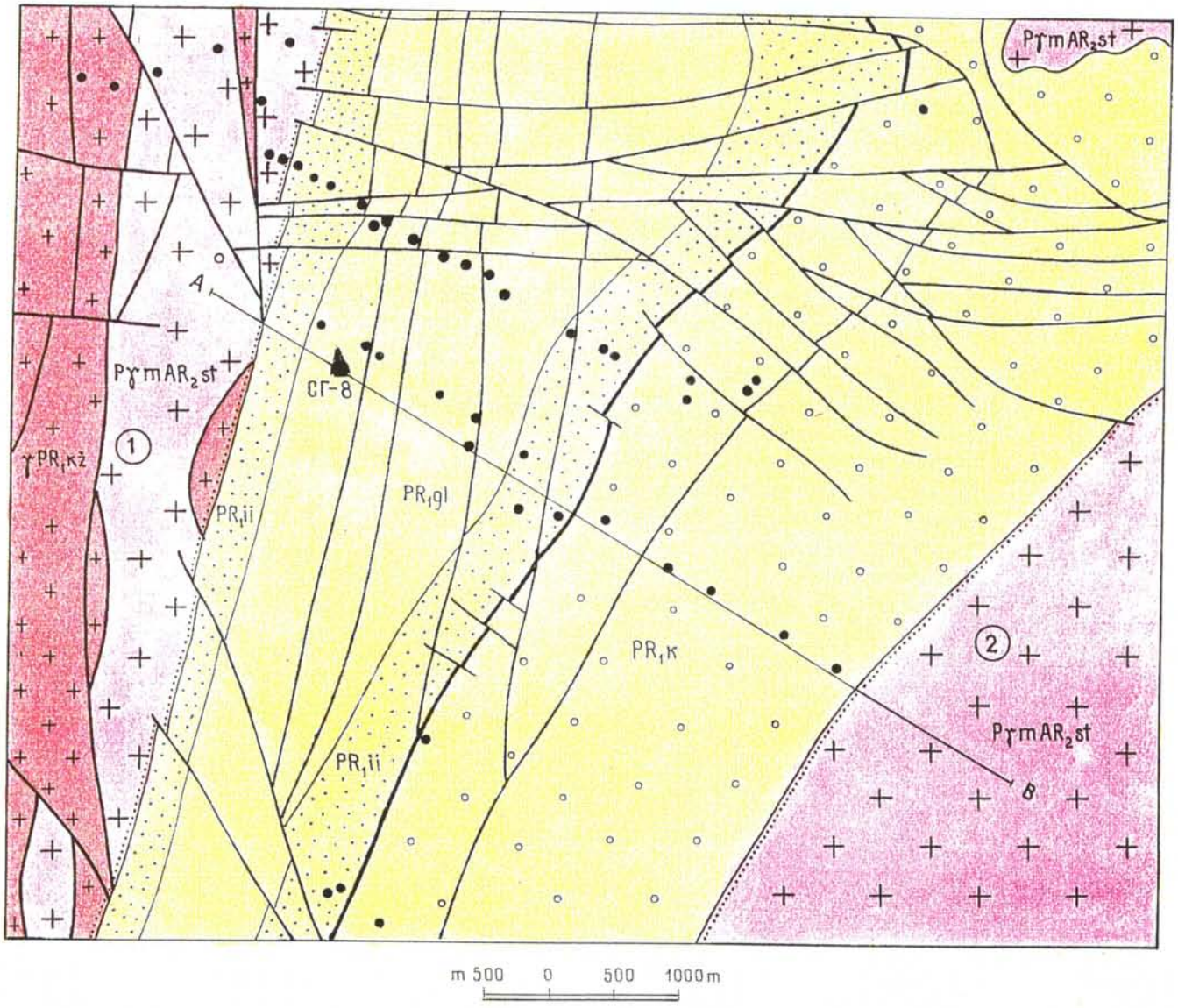

Fig. 4-4. Geological map of the central part of the Krivoy Rog-Kremenchug structure.

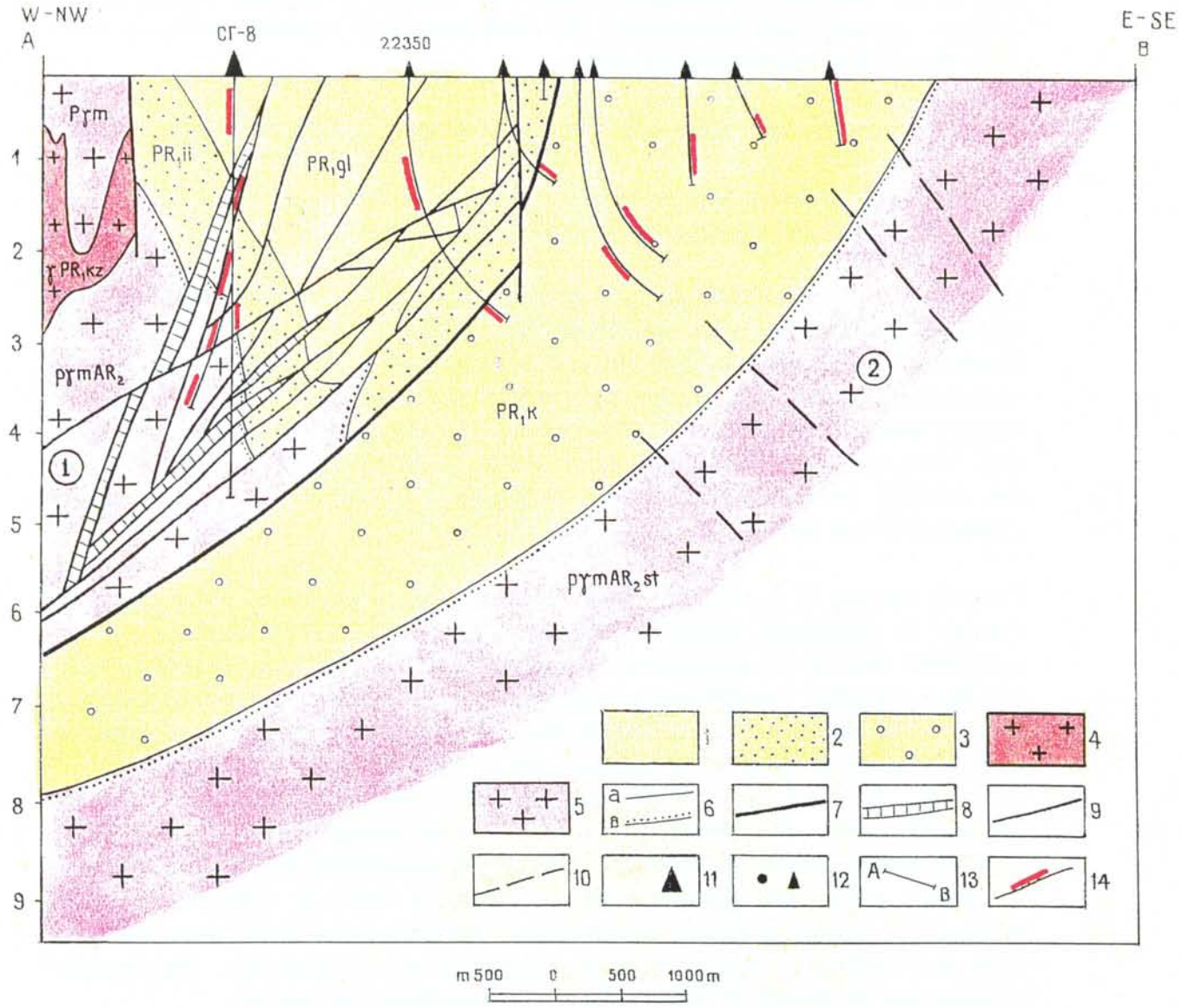

Fig. 4-5. *Geological section of the Krivoy Rog Superdeep borehole (SG-8) area.*

Original minerals in the plagiogranitoid rock are severely deformed and transformed into a blastic mass of quartz and muscovite. Crushing also took place in the lower part of the overlying metamorphic rock. With respect to physical properties like strength, porosity and permeability, the blastocataclasite mylonite does not differ from the original plagiogranitoid rocks.

In Krivbass and adjacent areas, two subtypes of tectonic fracture are distinguished:

1) Fractures connected with formation of plicative textures
2) Fractures accompanying tectonic faulting

Subtype 1) is a form of cleavage, and occurs in very hard and brittle, deformed beds of magnetite quartzite and jaspilite of the Saksagansky and Artemovsky suites. Observations in boreholes and excavations show that there is one system of concordant slip cleavage, and an other system of shear cleavage. The two systems forms a mutual angle of 40-45°, and subdivide the rock mass into blocks of variable size - from microscopic (in curves and folds) to 2-3 m (at the limbs). About 80% of the fractures are filled with quartz, carbonate, chlorite, and lamellar hematite ("micaceous iron ore").

Fracture subtype 2) is predominant in Krivbass. The formation of this category of fracture is genetically related to tectonic faulting and block displacements in monolithic rock. It is characterized by simple and, more often, complex extension and shear fractures, corresponding to the regional orientation of thrust and strike-slip faulting. The intensity of fracturing and the thickness of the fractured zones depends on the intensity of the tectonic process, and on the deformational characteristics of the rock. In hard and brittle rock with a Poisson's ratio of 0.15-0.21 (plagiogranitoids, iron-bearing formations, quartzite-sandstones, metaconglomerates) brittle deformation prevails, resulting in extensional and shear fracturing. In silicate schist and gneisses with a Poisson's ratio of 0.25-0.38, ductile deformation forms fine folding and plication. The orientation of the axial planes of folds and bedding coincides with the orientation of displacement. The fracture classification by Nevsky [2:14] is accepted for quantitative evaluation.

Most fractures, up to 75-80% of those observed in boreholes SG-8, No. 22 350 and others, are filled with quartz, calcite, dolomite, chlorite and sericite. Fracture filling found in plagiogranitoids are primarily quartz, calcite and dolomite. In crushed plagiogranitoids, albite is formed under the influence of tectonic processes. Biotite is mostly replaced by chlorite, sagenite and flake muscovite with and isotopic age of 1700-1800 Ma.

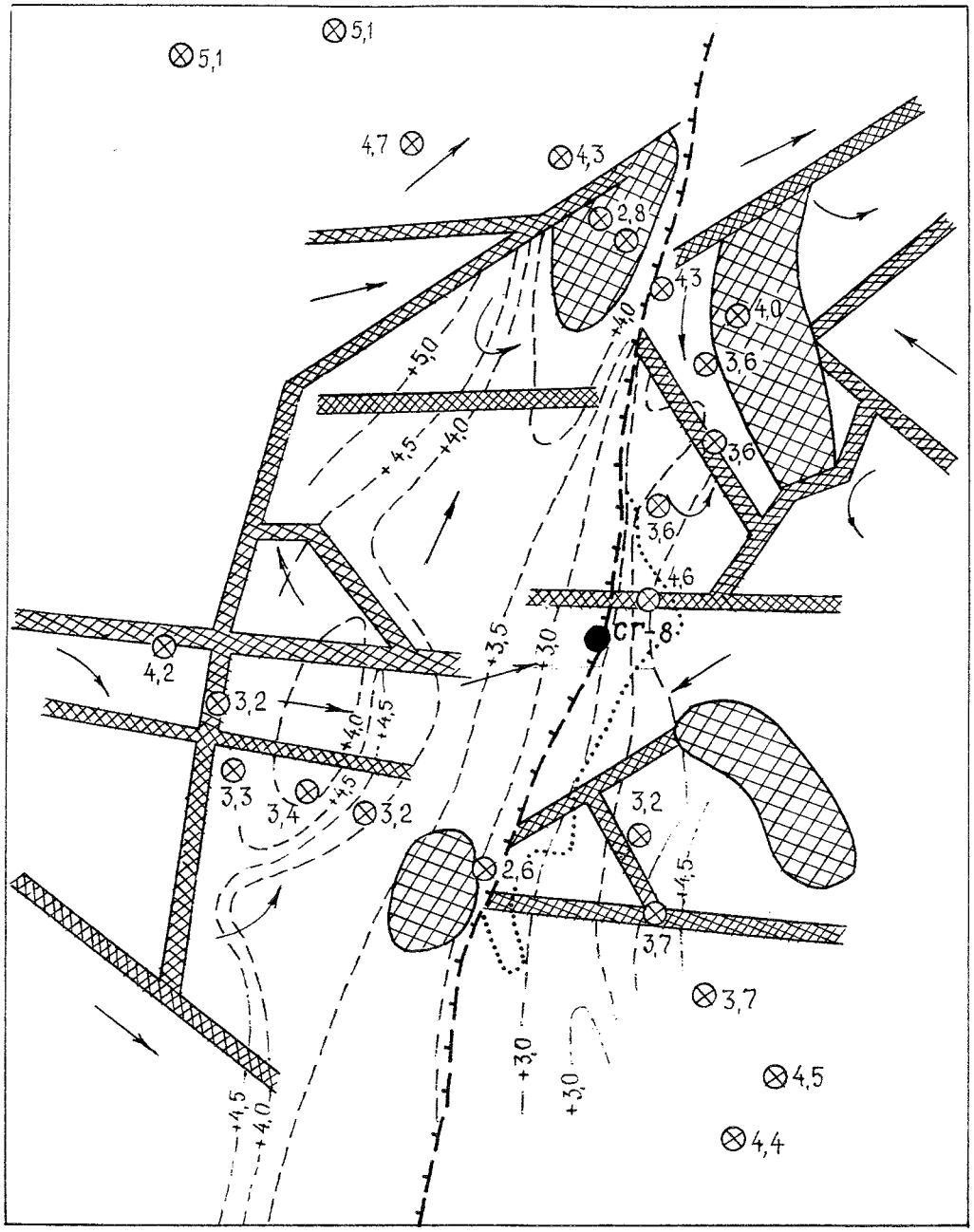

Fig. 4-6. *Results from geodetic measurements of block movements in the Krivoy Rog area.*

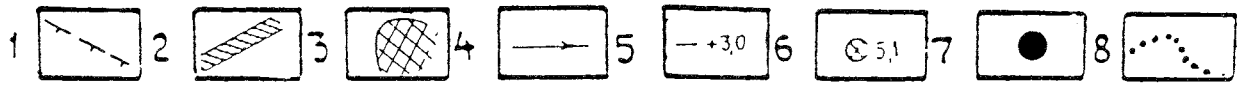

Legend

1 The Tarapakovsky regional overthrust
2 Fault zones
3 Zones of extension
4 Direction of horizontal movements
5 Isolines of block movements in mm/year
6 Horizontal velocities of block movements in mm/year
7 The Krivoy Rog borehole
8 Outline of the Krivoy Rog structure

Geodynamic investigations, conducted at Krivoy Rog during the period 1965-1975 using a method of repeated levelling, revealed horizontal and vertical movements of the Kirovogradsky and Predneprovsky blocks at rates of 2.5-5.1 mm/year (Fig. 4-6). The SG-8 borehole is located at the boundary between these blocks, where results indicate differential horizontal movements between the blocks (relative compression and shear, Fig. 4-6). These relative movements contribute to reactivation of the Tarapakovsky, Saksagansky and Eastern thrusts and their feather structures. This is indicated by the presence of open sub-parallel fractures in each tectonic zone, as noted especially in SG-8 (3620-3700 m and 3760-3850 m) and hole 22350 (2600-2700 m). Here, perfect slickensides and parallel grooves were observed on the fracture surfaces. These fractures intersect both the intact rock and older, filled fractures. Fractures caused by reactivation often have a thin coating (0.03-0.12 mm) of chlorite and hydromica. There is no such coating on artificial fractures, rock fragments or rupture surfaces from core-discing, occurring when drilling through intervals with high rock stresses.

General characteristics of faults, fracture zones and related fractures, alterations and minerals, as observed in boreholes SG-8 and 22 500 are given in Table 4-1. An example of a large-scale structure, as interpreted from geophysical logging data, in one of the tectonic zones (3620-3700 m) is given in Figure 4-9.

4.2 RESULTS FROM BOREHOLE INVESTIGATIONS

4.2.1 **Rock types, physical properties and fracturing**

The main geological characteristics of rock types within intervals subjected to deformation and associated formation of fractures and other tectonic features are given in Table 4-1 and Fig. 4-7 and 4-8. Table 4-2 presents petrophysical and mechanical parameters. The values given are averages, determined from data sets varying between 16 to 400 samples,and representing groups of similar rock types. Values representing individual samples are given in Fig. 4-8 and Table 4-3 for the parameters thermal conductivity and permeability respectively. Some of the physical parameters were derived on the basis of measurements of apparent resistivity (ρ), P-wave velocity (Vp) and bulk density (δ). The latter parameter was determined for the pilot hole only (depth 3551 m, diameter 215.9 cm).

The large number of fracture zones encountered is probably connected with the location of borehole SG-8, close to the Tarapakovsky transregional thrust. Boreholes No. 22 350 and 19929 intersected the thrust in its dip direction - and other boreholes in the direction of its strike. Borehole SG-8 is expected to intersect the thrust in the interval 4800-5200 m.

Analysis of the data shows that the frequency of feather fracture zones increases with proximity to the Tarapakovsky thrust. Their width, however, remains constant at 20-70 m. The upper zone, with a true width of 150 m (interval 870-1270 m),is an apparent exception, but is actually composed of three, 10-30 m wide neighboring zones, separated by two intervals of slightly deformed rock. In Figure 4-5, this is illustrated as single fracture zone, with a dip of 70-75°.

Tables 4-2, 4-4 and Fig. 4-7 and 4-8 show that the physical and mechanical properties (density, porosity, permeability, electrical resistivity, P-wave velocity, strength) within the fracture zones differ from those of intervals with undisturbed rock.

Increased porosity and permeability, and decreased density are directly correlated with fracture frequency, status of fracture filling and deformation of the basic rock minerals. For the identified fracture zones, the fracture frequency decreases below 400 m depth. However, a slight increase was noted within the zone of the Tarapakovsky thrust, as mapped in borehole 22 350. The degree of fracture filling remains constant at 70-85% except in two zones (3620-3700 m and 3760-3850 m) where it is approximately 60%.

The deformation of minerals within the zones is seen as wedging lamellae of biotite, chlorite, muscovite and amphibolite prisms, crushed garnet, andalusite and alunite. The aggregates formed have spiral shapes, microplicated tabular minerals in

association with microfolds, displacement of plagioclase twins and intense formation of Boehm Lamellae in quartz with typical and distinct gas inclusions. These alterations contribute to an increase in porosity and permeability.

Data shown in Fig. 4-7 and Table 4-2 indicate that the porosity of the undisturbed rock is generally low. In schist, it ranges from 0.45% to 1.2%, and in plagiogranitoids from 1.2% to 1.38%. On all hypsometric levels in fracture zones, porosity is enhanced by a factor of 2-6, reaching a maximum value of 5.3-7.43% in plagiogranitoids. The porosity is strongly dependent on fracture frequency and status of fracture filling.

Itabirite constitutes a considerable part of the metamorphic formations. Despite a massive texture of quartz and quartz-silicate-magnetite interlayers, it has a higher porosity than the other rock types. In unchanged varieties of this rock type, porosity averages 2.16%, and in the zone of hypergenesis (down to 500-600 m) it goes up to 6-8% due to leaching of silicate and carbonate and oxidation of magnetite. In heavily fractured zones (borehole 22 350) the porosity is 12-14%. This is caused by the presence of intense cleavage and shear fracturing, especially within intervals with steeply dipping bodies down to a depth of 2000-2500 m, where numerous drag folds and S-shaped fractures are found. The flattening of the iron formations with depth is accompanied by decreased drag folding which, in turn, results in a decrease of the porosity to 2-4%.

Permeability values of the plagiogranitoids are as follows:

Monolithic rock	$0.5\text{-}3.9 \cdot 10^{-15}$ m^2
Fracture zones	
medium fracturing	$8.9\text{-}65 \cdot 10^{-15}$ m^2
intense fracturing	$230 \cdot 10^{-15}$ m^2

Maximum permeability and porosity were recorded in tectonic zones at 3620-3700 m and 3760-3850 m. The highest frequency of open fractures, intense mineral deformation and frequent slickensides and the most pronounced caving were also observed at these intervals. The caving cannot be readily explained, but it may be related to the fact that the lithostatic pressure at 3500-4000 m (140-150 MPa) exceeds the compressive strength of the rock (120-130 MPa).

Table 4-1. Characterization of tectonic fractures in the area of the Krivoy Rog borehole.

No	Interval of fracture zone m	Rock subjected to tectonic deformations	Group of fracture zones	Fracture fillings		Type, morphology, and indications of tectonic deformation	Dip vz horizon of (deg.)		Thickness of tectonic zones (groups of zones in borehole), m	Extent, km		Order and type of faults	Identification method
				V, %	Vein material, typical alterations of minerals		Fractures	Tectonic zone		Vertical	Lateral		
SG-8													
1	870-1270	Metaconglomerates, apopsammite and apoaleurolite quartz-biotite schists	1	85	Chlorite, sericite, carbonate, quartz. Thickness from 0.1 to 6 mm	Shear fractures, ruptures; sections of ladder and net venation within three convergent displacements	15-20 40-80	70	400	1.5	10	III-local convergent group of displacement	Ground seismics, logging, cores
2	1650-1815	Quartz-biotite, graphite- schist, marble, itabirites	1	80	Chlorite, sericite, graphite, carbonate, pyrite (up to 3%)	Shear fractures, sections of intensive plication, flaggy-ness and cataclase	10-25 35-75	75	165	2.0	11	III-local feather displacement	-"-
3	2015-2058	Chlorite-talc-tremolite-schist	2-3	95	Carbonate, pyrite, pyrrhotite (1.5%)	Rare shear fractures, schistosity, plication	40-80	65	43	2.5	10	-"-	-"-
4	2960-3000	Plagiogranitoid blastocataclasite and blastomylonite subjected to later deformation	1	70	Chlorite, carbonate, quartz, albitization of plagioclase, full replacement of biotite by chlorite and sericite	Shear fractures and ruptures, sections of cataclase with slickensides, the core discing and vertical "peeling" of rock	50-70	25-30	40	5.5	No outcrop	III-local thrust	-"-
5	3410	Blastocataclasite of plagiogranitoids	2	70	Chlorite, carbonate, quartz; area of full dis-placement of biotite by muscovite and chlorite	Shear fractures, fractures of later origin with slickensides	60-70	50	80	5.5	10-12	III-local feather displacement	-"-
6	3620-3700	Plagiogranitoid trondhjemite blastoclasite and blastomylonite subjected to later deformations	1	60	Carbonate, quartz, chlorite, albitization of plagioclase, full replacement of biotite by muscovite and chlorite	Shear fractures and ruptures, sections of cataclase, open shear fractures of later origin with rectilinear configuration, wedge-shaped fragments of clastic rocks, slickensides, inten-sive "peeling" of rock, core discing with a sperical shape of rupture perpendicular to the core axis	30-40	40	30	5.0	No outcrop	-"-	-"-

Table 4-1. Continued

No	Interval of fracture zone m	Rock subjected to tectonic deformations	Group of fracture zones	Fracture fillings		Type, morphology, and indications of tectonic deformation	Dip vz horizon of (deg.)		Thickness of tectonic zones (groups of zones in borehole), m	Extent, km		Order and type of faults	Identification method
				V, %	Vein material, typical alterations of minerals		Fractures	Tectonic zone		Vertical	Lateral		
SG-8													
7	3760-3850	Plagiogranitoid blastocataclasite and blastomylonite subjected to later deformantions	1	60	Carbonate, quartz, chlorite, muscovite, albitization of plagiclase, full replacement of chlorite and sericite by biotite	Type, morphology of fractures and tectonic zones are identical to the ones in the adjacent upper interval of 3620-3700 m.	40-50	35-40	90	6.0	No outcrop	III-local feather displacement	Ground seismics, logging, cores
8	4060-4096	Crushed blastomylonite of plagiogranitoids	2-3	65-70	Carbonate, quartz, partial replacement of biotite by chlorite	Shear fractures, sections of cataclase of later origin, mylonite seams	45 55-60	35	36	6.0	-"-	-"-	-"-
9	4190-4240	Blastocataclasite, granitoids	2-3	65-70	Carbonate, quartz, chlorite	Shear fractures, individual slickensides	45 80-85	35	50	6.0	-"-	-"-	-"-
10	4304-4344	Crushed plagiogranitoid blastoclasite	2-3	75	Carbonate, quartz, chlorite, pyrite (up to 1%)	Shear fractures, mylonite seams, sections of monolithic rock (up to 1.5-2 m)	30-40 70	35	40	6.0	-"-	-"-	-"-
11	4468-4549	Crushed plagiogranitoid blastomylonite and blastocataclasite	2-3	75-80	Carbonate, quartz, chlorite, pyrite (up to 1%), albitization, biotite seritization	Shear fractures, mylonite seams (up to 5 cm), almost full replacement of biotite by chlorite growth of microcline	35-40 80	30-35	81	6.0	-"-	-"-	-"-
Borehole 22350 ("Sputnik-2")													
12	310-350	Apopsammite amphi-bole-biotite schist (cf SG-8 3410-3490 m)	2	85	Chlorite, sericite, carbonate, pyrite	Shear fractures, net venation, mylonite seams	55-70	55	40	5.5	10-12	III-local feather displacement	Ground seismics logging cores
13	1500-1530	Apopsammite amphibole-biotite gneisses (cf. SG-8 2960-3000 m)	1	75	Chlorite, muscovite, quartz, pyrite, microcline	Shear fractures, ladder veins	50-70	25-30	30	5.5	No outcrop	III-local thrust	-"-

Table 4-1. Continued

No	Interval of fracture zone m	Rock subjected to tectonic deformations	Group of fracture zones	Fracture fillings		Type, morphology, and indications of tectonic deformation	Dip vz horizon of (deg.)		Thickness of tectonic zones (groups of zones in borehole), m	Extent, km		Order and type of faults	Identification method
				V, %	Vein material, typical alterations of minerals		Fractures	Tectonic zone		Vertical	Lateral		
Borehole 22350 ("Sputnik-2")													
14	2020-2070	Graphitic gneisses, quartzite-sandstone, calciphyre, talc-amphibole schist cf. SG-8; 3760-3850, 4466-4549 m	1-2	65	Chlorite, graphite, carbonate, pyrrhotite, quartz, microclinization, formation of apatite and diopside	Complex shear fractures, slickensides, mylonite seams, partial plication	50-70	40	10-50	5.5	No outcrop	III-local feather displacement	Ground seismics, logging, cores
15	2620-2700	Magnetite quartz, graphitic gneisses, actinolite, muscovite-fibrolite schist	1	70-80	Graphite, carbonate, diopside, pyrrhotite, muscovite, pyrite processes are growing in the area of 300 m	Shear fractures, intensive plication, schistosity, thick mylonite seams (up to 1.2-1.5 m)	70-90 45	30-2000	80	6.0	>100	I-transregional thrust	Ground radio survey logging cores
16	3009-3044.6	Biotite and graphitic schist, marble, quartzite (the borehole did not penetrate the tectonic zone)	1	75	Graphite, carbonate, quartz, pyrite, microcline, apatite	Shear fractures, plication, boudinage of quartzite layers, formation of pseudoconglomerates	80 45	45-50	60-100	3.0	>20	II-regional concordant displacement	-"-

Legend to Fig. 4-7.

1 Depth, m
2 Suite, complex
3 Lithological column
4 Rock characterization
5 Fractured zones, see legend Fig. 4-9
6 Resistivity ohmm
7 Neutron-gamma ray log, cps/s
8 Acoustic log, mcs/m
9 Borehole diameter, mm
10 Borehole configuration, ratio between long and short axes
11 Density of core samples, g/cm^3
12 Density from neutron-gamma logging, g/cm^3
13 Velocity of P-waves, from core samples, km/s
14 Velocity of P-waves from acoustic logging, km/s
15 Porosity of core samples, %

Legend to Fig. 4-8.

1 Depth, m
2 Fractured zones, see legend Fig. 4-9.
3 Tensile strength, MPa
4 Compressive strength, MPa
5 Poisson´s ratio
6 Velocity of P-waves parallel to core axis, km/s
7 Velocity of P-waves perpendicular to the core axis, km/s
8 Anisotropy coefficient
9 Stability coefficient
10 Thermal conductivity, W/mK
11 Thermal gradient °C/100 m
12-17 Gas content in flushed fluid in relative percentages
- 12 CO_2
- 13 O_2
- 14 CO
- 15 CH_4
- 16 H_2
- 17 N_2

18-19 Gas content in flushed fluid in absolute percentages
- 18 $CH_4 + C_6H_{1.4}$
- 19 $He \cdot 10^{-4}$

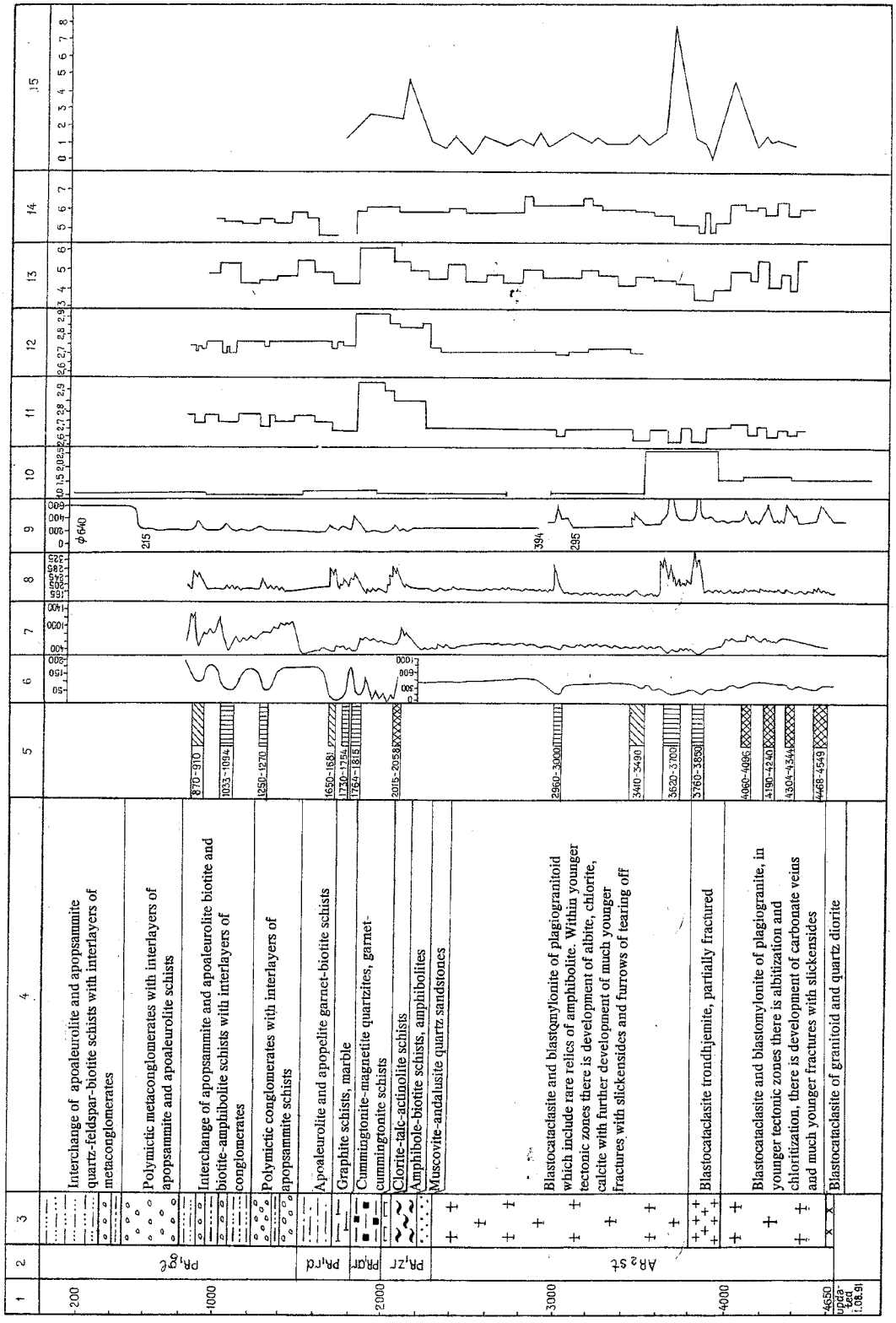

Fig. 4-7. *Characterization of the Krivoy Rog borehole based on geophysical and petrological investigations.*

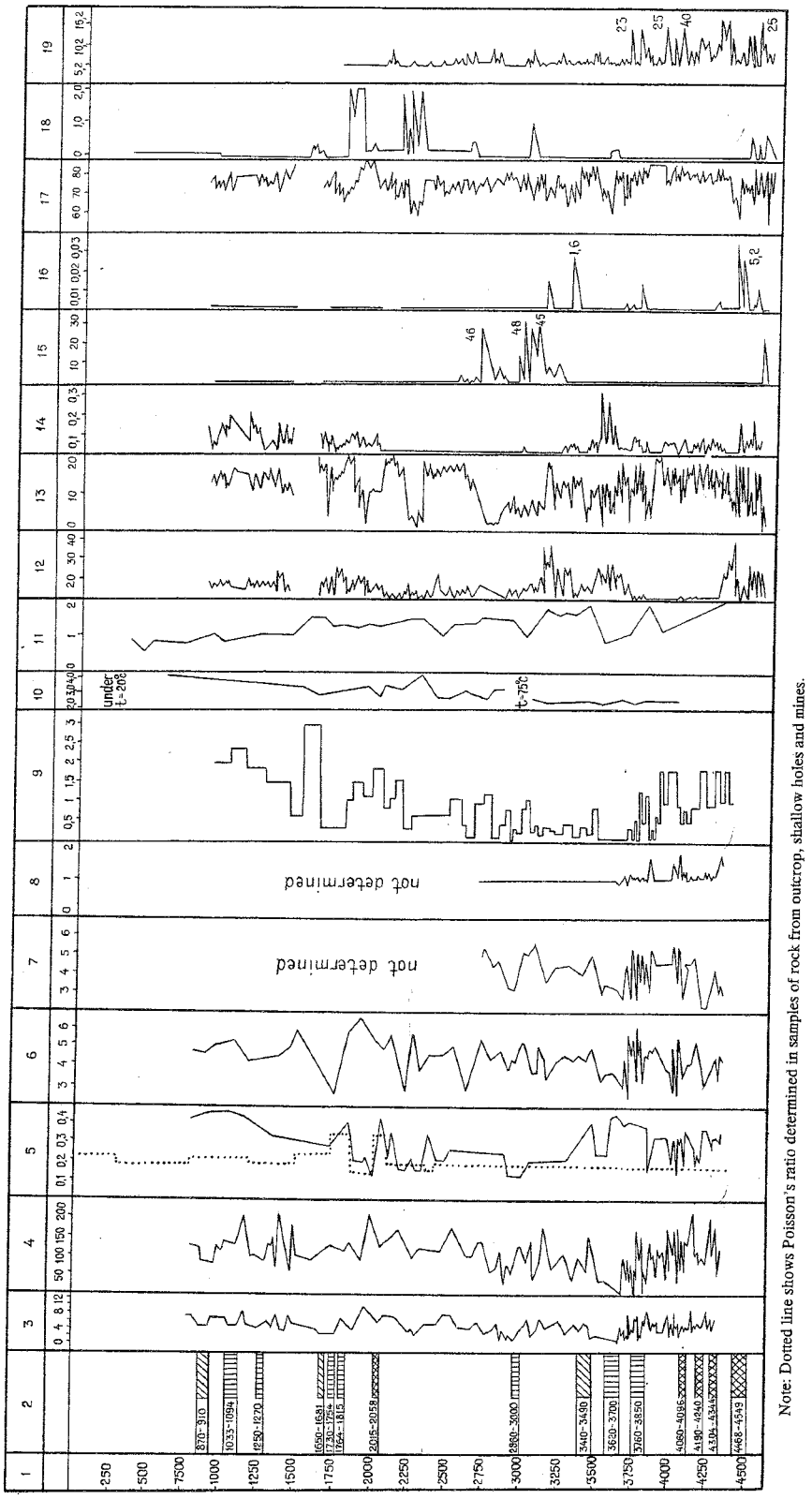

Fig. 4-8. *Characterization of the Krivoy Rog borehole based on physical, mechanical, thermal and mud logging.*

Table 4-2. Geological characterization of rock and zones of fracturing.

Series (complexes)	Suite	Depth to the upper boundary, m	Rock-type	Minerals and mechanical changes in original mineral	Fracturing			Physical and physical-mechanical properties													
					Interval, m	Group of fractures	True width m	Apparent resistivity ρ_a, Ωm		Velocity of P-waves, V_p m/s				Bulk density (core) g/cm^3		Tensile strength, MPa		Compressive strength, MPa		Total porosity, % m_t		Permeability, Kp n · 10^{-15} d m^2	
										Acoustic log		Core											
								Monolithic rock	Fracture zone	Monolithic rock	Fracture zone	Monolithic rock	Fracture zone	Monolithic rock	Fracture zone	Monolithic rock	Fracture zone	Monolithic rock	Fracture zone	Monolithic rock	Fracture zone	T= 20°C	T= 300° C
	Gleevatskaya	300	Apopsammite and apoaleurite amphibole-biotite					320		5260		5560		2.78		3.77		129.5		0.45		*	*
			Polymictic conglomerates					410		6600		5200		2.75		6.55		164.0		0.87		*	*
			Interchange of amphibole-biotite schist and metaconglomerates	Chlorite, sericite, carbonate, quartz, wedging biotite	870-1270	1	150	315	40	6250	3597	5162	4170	2.77	2.70	5.13	3.41	132.1	87.3	0.99	2.53	*	*
Ingulo-Inguletskaya	Rodionovskaya	1509	Apoaleurite amphibole-biotite schist					400		5000	3660	6030	3820	2.82	2.71	4.38	3.38	129.5		0.99	2.78	*	*
			Apoaleurite-apopelite garnet-biotite schist with graphite and pyrite	Graphite, chlorite, carbonate, wedging biotite, crushing of garnet	1650-1815	1	60	285	33	4761	3700	5920	3420	2.82	2.69	4.00	3.79	118.6	94.4	0.45	2.80	*	*
	Artemovskaya	1815	Graphitic biotite schist with pyrite					90	20	4440	3120	5810	4070	2.81	2.73	3.85	3.79	82.3	74.2	1.2	2.84	*	*

Table 4-2 continued.

Ingulo-Inguletskaya	Artemov-skaya	2015	Cumming-tonite-magne-tite quartzite with inter-layers of garnet-cum-mingtonite schist	Wedging of talc and shear aggregates of actinolite	2015-2058	2	20	45	17	7100		6000		3.20	3.10	4.25	4.00	140.2	131.9	2.16	4.48	1.9	0.1
	Zelenore-chenskaya	2058	Talc actinolite schist with pyrrhotite					256	44	6200	3508	5800	4000	2.90	2.82	5.00	2.65	30.0	28.0	1.16	2.07	*	*
			Biotite-amphibolite schist and amphibolite					750		6250		6200		2.88		6.10		136.4		0.98		0.04	0.24
			Andalusite-muscovite quartzite sandstone	Crushing of andalusite				570		5900		5750		2.72		3.30		132.1		0.21		1.2	0.9
Surskolokovsky		2351	Plagio-granitoid blastocata-clasite and blastomylonite with rare relicts of amphibolite	Crushing of plagioclase, shifts of its twins, extensive growth of Boehm Lamella in quartz, wedging and plication of biotite and muscovite blades, fractures are filled with quartz and carbonates	2960-3000	1	30	520	62	5600	3225	5000	3830	2.70	2.67	5.60	5.33	121.4	54.2	1.27	3.20	8.9-65.0	*
					3410-3490	2	60	500	80	5600	3730	5420	3730	2.68	2.66	5.11	2.57	124.7	64.2	1.27	2.8	*	*
					3420-3700	1	50	500	37	5600	3420	5110	3420	2.68	2.62	4.77	1.43	100.1	21.9	1.38	7.43	230.0	*
					3760-3850	1	70	480	40	5600	3200	4800	3200	2.67	2.62	5.11	1.73	129.8	40.4	1.30	5.30	*	*
					4304-4344	2-3	30	530	270	5600	3820	5200	3820	2.68	2.65	5.20	3.11	130.6	28.1	1.20	2.30	14.0	*

* *Not evaluated*

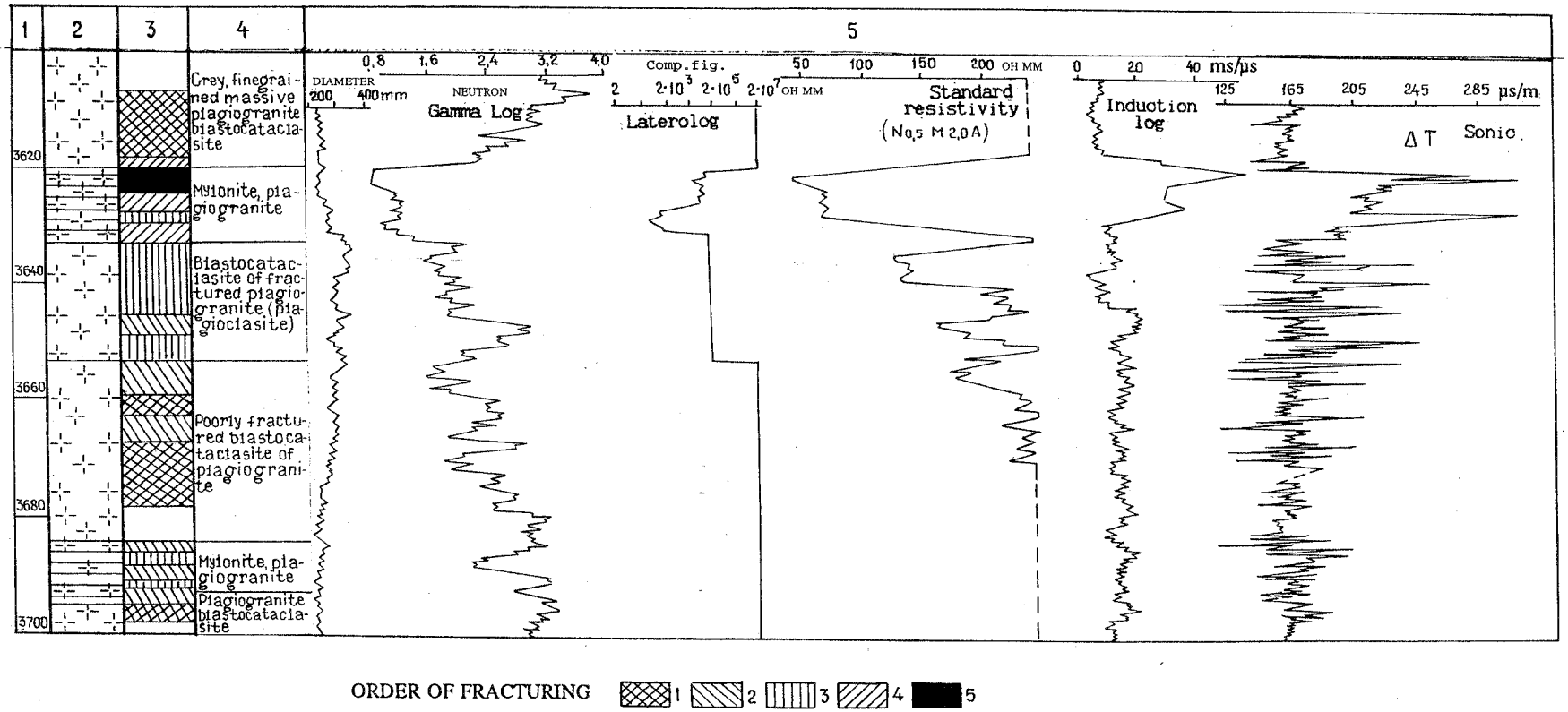

Fig. 4-9. *Geological and geophysical characterization of a ruptured tectonic zone between 3620 and 3690 m.*

Legend:

Order of fracturing:	*(1) very weak*	*(2) weak*	*(3) average*	*(4) heavy*	*(5) very heavy*
Vertical column:	*(1) depth, m*	*(2) lithology*	*(3) order of fracturing*	*(4) rock characteristics*	*(5) borehole geophysics*

Table 4-3. *Permeability of rocks from the Krivoy Rog superdeep borehole.*

No.	Depth interval, m	Rock type	Permeability , Kp, n·10 D/m³	
			20°	300°
1	1899-1970	Quartzite schists	1.9	0.14
2	2080-2192	Sandstones	0.04	0.24
3	2369.5	Blastoclasite	1.2	0.9
4	2522.0	Blastoclasite of plagiogranitoid	0.24	0.17
5	2728	-"-	0.37	0.35
6	2764	-"-	3.8	0.49
7	2787	-"-	38.0	4.6
8	2829.5	-"-	65.0	2.4
9	2896-2902	-"-	3.9	-
10	2906	-"-	2.5	-
11	3000	-"-	41.1	-
12	3020	-"-	1.0	-
13	3095	-"-	1.0	-
14	3151.9	-"-	5.0	-
15	3200	-"-	8.5	-
16	3300	-"-	2.5	-
17	3400	-"-	14.0	-
18	3620-3648	-"-	230.0	-
19	3912	Blastocataclasite of trondhjemite	0.05	-
20	4005	Blastocataclasite of plagiogranite	50.0	-

4.2.2 Stress conditions

At Krivbass, the Earth's crust is undergoing upwarping. The geodynamic investigations (Fig. 4-6) show ongoing block displacements. Differential, horizontal block movements cause accumulation of shear deformation across the Tarapakovsky thrust and its feather tectonic zones.

No rock stress measurements have been conducted in borehole SG-8. However, borehole observations, relating to the characteristics of the stress field, include:

1 Below 3000 m, lateral stress (gravitational and tectonic) was indicated, in the form of spalling of the hole wall. Initially thin (0.5-3 mm), and then thicker (0.5-1 cm) rock fragments were formed parallel to the borehole periphery.

2 Core discing initiated below 3125 m, became more intense in the interval 3620-3850 m, and decreased again below this interval. The disc surfaces formed were spherical and oriented perpendicular to the hole axis. They showed no sign of secondary mineral alteration.

3 Caving occurred throughout the borehole. Down to a depth of 3500 m, the caving was highly progressive for a period of 2-2.5 months. Then it ceased almost completely, and was replaced by sporadic fall-outs, occurring primarily in sections with talc-amphibolite and graphitic schist. The borehole cross section was near-circular or oval. Below 3500 m, caving was particularly intensive. Drilling stoppages were encountered and borehole stabilization measures were required. The most severe break-outs occurred in sections of highly fractured rock (3620-3700 m and 3760-3850 m). Here, the borehole cross-section was elliptical with a high axis ratio (Fig. 4-7).

Analysis of the data shows that both the lithostatic pressure and dynamic tectonic forces contribute to the current stress field. In the very ductile biotite-graphite and talcy schist, the lithostactic pressure is 62-70 MPa. Horizontal stress magnitudes, inferred from analysis of borehole cross-sectional geometries, were 24-25 MPa. This stress field caused the observed break-outs, which ceased after some time. Starting at 3500 m, a tectonic component, related to the flattening of a tectonic zone, is superimposed on the horizontal, gravitational component. The resulting, net horizontal stress is 68-75 MPa. This initiates the observed, intense spalling of the borehole walls, core discing and fall-outs of large rock fragments. The strength properties show a wide scatter. Excessive values of Poisson's ratio, and low values of the coefficient of stability are encountered (Fig. 4-8).

4.2.3 Hydrogeology, groundwater chemistry and gases

In Krivbass, systematic observations of groundwater circulation and hydrochemistry, in boreholes and mine workings at depths exceeding 1000 m, have been performed over a long period of time. This work has important implications with respect to iron ore mining in the area. The information obtained in boreholes 22350 and 20500, located within a mining area neighbouring on SG-8 to the east, is given in Tables 4-4, 4-5 and 4-6.

Groundwater was found in almost all types of rock in the area surrounding the SG-8 borehole. The conductivity is controlled by the porosity and the extent of tectonic fracturing. With respect to groundwater circulation, the formation can be characterized as a fractured medium. Within the mining area, conductivity measurements were made using packer tests and suction pump tests. The tests were made in diamond drilled boreholes, with diameters 59-93 mm. A bentonite drilling mud with a filter loss of 22-26 cm^3/min was used. Results are presented in Table 4-4.

Table 4-4. Water in the Krivbass rock (northern part).

No	Strati-graphical index	Rock type	Number of fractures per cored metre	Bore-hole no.	Obser-vation interval, m	Yield (Q), m^3/h	Conductivity (Km), m^2/day	Filtration coefficient (Fc), m/day	Type of test	Notes
1	PR, gd	Quartz-biotite schist		*	50-480	1-2.6		0.0022-0.027	Suction rod pump	Space between the Tarapakovsky and Saksagansky thrusts
2	-"-	-"-	7-20	*	597-941	0.32-0.35	0.06-0.13	0.0004-0.006	Packer test	-
3	PR, sx	Itabirite	7-20	*	20-750	0.03-3.00	not determined	0.0012-0.016	Suction rod pump	Zone of influence of the Saksagansky thrust
4	-"-	-"-	>7	*	400-1257	0.08-1.20	0.01-1.36	0.002-610	Packer test	Space between the Saksagansky and eastern thrusts
5	-"-	-"-	-"-	*	725-1500	0.03-0.40	0.016-0.0006	110-310	-"-	-"-
6	-"-	Itabirite	-"-	*	760-1200	2.43-9.0	Not determined	0.011-0.039	Suction rod pump	-"-
7	-"-	-"-	-"-	*	950-1970	0.08-1.5	0.005-0.33	0.001-310	Packer test	-
8	PR, gl	Metaconglomerate	-"-	20500	0-305	3.7	0.080	0.035	-"-	Zone of influence penetrated by SG-8 in the interval from 870 to 1270 m.
9	-"-	-"-	7-15	-"-	600-705	3.0	1.800	0.037	-"-	-
10	-"-	-"-	-"-	-"-	702-844	1.1	0.460	0.035	-"-	-
11	-"-	Metaconglomertates and schist	-"-	-"-	898-1018	0.1	0.004	0.030	-"-	-
12	-"-	Gneisses and schist	Relatively monolithic rock with "cicatrized" fractures	22350	700-800	0.7	0.002	0.0002	-"-	Space between displacement and thrust penetrated in the interval from 310 to 350 and 1500 m
13	-"-	-"-	-"-	-"-	694-915	7.0	Not determined	0.010	Suction rod pump	-"-
14	-"-	-"-	< 7	-"-	800-915	0.6	0.100	0.001	Packer test	-"-

Table 4-5. Variations in water mineralization with depth.

Horizon, m	Mineralization, g/l		
	Minimum	Maximum	Average
607	6.3	23.0	12.8
680	5.4	30.5	17.3
750	3.7	35.8	20.7
825	5.3	44.9	27.4
900	6.6	57.0	30.1
975	7.5	58.0	33.2

Water inflows of 11-23 m^3/h were recorded in connection with shaft sinking. Furthermore, drilling water was lost when exploration holes were penetrating the Tarapakovsky, Saksagansky and Eastern thrusts. This was observed especially in boreholes 20 500 (468.9-478.5 m 672.4-726.6 m, 996.0-1008.0 m) and 22 350 (314.7-369.2 m, 1493.0-1538.5 m). Water quantities lost were 0.03-0.65 m^3/h. Water losses were eliminated by applying a drilling fluid with a filter loss of 10-14 cm^3/min. No water losses were observed when drilling the pilot and main boreholes of SG-8. Not even application of a 15 MPa gaugepressure in the most heavily fractured interval (3760-3850 m) for a period of 30 min caused any loss of water into the formation. Furthermore, packer tests in borehole SG-8 (intervals 3380-3500 m and 3509-3550 m), conducted at a differential pressure of 12 MPa and for a duration of 12 hours, did not show any water inflow. However, a comparison of the chemistry of a mud filtrate before pumping in and after pumping out as well as the results of logging indicate that fluid inflows occurred during the drilling process.

Analysis of data given in Table 4-4 shows that pumping tests using a suction pump produced the most reliable results. Applied under similar geological conditions, packer testes are less reliable, due to partial closure of pores and cracks. Nevertheless, the packer test results from boreholes 20 500 and 22 350 do indicate that the hydraulic properties of individual rock types depend on the degree of tectonic impact. In borehole 20 500, greater fracturing is accompanied by increased conductivity.

The annual discharge of groundwater from the Krivbass workings amounts to $25 \cdot 10^6$ m^3. Brines account for 1/3 of this volume. In the central part of the Kirovogradsky block, the conductivity is much higher due to the presence of open fractures formed under extensional strain. Some holes yield outflows of about 80 m^3/h. The water is characterized by a high content of radon and a low degree of mineralization (0.5-3.6 g/l).

Table 4-6. Ground water chemistry.

Depth, m	General mineralization, g/l	Sampling place	Sampling method	pH	Components, g/l (min, max and average values)						
					HCO_3^-	Cl^-	SO_4^{2-}	Ca^{2+}	Mg^{2+}	Na^+	K^+
0-500	0.41-7.20	Mine	Direct	7.0-8.3	0.10-2.70/0.87	1.6-38.3/3.20	0.20-1.77/0.73	0.13-2.65/0.13	0.14-2.65/0.80	0.98-17.5/2.41	0.04-0.36/0.05
		20500 Borehole									
		0-305.0 m	Packer test	7.1	1.49	2.94	0.004	0.23	0.27	1.67	0.001
		300.2-390.0	-"-	6.9	1.46	2.41	0.20	0.22	0.24	1.45	0.001
500-1000	7.0-33.2	Mine	Direct	7.0-8.3	0.12-1.84/0.65	1.61-39.4/4.2	0.45-2.10/0.61	0.26-2.48/0.76	0.29-3.10/0.83	1.47-16.3/5.83	0.001-0.39/0.05
		20500 Borehole									
		600.0-705.1	Packer test	6.9	1.59	3.51	-	0.38	0.28	1.88	0.001
		702.1-844.6	-"-	7.2	0.98	7.23	-	0.76	0.43	3.33	0.002
		898.0-1018.0	-"-	7.1	1.31	6.03	-	0.74	0.44	0.27	0.002
		22350 Borehole									
		694.0-723.0	Suction rod pump	7.1	0.35	0.34	2.02	0.34	0.27	9.77	0.018
		694.0-799.0	Packer test	7.0	0.22	0.41	2.06	0.32	0.22	13.43	0.025
1000-1500	27.1-69.0	A group of holes within a mining area	Packer test	6.8-7.6	0.07-0.33/0.17	1.58-40.2/4.70	0.58-2.12/0.64	0.08-2.26/0.77	0.02-2.80/0.78	0.94-16.4/4.80	0.06-0.46/0.14
1500-2500	98.0-142.0	-"-	Packer test and suction rod pump	6.9-8.2	0.04-2.93/1.0	2.14-57.0/16.0	0.19-1.81/0.86	0.24-2.66/0.96	0.18-3.21/1.12	1.06-32.3/9.91	0.016-0.38/0.14

Notes: During chemical characterization of the water from workings and holes (1000-1500 m and deeper) the numerator indicates minimum and maximum content of the component and the denominator - average.

Results from investigations performed on permeable rocks (mainly granitoids) were given in a previous section and in Table 4-3. With respect to the degree of mineralization of groundwater, the formation can be subdivided into four zones:

Zone 1	Active circulation	Depth 0-500 m	Mineralization 0.4-7.2 g/l
Zone 2	High circulation	500-1000	7.0-33.2g/l
Zone 3	Low circulation	1000-1500	27.1-69.0g/l
Zone 4	Deep water	Below 1500 m	98.0-142.0 g/l

The increase in the degree of mineralization with depth was verified by systematic observations performed in a mine during the period 1967-1984. Total mineralization at different depths is given in Table 4-5. Further details on sampling method and distribution of constituents are presented in Table 4-6.

The groundwater is characterized by a multi-component composition. In the upper parts, it contains hydrocarbonate-chloride-calcium-sodium components. With increasing depth, this composition gradually changes over to a chloride-sodium-hydrocarbonate water. The contents of copper, molybdenium, nickel, titanium, zinc, beryllium, lead, cerium, germanium, chromium, vanadium and bismuth do not exceed values typical for natural water basins. Anomalous contents of cesium, rubidium and lithium were observed. In this part of Krivbass, the water is aggressive to sulphate cements and metals. Analysis of mud filtrate from SG-8 revealed that below 1600 m, the contents of chlorine, hydrocarbonate and sodium increase from 1.2 to 2.1, from 2.5 to 5.2 and from 1.4 to 3.7 g/l respectively. The maximum contents were measured within heavily fractured intervals of metamorphic and plagiogranitoid rocks. The fractures were also affected by metasomatic alteration, including quartzilization, carbonation and albitization. The minerals form veins, containing abundant gas-fluid inclusions, which impregnate the rock. The salt content of inclusions was studied using a method of triple water extraction. It was found to consist of ($n \cdot 10^{-6}$ mg/eq.) sodium (3.71-4.86), potassium (0.56-1.21), chlorine (0.97-1.42) and hydrocarbonate (5.81-7.44). It is likely that these components are added to the water in a zone of deep circulation, since corresponding concentrations in the water in a zone of hypergenesis are considerably lower (Table 4-6). The indications of deep circulation below 1600 m are further supported by the following observations:

- Proterozoic, and younger, vegetable fragments are present in fracture zones above 1650 m - but absent below 1650 m.

- Isotopic analysis of carbon and oxygen from carbonate veins indicates that the content of heavy isotopes increases above 1650 m and decreases below this depth (Table 4-7). It is believed that carbonate absorbs heavy isotopes in the zone of free circulation. Below 1650 m, there is no absorption since meteoric water does not penetrate below this depth.

Results from analyses of gas sampled in connection with drilling are given in Table 4-8. The gas distribution is shown in Fig. 4-8. The data shows that the gas distribution in borehole SG-8 is complex, and probably controlled by several factors. However, the two most important factors are the composition of the rock hosting fluids, and the extent of fracturing.

There is a clear trend in the distributions of carbon monoxide, hydrogen and helium. All rock types show low average contents of these gases, and concentrations increase at depths below 3200-3500 m. This is particularly evident within the interval 3500-4500 m. Gases might be of mantle origin, and their migration paths could be along the Tarapakovsky deep thrust. The abiogenic nature of gases, for example carbon monoxide, is suggested by a very low content of carbon (δC^{13} = -12 to -21). Unlike hydrogen and helium, carbon monoxide is found in sedimentary-metamorphic rock of the Gleevatsky and Rodionovsky suites. Here, the high content is caused by graphite and fragments of seaweeds.

Carbon dioxide and oxygen both occur throughout the investigated interval. Carbon dioxide tend to be accumulated in fracture zones, whilst Oxygen is lacking in fracture zones. This was clearly observed at depths below 300 m, excluding, however, a fracture zone at 3700-3850 m, were the relative oxygen content reached 23%. Nitrogen occurs fairly uniformly distributed with depth, with the exception of distinctly higher concentrations measured at intervals 1650-1812 m, 3620-3850 m and at the contact between metamorphic and plagiogranitoid rocks.

The total hydrocarbon concentration in all rock types is very low. Distinct anomalies occur mainly in tectonic zones, especially in the interval 1650-1815 m, where abiogenic gases are reinforced with gases which were previously guest components of hydrocarbon formation.

Table 4-7. Contents of O^{18} and C^{13} isotopes in carbonate veins in SG-8.

Depth, m	Content, per mille	
	O^{18}	C^{13}
1	2	3
286	+24.4	-4.6
382	+18.2	-3.8
512.4	+27.3	-1.0
652.2	+25.6	-2.1
805.6	+20.3	-5.0
1006	+16.9	-11.4
1153	+19.7	-8.7
1213	+19.2	-14.3
1424.7	+16.8	-7.2
1708	+17.5	-9.1
1767	+15.3	-12.3
1823	+15.5	-7.5
2010	+15.2	-5.2
2112.6	+15.5	-6.7
2219.7	+16.2	-7.2
2424.7	+14.5	-7.2
2887	+14.9	-9.9
2908	+14.4	-9.4
2958	+11.8	-11.2
3038.8	+13.3	-8.1
3480.9	+12.7	-8.8

Table 4-8. Results from gas analyses of the drilling mud. Relative percentages.

Zones of fracturing	CO_2		O_2		CO		H_2		CH_4		N_2		He ($n \times 10^{-4}$)	
	Monolithic rock	Fracture zone	Monolithic rock	Fracture zone	Monolithic rock	Fracture zone	Monolithic rock	Fracture zone	Monolithic rock	Fracture zone	Monolithic rock	Fracture zone	Monolithic rock	Fracture zone
870-1270	2.4-15.0 8.2	4.0-10.0 6.7	10.2-16.2 12.6	10.5-17.6 14.0	0.025-0.18 0.1	0.015-0.21 0.11	Not evaluated	Not evaluated	0.01-0.09 0.03	0.0-0.19 0.04	71.5-87.1 79.1	75.1-84.3 79.0	Not sampled	Not sampled
1650-1815	0.05-12.0 0.3	1.8-18.1 8.5	4.0-20.0 19.8	2.3-20.2 16.0	0.01-0.13 0.122	0.0-0.1 0.014	Not evaluated	Not evaluated	Not evaluated	Not evaluated	74.5-86.1 80.2	69.3-90.0 82.5	5.2	5.2-5.7 5.4
2015-2058	0.1-7.5 3.3	0.2-1.7 0.7	14.0-20.2 17.4	17.0-19.6 18.7	Not evaluated	Not evaluated	Not evaluated	Not evaluated	0.0-4.4 0.5	Not evaluated	71.6-82.5 80.1	79.6-81.4 80.6	5.0-7.08 5.4	6.1-9.7 7.0
2960-3000	2.0-16.2 5.0	5.0-10.3 6.7	0.8-18.7 12.4	4.8-7.8 6.0	0.0-0.03 0.003	0.01-0.04 0.02	Not evaluated	Not evaluated	0.0-46.0 3.2	0.8-48.1 30.3	69.2-89.9 78.1	39.1-86.6 56.9	5.2-9.04 5.8	5.2-9.2 5.7
3410-3490	2.2-12.7 6.6	1.0-20.5 9.2	0.5-20.7 9.4	3.9-15.8 9.9	0.0-0.05 0.01	0.0-0.098 0.04	Not evaluated	Not evaluated	0.03-39.2 5.4	0.0-0.19 0.04	77.9-92.7 84.5	71.1-90.2 80.8	5.2-10.8 5.9	5.2-8.9 6.5
3620-3700	8.7-26.7 18.7	2.0-20.1 8.8	6.3-14.8 11.7	2.4-19.5 14.4	0.0-0.05 0.16	0.0-0.11 0.04	Not evaluated	Not evaluated	0.1-1.47 0.8	Not evaluated	61.9-86.6 68.6	78.0-90.1 84.5	5.2-8.8 6.2	5.2-23.7 8.7
3760-3850	0.4-6.5 2.5	0.0-5.9 1.8	6.5-19.2 13.4	1.3-19.9 11.6	0.02-0.09 0.05	0.01-0.08 0.02	0.0-0.018 0.009	Not evaluated	Not evaluated	Not evaluated	78.5-89.9 85.7	89.9-90.4 90.0	5.2-8.2 5.9	5.2-8.2 5.6
4304-4344	0.0-34.3 4.8	0.3-16.9 6.0	1.6-20.8 13.3	10.2-17.3 14.1	0.0-0.097 0.02	0.009-0.04 0.01	0.0-5.22 0.0007	0.0-0.056 0.007	0.0-29.5 0.41	0.0-0.11 0.06	46.7-95.9 81.3	71.1-86.4 79.8	5.2-37.2 7.8	5.2-19.2 10.3

Notes: The contents of hydrogen, methane and carbon monoxide in some of the samples was not evaluated due to the release of insufficient gases to permit correct analysis.

4.2.5 Thermal conditions

In the Krivoy Rog hole and other exploration holes, the temperature was measured at 400-600 m intervals. Prior to measurements, conditions were allowed to stabilize for a period of 7-10 days. The accuracy was ± 0.01 K. For many years, observations of the thermal regime were made in 23 exploration holes within the Krivoy Rog area, at depths ranging from 500 m to 2500 m. The results show a geothermal gradient averaging 11.2 K/km and ranging between 6.3 and 17.0 K/km. Temperature data obtained from boreholes SG-8, 22 350 and 19929 are given in Table 4-9. Figure 4-8 shows the geothermal gradient in the Krivoy Rog borehole, together with geological and tectonic information. Interpretation of the data enabled five thermal zones to be distinguished:

1)	Seasonal variations	from 0 m to 20-70 m
2)	Uniform temperature	20-70 m to 200 m
3)	Stable, low gradients	from 200 m to 1400 m
4)	Average gradients	from 1400 m to 2500 m
5)	Irregular, increasing gradients	below 2500 m

Fig. 4-10 illustrates the distribution of paleotemperatures in a vertical section [2:5, 2:8 and 2:11]. There is a distinct paleothermal anomaly which corresponds to the Tarapakovsky thrust. The formation of this zone started during Early Proterozoic time. The thermal regime in the zone is probably influenced by its ongoing deformation, as caused by differential block movements (Fig. 4-6). This is verified by the 400-500 m upward shift of isotherms in the section, and by the 1500-1600 m shift in thermal zones 4) and 5), in hole 22 350 as compared with SG-8. Furthermore, in borehole 22 350, anomalous thermal gradients (14-20 K/ km) were observed within the thrust zone and overlying faults (1700-2100 m). Similar conditions were observed within a heavily distorted interval (3500-4400 m) in borehole SG-3. In SG-8, the thermal gradients increase significantly towards the Tarapakovsky thrust. Within the metamorphic rock in the upper part of SG-8, thermal gradient anomalies coincide with a series of faults located in the interval 1250-2058 m. Fracture zones are thus found to significantly influence the thermal regime, and to govern the direction of heat flow.

In hole 19 929 the influence of deep heat flow disappears almost completely. This may be attributed to the effect of downward flow of meteoric water, which ceases at a depth of 1000-2000 m. This supports the definition of the upper boundary of the zone of highly mineralized deep water, as discussed in Section 4.2.4.

Table 4-9. Temperatures and thermal gradients measured in the Krivoy Rog, 22350 and 19929 boreholes.

Krivoy Rog				22350				19929			
Depth, m	Temperature, °C	Thermal gradient °C/100 m	Thermal zone	Depth, m	Temperature, °C	Thermal gradient °C/100 m	Thermal zone	Depth, m	Temperature, °C	Thermal gradient °C/100 m	Thermal zone
0				0				0			
100			1-2	100			1-2	100	12.50		1-2
200	16,80	0.78		200	19.30	0.63		200	13.30	0.80	
300	17.70	0.90		300	20.15	0.85		300	14.15	0.85	
400	18.21	0.51		400	21.00	0.85		400	15.15	1.00	
500	19.00	0.79		500	21.85	0.85	3	500	16.10	0.95	
600	19.79	0.79		600	22.80	1.05		600	17.20	1.10	3
700	20.59	0.80		700	23.85	1.05		700	18.25	1.05	
800	21.47	0.88	3	800	24.90	1.05		800	19.35	1.10	
900	22.47	1.00		900	26.05	1.15		900	20.35	1.00	
1000	23.32	0.85		1000	27.20	1.15		1000	21.55	1.20	4
1100	24.22	0.90		1100	28.40	1.20	4				
1200	25.24	1.02		1200	29.40	1.00					
1300	26.25	1.01		1300	30.60	1.20					
1400	27.20	0.95		1400	31.80	1.20					
1500	28.60	1.40		1500	33.20	1.40					
1600	30.00	1.40		1600	34.56	1.36					
1700	31.25	1.25		1700	36.20	1.64					
1800	32.46	1.21	4	1800	37.42	1.21					
1900	33.74	1.28		1900	38.93	1.53					
2000	35.00	1.26		2000	40.42	1.49					
2100	36.37	1.37		2100	41.63	1.21	5				
2200	37.84	1.47		2200	42.75	1.12					
2300	39.24	1.40		2300	43.91	1.16					
2400	40.24	1.00		2400	44.92	1.01					
2500	41.53	1.29		2500	46.93	2.01					
2600	42.90	1.37		2600	48.15	1.22					
2700	44.45	1.55		2700	49.40	1.25					
2800	45.80	1.35									
2900	47.30	1.55									
3000	47.91	0.80									
3100	49.20	1.30									
3200	50.00	1.40									
3300	52.80	2.20									
3400	54.51	1.70									
3500	56.20	1.70									
3600	58.00	1.80	5								
3700	58.74	0.74									
3800	61.20	2.46									
3900	62.00	0.80									
4000	62.73	0.73									
4100	64.05	1.32									
4200	65.10	1.05									
4300	66.42	1.32									
4400	68.41	2.00									

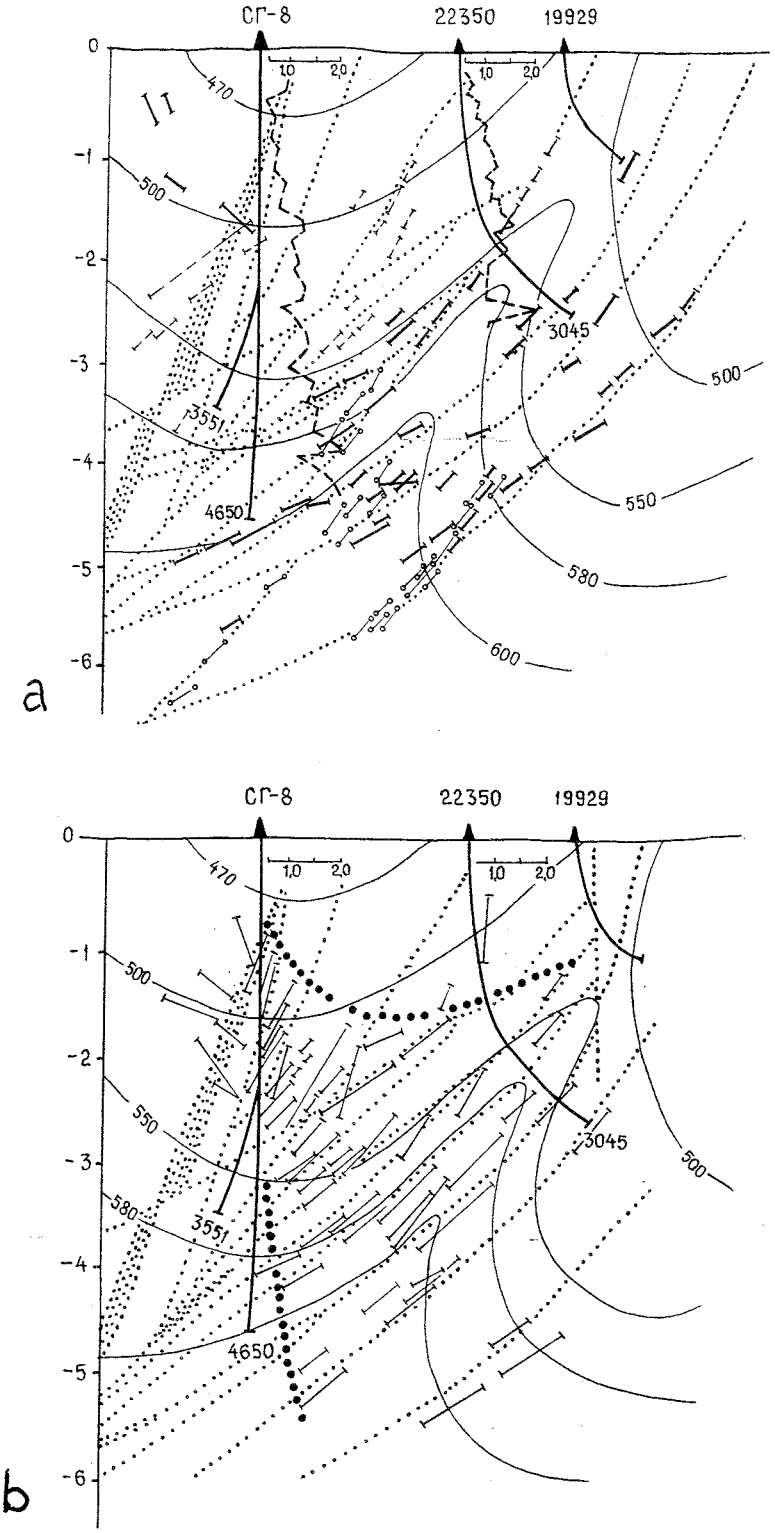

Legend

1) Reflections corresponding to wave intensity
2) Reflections corresponding to weak intensities
3) Reflection corresponding to a single signal
4) Seimic boundaries
5) Shadow zone
6) Tectonic disturbance
7) Paleoisotherms
8) Temperature gradient

Fig. 4-10. *Results from surface seismic surveys in the Krivoy Rog borehole*
(a) Reflecting deep point
(b) Vertical seismic profiling

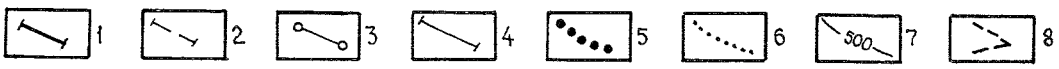

4.3 SUMMARY OF THE RESULTS FROM THE KRIVOY ROG BOREHOLE

The major results from the investigations in borehole SG-8 and its surroundings in the Krivbass area can be summarized as follows:

1 The Krivbass area is characterized by the tectonic and geological structure prevailing within the central part of the Ukrainian Shield. The Tarapakovsky transregional thrust zone and its feather faults of second and third order are major elements with respect to the overall geological setting in the area. Fault zones have dip angles of 70-90° down to a depth of about 2000 m. Below this depth they tend to flatten gradually, to dip angles of 20-30°.

2 Down to a depth of 4650 m, borehole SG-8 penetrated 11 different faults with widths varying between 20 and 150 m. The fracture zones occur throughout the investigated horizon. With respect to intensity of fracturing, the zones are classified as being of first, second and third categories. The fracture intensity tends to decrease below 4000 m. Significant tectonic faults are observed in the interval 3600-3850 m, where the relative frequency of "non-cicatriced" fractures increases up to 40%, to be compared to 5-20% for other fracture zones. The fracturing in this interval appears to be genetically related to neotectonic block movements, causing reactivation of fracture zones. The rate of block movements is up to about 5 mm/year.

3 The fault zones are characterized by anomalies in porosity, permeability, density, strength properties and borehole stability. Anomalies are especially evident in the interval 3600-3850 m.

4 Gas is generally encountered when drilling through fracture zones. The most common gases are carbonic acid, carbon monoxide, hydrogen and especially helium. The content of helium increases gradually with depth.

5 The groundwater flow regime is characterized by zonation in terms of flow characteristics and, interrelated, also by the degree and type of mineralization. An important conclusion is that active circulation is limited to depths less than 1500-1700 m. At larger depths, the water is of a hypogene character with a high degree of mineralization.

6 Observed thermal anomalies are partly related to heat transport in fracture zones. The direction of heat flow is largely controlled by the Tarapakovsky thrust zone.

5 THE TYRNAUZ DEEP BOREHOLE

5.1 GEOLOGICAL AND TECTONIC SETTING

The Caucasus is a complex system of Alpine folded structures deposited between the Black Sea and the Caspian Sea. It is separated from the ancient Russian platform by the Skifsky plate. As shown in Fig. 5-1, the main tectonic features of the Caucasus are oriented towards the west-north-west.

The Pshekish-Tyrnauz sutural zone forms the boundary between the folded area and the Skifsky plate. This zone is a wide, sublatitudinal disjunctive system which geomechanically corresponds to strike-slip or reversal conditions [3:11]. It forms a system of closely spaced ruptures, separated by tectonically deformed Paleozoic and Upper Paleozoic rocks that are fragments of originally large structural and facial zones. The ruptures building up the zone were formed from the Middle Paleozoic to the Mesozoic and Cenozoic. The process was accompanied by intrusion of different ages. The Tyrnauz deep borehole is located within one of these intrusive bodies - the Eldjurtinsky granite massif.

An anticline zone that appears to be an extension of the Pshekish-Tyrnauz sutural zone to the east is traced up to the Caspian Sea. To the west, it probably corresponds to a zone of convergence of the north-western Caucasus and an adjoining marginal zone through the Skifsky plate. To the south, the Pshekish-Tyrnauz sutural zone is flanked by schists and gneisses of the megantclinorium of the Great Caucasus, which were formed during Proterozoic to Early Paleozoic times.

Knowledge about the zone is incomplete, and there are different theories as to its evolution. Thus, some scientists claim that it is a surface extension of deep, undercrust structure [3:8, 3:13]. Others argue that, as a rule, the most ancient rock complexes of this zone are allochthonous tectonically overlying different Devonian-Carbon horizons, and together with them forming post-thrust sinformal and antiformal sublatitudinal folds (Fig. 5-2) [3:1, 3:2 and 3:3]. Allochthonous lamellae have a complex composition. Some of them occur both upside-down and normally [3:2, 3:3, 3:4]. According to this theory, the thrust evolved from the south. On the basis of geophysical data, the zone is here considered to be a thrust zone.

Tectonic faults within the Pshekish-Tyrnauz zone are classified into three orders:

- First order faults - *Regional faults* - are traced for distances of tens or hundreds of kilometres, and have displacement amplitudes from several hundreds of metres to a few kilometres. Fault zones are up to 100 m wide.

- Second order faults - *Intrastructural faults* - are secondary (feather) structures to the regional faults. These faults extend several kilometres, amplitudes are up to several hundres of metres, and widths several metres or tens of metres.

- Third order faults - *lateral and oblique faults* - are abundant, and their lengths are controlled by the higher-order faults. They are characterized as up-thrusts and strike-slip faults with amplitudes of up to several metres.

The eastern part of the Pshekish-Tyrnauz sutural zone is to the north bounded by a 1st order fault. Within the Tyrnauz ore field, it is 15 km long and traced down to 2 km in river valleys. The width of the fault zone is 80 m. In the Baksan river valley, the fault plane dips 80° to the south. Another 1st order fault bounds the Pshekish-Tyrnauz zone to the south. This fault dips steeply towards the south-west, and has an amplitude of about 2.5 km.

The largest 2nd order fault is the Central fault, striking sublatitudinally and dipping 75-80° north. It is characterized by mylonitization with a thickness of up to 10 m.

Plicate tectonics are common in the area. They are mainly observed in formations of sedimentary and metamorphic complexes, in which folds of different orders are exceptional.

Geologically, the Pshekish-Tyrnauz sutural zone is built up of Proterozoic metamorphic formations, Paleozoic (Devonian, Carbon, Permian), Mesozoic (Jurassic), Cenozoic tuffaceous-sedimentary and sedimentary rocks, intersected by numerous intrusions (Fig. 5-3).

The youngest intrusion is the stock-shaped Eldjurtinsky granite massif. It occurs both on the surface and in underground workings, extending more than 7 km southeast-northwest, and having a width of 2-2.3 km. The roof of the massif dips 25-30° SE, underlying hornfels, marble and granite-pyroxene wollastonite-vesuvianite skarns of the Tyrnauz tungsten-molybdenum deposit. The scarned rocks were traced vertically over hundreds of metres from absolute levels of +3100 to +2900 m to the roof of the Eldjurtinsky granite. The highest mark of a granite outcrop is +2550 m. The total volume of the massif, included eroded parts, exceeds 90 km^3. The absolute age of the granite is estimated at 1.8-1.9 Ma, which corresponds to Pleistocene.

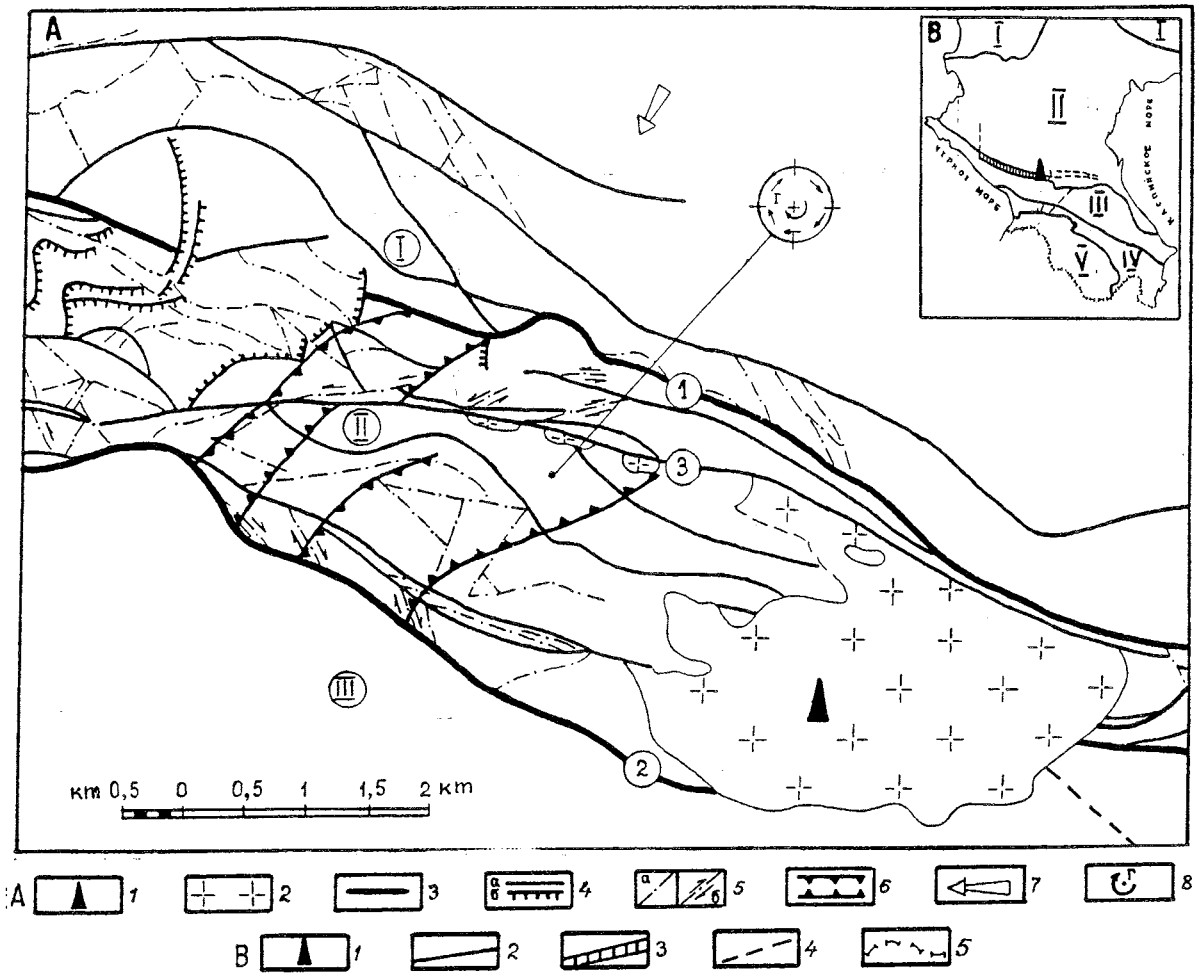

Fig. 5-1. Tectonic map of the Tyrnauz ore field (A) and map of the main structures of the Caucasus (B).

Legend

A

Main tectonic blocks

I The Betchasinskaya zone Skifsky plate II The Pshekish-Tyrnauz sutural zone

III The meganticlinorium of the Great Caucasus

Legend

1 Location of the Tyrnauz borehole 2 The Eldjurtinsky granite massif

3 Tectonic disturbance of the 1-st order (1 - Northern fault; 2 - Southern fault).

4 2nd order; a- fault; b- overthrust (3 - central fault)

5 3rd order; a-fault; b- thrust 6 Flexures

7 Axis of maximum compression 8 Axis of rotation

B

Main tectonic blocks

I The Russian platform II The Skifskaya epihercynian plate

III The meganticlinorium of the Great Caucasus

IV The Transcaucasus intramountain zone V The folded structure of the Little Caucasus

Legend

1 Location of the Tyrnauz borehole 2 Tectonic boundaries of the main structures

3 The Pshekish-Tyrnauz sutural zone 4 Faults and overthrusts

5 The state border

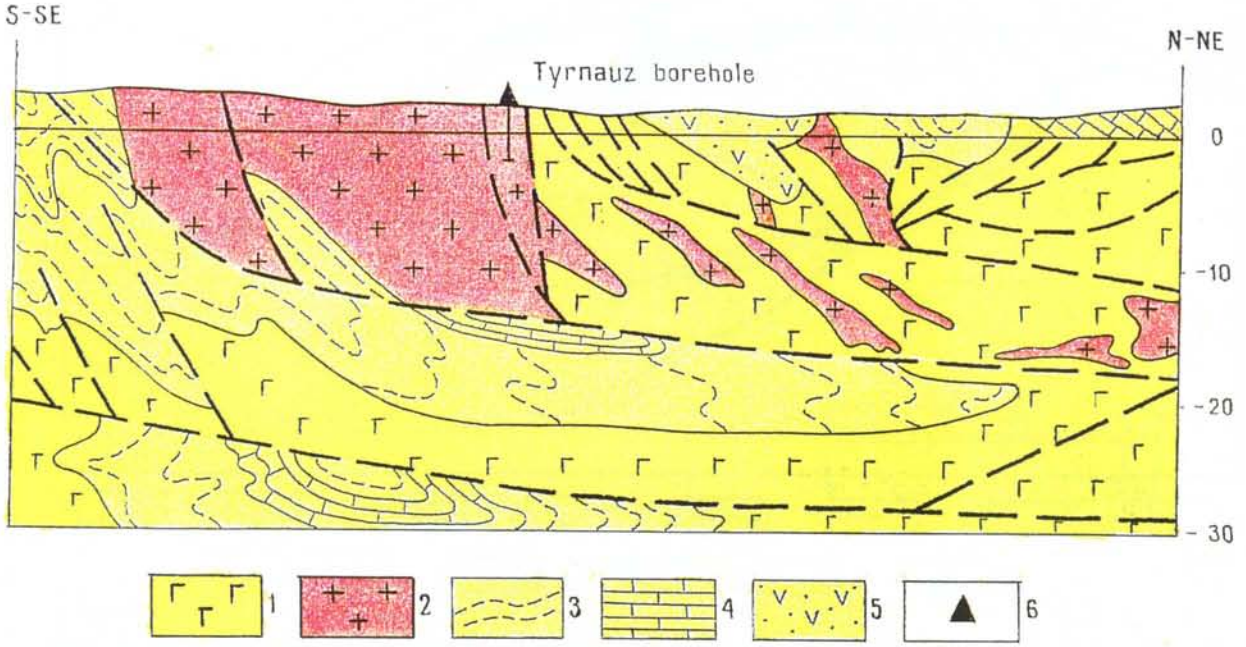

Fig. 5-2. *Geological section of the Earth's crust of the Caucasus.*

Legend

Paleozoic rocks

1 Basic volcanogenic-sedimentary and volcanic rocks

2 Granite, granitoid, orthogneisses (PZ)

Mesozoic rocks

3 Metamorphosed terrigenous deposits of shale phyllite. Intensively deformed.

4 Carbonate rocks

5 Intermediate volcanogenic-sedimentrary and volcanic rocks

6 Location of the Tyrnauz borehole

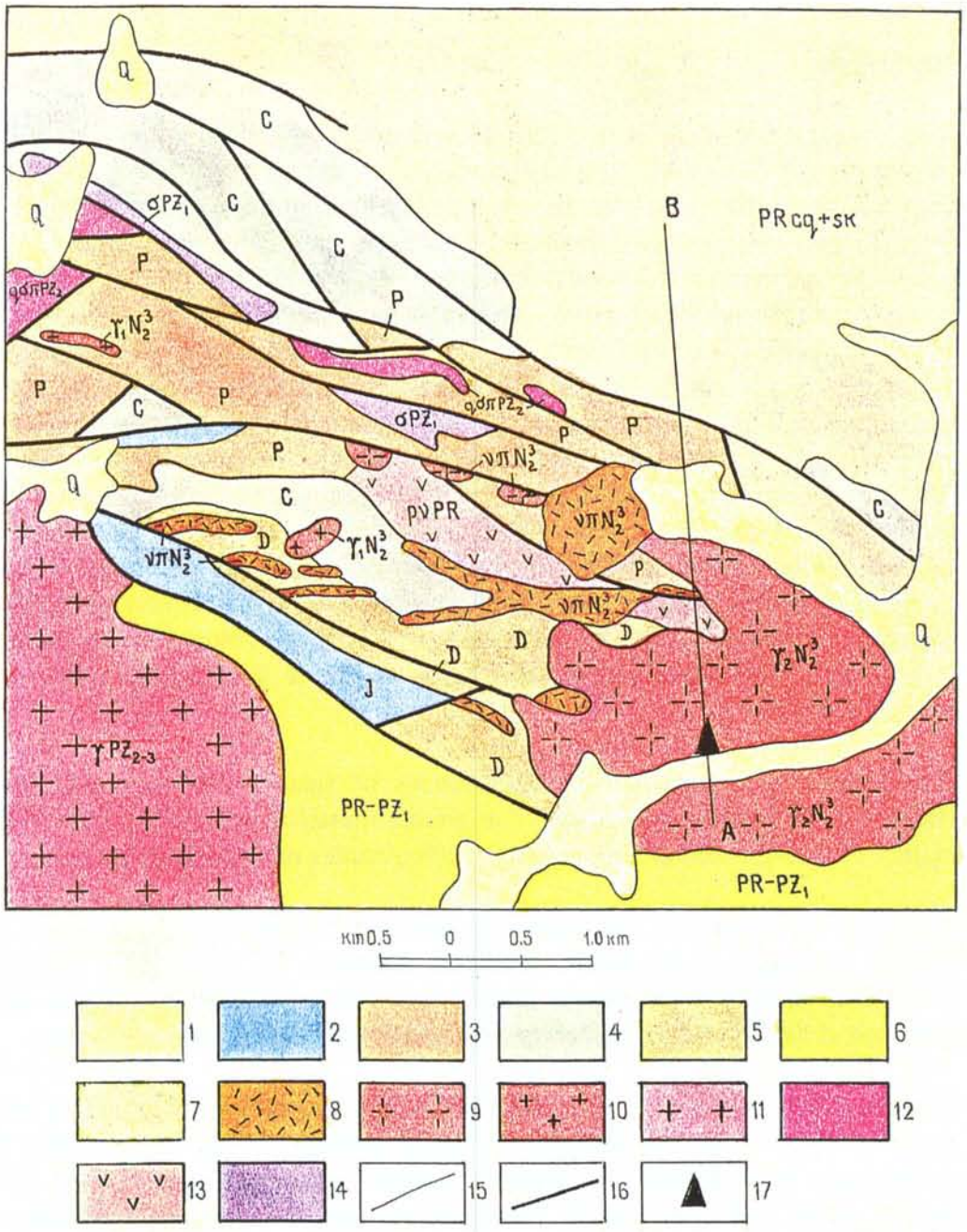

Fig. 5-3. Geological map of the Tyrnauz borehole area.

Legend:

(1) Freshwater and glacial deposits (2) Sandstone and aleurolite (3) Conglomerate, gravelite and aleurolite (4) Conglomerate, sandstone, limestone and phyllite (5) Limestone, sandstone, hornfels, conglomerate, tuff, phyllite and aleurolite (6) Micaceous and chloritic schist (7) Muscovite-albite and chlorite-albite schist (8) Liparite (9) The Eldjurtinsky granite (10) Leucocrate granite (11) Granite, plagiogranite (12) Quartz, diorite-porphyry (13) Plagiogranite (14) Hyperbasite (15) Boundary (16) Rupture (17) Location of the Tyrnauz borehole

5.2 RESULTS FROM BOREHOLE INVESTIGATIONS

5.2.1 **Rock types**

The Tyrnauz deep hole was drilled to a depth of 4001 m within the Eldjurtinsky granite massif. The rock type distribution over the penetrated horizon is shown in Fig. 5-4 and Table 5-1. It comprises Tertiary alluvial deposits in the upper part (0-290 m) and then massive granite of variable granularity and composition. The granite is macroscopically subdivided into pink (290-715 m), grey (715-3835 m) and leucocratic (3835-4001m) types. The mineral compositions of these varieties are given in Table 5-2. The pink granite is porphyritic with biotite enrichments. Impregnated quartz and feldspar with grain sizes 0.5-5 cm constitute 55-60% of the volume. The main matrix consists of the same minerals, with grain sizes 0.2-2.0 mm. The grey granite is coarse-grained porphyritic with evenly distributed biotite. The impregnated quartz and feldspar grains ranges in size from 0.3 cm to 3 cm, and accounts for 35-50% of the volume. The grain size of the main matrix is predominantly 0.3-0.5 mm in the upper part of the section and 1.0-2.0 mm in the lower. Leucocratic granite is dispersed porphyritic with a relatively even distribution of biotite. Impregnated quartz and feldspar (5-10% by volume) have grain sizes of 0.5-1.5 cm. The grain size of the main matrix is 0.7-2.0 mm. Schlieren and zenoliths are found.

The section is complicated by occurrences of liparite and granite-aplite dykes, fracture zones and crushed zones. The granite massif is cut by thin vein formations, mainly of fine-grained and more acidic differentiates of the granite magma.

As shown in Figure 5-5, the granite section is characterized by a high and uniform density, averaging 2.60 g/cm^3. Schlieren accounts for the highest density (2.74 g/cm^3) and aplite for the lowest (2.54 g/cm^3). A significant decrease in density is observed at 3830-4001 m, corresponding to the leucocratic granite deposits.

There is a certain regularity in the distributions of petrogenic oxides and a number of elements (Fig. 5-6). An increase in silica content in the interval 600-2000 m corresponds to a decrease in alumina content, inadequate reaction of ferric and ferrous oxide and also slightly increased contents of titanium and lithium. The interval 2000-3830 m displays an abrupt decrease in silica content and increased contents of all petrogenic oxides. Below that level, the silica content increases considerable, with a corresponding decrease petrogenic oxides and a number of elements.

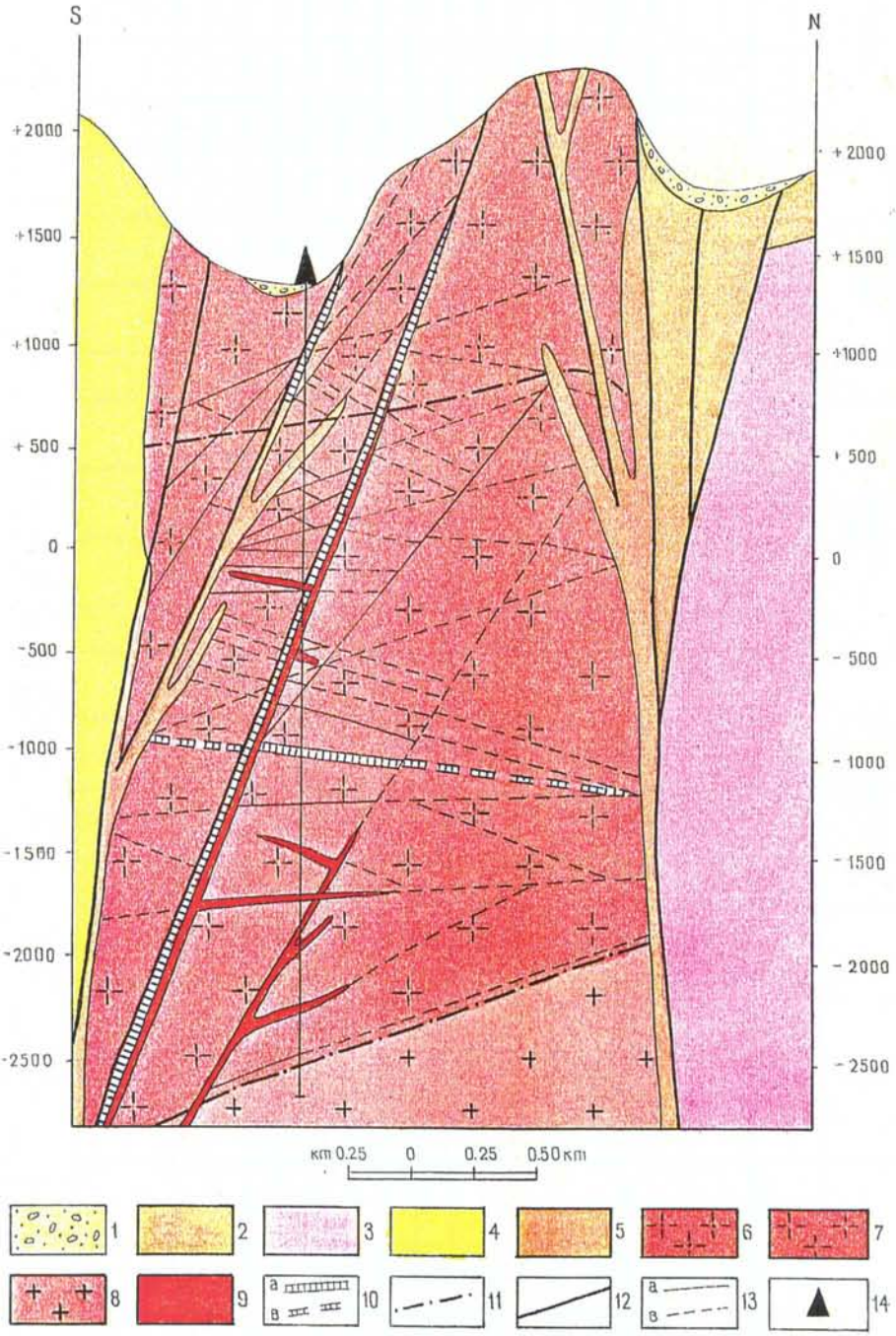

Fig. 5-4. *Geological section of the Tyrnauz borehole area.*

Legend

(1) Freshwater and glacial deposits (2) Limestone, sandstone, hornfels conglomerates, tuff, phyllite, aleurolite (3) Muscovite-albite and chlorite-albite schist (4) Micaceous and chlorite schist (5) Liparite (6) "Pink" granite (7) "Grey" granite (8) Leucocratic granite (9) Aplite (10) Crush zones: (a)-existing; (b)-anticipated (11) Representative contours facies of granite (12) Faults (13) Fracture zones: (a)- existing; (b)-anticipated (14) Location of the Tyrnauz borehole

Table 5-1. Petrotypes and physical properties of granites of the Eldjurtinsky massif.

Bore-hole No	Interval m	Granite	SiO_2 content %				Open porosity, (Kp), %				Permeability (Kpr),				Thermal conductivity W/mk				Compressive strength MPa				Tensile strength, MPa				Density g/cm^3			
		Petro-type	No.	C min	C max	C aver	No.	Kp min	Kp max	Kp aver	No	Kpr min	Kpr max	Kpr aver	No	min	max	aver	No.	min	max	aver	No.	min	max	aver	No.	min	max	aver
500	260-350	Pink granite	6	70.05	71.53	70.94	10	0.60	3.00	1.84	4	13.4	56.8	37.0	70	1.99	2.65	2.39	2	105.4	155.2	130.3	2	8.4	8.8	8.6	12	2.60	2.62	2.61
	350-500	-"-	4	70.25	71.44	71.00	35	1.25	2.05	1.61	13	1.13	6.4	4.2	105	1.84	2.87	2.38	8	140.1	191.5	164.7	8	6.1	8.9	6.8	13	2.59	2.61	2.60
	500-715	-"-	5	68.04	70.37	69.82	49	0.75	1.85	1.29	57	0.65	10.0	4.0	191	1.98	3.09	2.37	28	129.3	194.2	154.0	28	5.1	13.8	8.4	55	2.57	2.63	2.61
	715-1000	Grey granite	11	69.73	72.51	71.56	30	0.90	1.75	1.32	6	3.80	6.4	5.1	158	1.87	2.92	2.31	29	131.0	187.3	146.6	30	6.9	14.4	9.4	36	2.52	2.63	2.61
	1000-1300	-"-	7	70.22	73.22	71.84	24	1.15	2.10	1.43	-	-	-	-	101	1.87	2.87	2.31	8	122.0	169.8	136.6	8	6.1	9.0	7.6	22	2.59	2.63	2.61
	1300-1650	-"-	6	71.10	71.81	71.45	27	0.60	1.65	1.37	-	-	-	-	32	1.91	2.72	2.31	4	110.8	163.0	134.5	4	6.4	7.3	6.8	21	2.60	2.64	2.62
	1650-1800	-"-	4	70.23	71.25	70.69	6	1.40	2.00	1.59	7	2.4	12.4	6.0	-	-	-	-	3	103.5	173.6	139.3	3	5.7	8.9	7.8	9	2.60	2.61	2.61
T1	1400-1600	-"-	10	69.25	72.47	70.62	5	1.30	1.70	1.44	19	0.5	6.2	2.5	15	2.16	3.00	2.43	-	-	-	-	-	-	-	-	18	2.59	2.69	2.61
	1600-2000	-"-	20	68.51	73.56	71.50	19	1.25	2.00	1.66	22	0.5	21.0	5.2	44	1.78	2.70	2.25	10	114.5	200.0	142.4	-	-	-	-	26	2.59	2.72	2.62
	2000-2600	-"-	15	68.32	73.33	70.73	13	1.37	2.55	1.93	9	0.2	24.0	10.7	79	1.72	3.84	2.07	20	72.6	177.6	138.8	11	4.2	10.3	5.9	16	2.49	2.74	2.61
	2605-2850	-"-	5	69.04	70.85	69.70	18	1.70	2.35	2.15	5	3.7	47.0	24.0	24	1.66	2.54	2.01	7	67.4	175.6	114.5	8	3.7	9.7	5.4	34	2.57	2.72	2.60
	2850-3000	-"-	4	67.40	69.43	69.02	11	2.05	2.77	2.58	2	35.0	85.0	60.0	5	1.66	1.90	1.80	2	103.5	130.6	117.0	3	3.5	6.2	4.8	16	2.58	2.62	2.60
	3000-3525	-"-	14	69.02	73.02	70.64	33	1.60	2.82	2.10	10	0.45	24.0	11.0	65	1.58	2.67	2.14	22	61.2	184.2	118.5	49	3.5	10.5	4.9	93	2.55	2.74	2.59
	3525-3750	-"-	4	69.05	70.84	69.87	32	1.82	2.80	2.28	-	-	-	-	16	1.62	2.43	2.01	2	64.6	106.6	85.6	15	3.2	5.3	4.4	82	2.57	2.63	2.59
	3750-3835	-"-	4	71.10	71.48	71.48	8	1.45	2.87	2.04	-	-	-	-	6	1.52	2.22	2.05	1	106.4	106.4	106.4	6	3.7	7.4	5.0	12	2.57	2.60	2.59
	3835-4000	Leuco-crate granite	32	72.21	76.44	74.10	12	2.02	2.40	2.13	-	-	-	-	31	1.58	2.48	1.81	4	75.0	88.8	83.7	4	2.9	6.4	4.3	26	2.55	2.58	2.57

Table 5-2. Mineral composition of granites in the Eldjurtinsky massif.

No.	Rock type	Potassium feldspar	Plagioclase	Quartz	Biotite	Muscovite	Accessory minerals
1	Medium to coarse-grained "grey" granite	26.6	39.2	27.0	7.1	-	0.1
2	Fine to medium-grained "grey" granite	24.2	41.5	26.9	7.3	-	0.1
3	Medium to coarse grained "pink" granite	23.6	40.6	27.6	8.2	-	T*
4	Medium grained "pink" granite	26.8	41.0	25.9	6.3	-	T*
5	Leucocratic granite	34.1	27.5	32.5	6.5	1.5	T*
6	Granite-aplite dykes	23.6	32.9	40.7	2.6	0.2	T*

* *Mineral present only as traces*

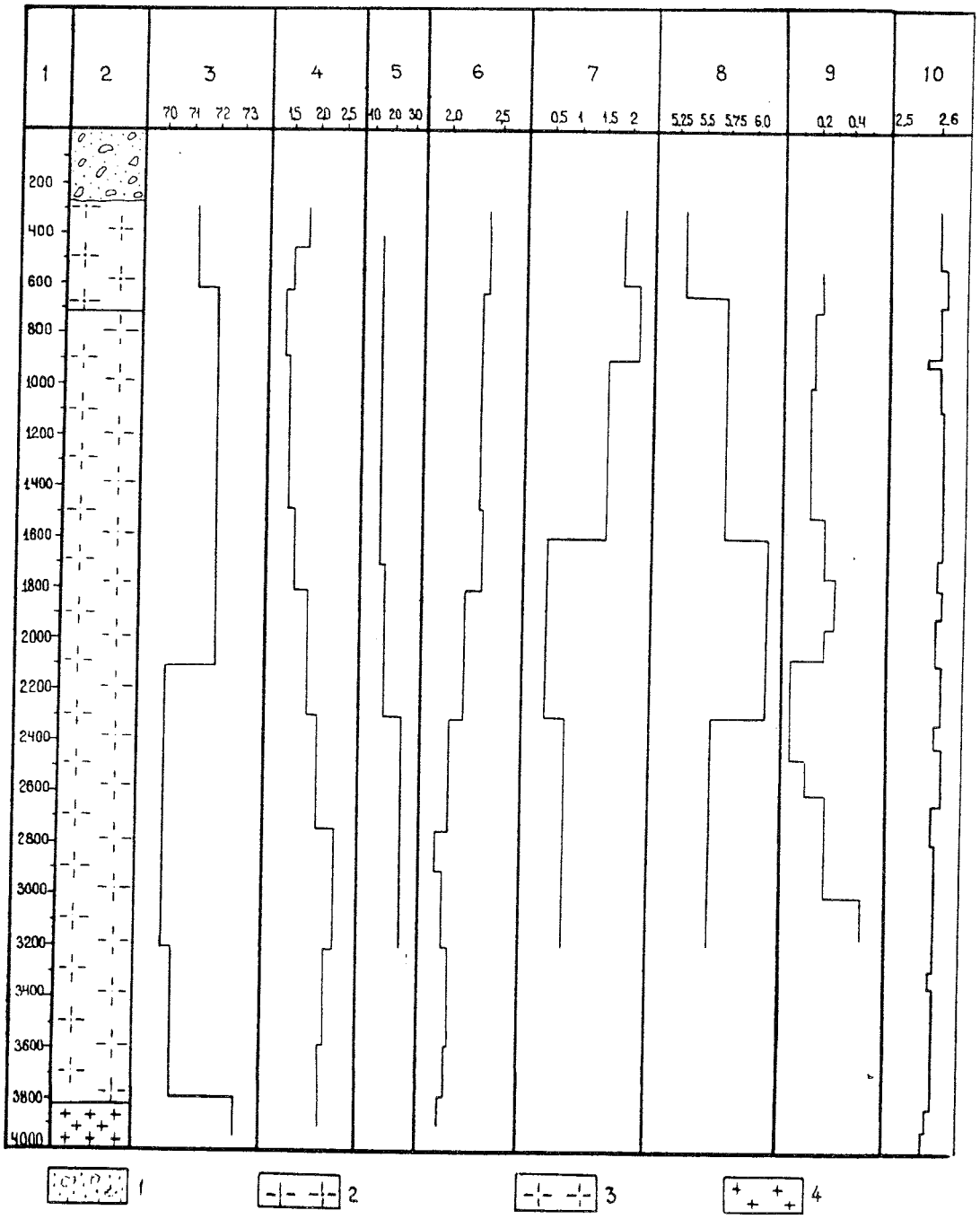

Fig. 5-5. *SiO_2 content and petrophysical parameters in the Tyrnauz borehole.*

Legend

(1) Freshwater and glacial deposits (2) "Pink" granites (3)"Grey" granites (4) Leucocratic granites

Vertical column

(1) Depth, m (2) Geological column (3) SiO_2 content, % (4) Open porosity, % (5) Permeability, mD . 10^{-2} (6) Thermal conductivity, W/mK (7) Fracture frequency, 1/m (8) Formation velocities from VSP (Vp), km/s (9) Poisson's ratio (10) Density, g/cm^3

Legend to Fig. 5-6.

1) Depth, m
2) Lithological column


Pink granite

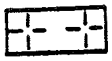
Grey granite

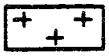
Leucocratic granite

3) SiO2, %
4) Al2O3, %
5) Fe2O3, %
6) FeO, %
7) CaO, %
8) Ti, ppm
9) Cs, ppm
10) Ni, ppm
11) Li, ppm
12) Rb, ppm
13) carbonate
14) chlorite
15) sericite
16) muscovite
17) quartz

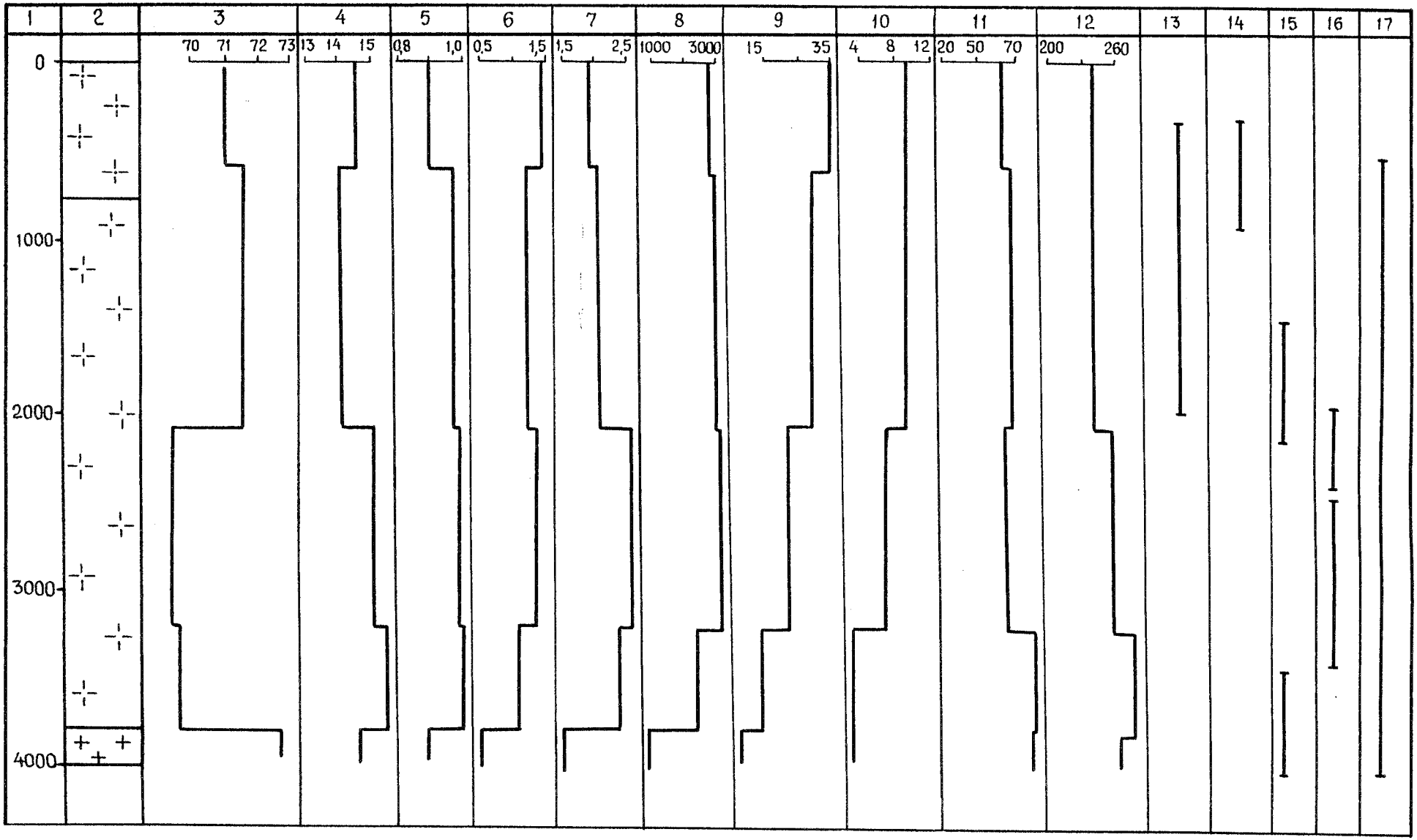

Fig. 5-6. *Petrogenic oxides, geochemical characteristics and fracture fillings in the Tyrnauz borehole.*

5.2.2 Fractures and fracture zones

Identification and characterization of fracture zones (Table 5-3) was done on the basis of core information and borehole geophysics (Fig. 5-7) including:

- broad-range acoustics
- neutron-gamma logging
- gamma-gamma logging
- neutron-neutron logging
- caliper logging
- caliper and dipmeter logging
- borehole televiewer.

Two groups of tectonised zones are found in the penetrated section:

Crush zones — Zones of intense stress-induced fracturing and shattering. Slip surfaces are perpendicular or parallel to the direction of the zone. Mylonite and cataclasite may be present.

Fracture zones — Bands with a dense network of tectonic fractures, such that the fracture frequency is markedly higher than in the surrounding rock. Zones are characterized by formation of tension fractures parallel to, or at an angle to the strike of the zone.

Crush and fracture zones were characterized by maximum values of magnetic susceptibility in combination with decreased apparent resistivity and thermal gradient. Crush zones and, very rarely, also fracture zones were characterized by low rock strength and constant gamma-ray activity. In very few cases, an increase of gamma-ray activity related to hydrothermal mineralization could be observed. Acoustic methods clearly showed changes in rock mass integrity.

Investigations of the near-borehole environment helped to define five fracture systems [3:7]:

1) A system of steeply dipping (80-85° $\pm$10°) fractures,striking 280-290°. Most of the aplite dykes are connected to this system. Fractures are rectilinear with rough surfaces. They are defined as ruptures.

2) A system of steeply dipping (80-85° $\pm$10°) fractures, striking 0-10°. Fractures are usually closed, and have no connection to dykes.

3) A system of conjugate fractures striking 310-320° and forming an angle of 45° with ruptures.

4) A system of conjugate fractures striking 40-50° and forming an angle of 45° with ruptures.

5) A system of gently dipping (10-30°) fractures, striking 260-270°.

Fracture zones identified in the borehole were grouped in three types:

Type I Strike 286° and dip angle 60-80° SW, extending up to 10-15 km.

Type II Strike 331-356°, dip angle 40-80° SW, extending up to 2 km.

Type III Strike 3-26°, dominating dip angles 60-80° NW, extending up to 1 km.

Fractures within fracture zones are oriented symmetrically, asymmetrically and chaotically. In crush zones with cataclastic and mylonitized rock, fracturing is non-systematic. Mineralized fractures were found in all three types of zone. Their typical width was 3-15 mm, compared with 3 mm for mineralized fractures in sections outside fracture zones.

Subhorizontal fractures of both tectonic and artificial (drilling-induced) origin were also recorded along the borehole. However, due to the difficulties encountered both in detecting these fractures and identifying their origin, they will not be further discussed.

Table 5-3. Classification of fracture zones.

Fracture zone interval, m	Width of fracture zone, m	Dip, deg.	Strike, deg.	Coefficient of total porosity by NNL	Notes
I type					
326.0-327.7	0.75	64	286	4.0	
365-372	2.4	80	286	5.0	Crush zone
526-533	1.5	78	286	3.0	
795-801.5	4.0	72	286	5.0	
1580-1700	50.4	65	286	16.0	Crush zone
2032.7-2034	0.3	75	286	2.0	
3140-3205	16.2	75	286	5.0	
II type					
355-365	3.6	80	331	5.0	Crush zone
772-775	2.0	49	331	4.0	
1007-1017	4.7	43-60	331	9.0	
1138.7-1156.5	3.9	40-77	331	4.0	
1260.5-1262.8	1.6	46	336	7.0	
1317-1335.5	6.3	68	356	4.0	
1907-1921.3	6.4	56-63	331	6.0	
2563.3-2566.1	0.6	77	356	4.0	
3013-3045.6	11.1	51-80	356	5.0	
III type					
341-343.2	0.63	73	3	3.5	
398.6-409.5	2.1	79	16	6.0	
464-478	4.8	71	20	6.0	
514-518.5	1.4	72	26	3.0	
613-621	4.0	60	41	11.0	Not clearly distinguished crush zone
900-931	5.9	79	16	10.0	
931-940	3.1	69	20	6.0	
1025-1034.1	4.0	64	16	9.0	
1178.5-1193.3	3.3	69	6	6.0	
1400-1440	12.4	41-72	6	6.0	Strike is determined conditionally
144.5-1449.3	13.2	66-76	16	5.0	
1528-1534.6	2.2	64-71	6	4.0	
1758.4-1760.8	0.6	75	26	2.0	
1766-1805	8.2	78	16	2.0	
1841-1889.5	8.2	80	16	1.5	
1940-1998	10.0	80	16	1.5	
2072-2073.6	0.6	79	16	4.0	
2287-2312.6	16.9	49	16	4.0	Crush zone
2884.2-3013	5.2	79	16	4.5	
Non-classified zones					
3475-3489	4.0	N. d.	N. d	N. d	
3510-3523	4.0	N. d	N. d	N. d	
3600-3616	4.0	N. d	N. d	N. d	
3707-3720	45.0	N. d	N. d	N. d	
3863-3866	N. d	N. d	N. d	N. d	

N.d: Not detected

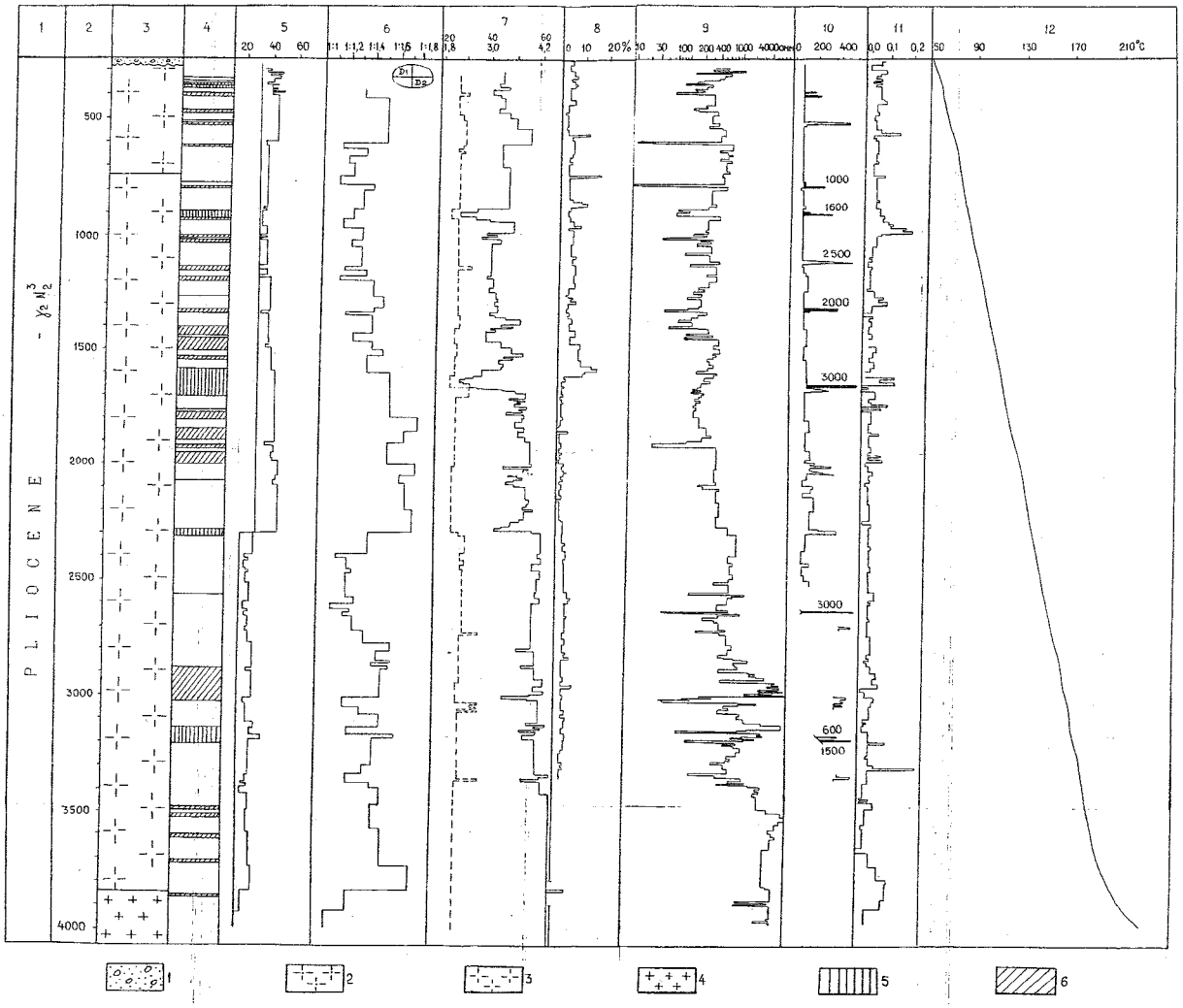

Fig. 5-7. Geophysical borehole logging results and inferred fracture zones.

Legend

1 Freshwater and glacial deposits
2 "Pink" granite
3 "Grey" granite
4 Leucocratic granite
5 Crush zones
6 Fracture zones

Vertical column:

1 Age, index
2 Depth, m
3 Geological column
4 Fractured and crushed zones

Results of geophysical investigations (5-12)

5 Caliper log, cm
6 Ratio between long and short axis of the borehole cross section
7 Gamma-ray log, mcr/h and neutron gamma-ray log, arbitrary units
8 Coefficient of total porosity, from neutron-neutron log data, %
9 Lateral log, Ohmm
10 Magnetic susceptibility log,CI-units
11 Thermal gradient, K/m
12 Temperature, °C.

5.2.3 Stress conditions

Evaluation of the regional stress field and its history as related to the tectonic evolution was based on structural-paragenetic analysis of fracture tectonics, faults and other zones of deformation. The Caucasus is characterized by submeridian compression. This is manifested by the presence of disjunctive shear structures (sublatitudinal faults and thrusts, right-lateral separation with north-eastern strike) of different orders - from fractures to transregional deformation zones [3:11].

An other stress regime, related to the Alpine folding and having its origin in the global tectonics of the Caucasian region, can also be distinguished. It is characterized by highly anisotropic horizontal stresses, with the maximum compression oriented northeast-southwest. Compressional, shear- and extensional structures attributable to this stress field are found. They are overlain on the structural pattern related to the main paragenesis, and are oriented 30-45° clockwise to this pattern.

Field investigations of the structural paragenesis often showed effects of stress alterations governed by specific structures. Extensive fracture mapping at some locations within the Pshekish-Tyrnauz zone revealed disjunctive deformation corresponding to a considerable diversity of geomechanical conditions. In the eastern part of the Pshekish-Tyrnauz zone, highly compressed, sometimes inverted, narrow linear folds with sublatitudinal strike occur. This, together with a large variety of fracture patterns, indicates the presence of thrust- and-strike slip faults.

The stress field within the Eldjurtinsky granite massif was indirectly characterized on the basis of results from regional geodynamic investigations, borehole geophysics and laboratory investigations of core samples. Furthermore, observations of borehole geometry and stress measurements were made in the Tyrnauz borehole. Horizontal compression is a predominate characteristic of the stress field. This has been verified by analyses of focal plane mechanisms for earthquakes in Caucasus, which also show a northeast southwest orientation of the maximum horizontal stress (Fig. 5-1).

Investigations of thin sections also revealed randomly distributed artificial cracks. The nature of this cracking showed that it was initiated as a consequence of relief of high compressive stresses. The intensity of cracking increased with depth. Furthermore, core discing was observed in all holes previously drilled in the Eldjurtinsky massif. In the Tyrnauz borehole, core discing started at a depth of 520m, corresponding to +800 m in terms of absolute level. In the upper part, the initiated fractures were spaced several metres along the hole, at 1200-2000 m by up to several centimetres, and down to a depth of 3870 m spacings were several millimetres to several centimetres.

Stress anisotropy in the horizontal plane was inferred from determinations of borehole geometry by means of caliper logging (Fig. 5-7), and also from hydraulic

fracturing stress measurements. The borehole cross section was generally found to be elliptical, with an axis ratio that varied with depth. The orientation of the elongations, however, was not dependent on depth, structural-textural conditions or mineralogical composition (excluding granite-aplite and liparite dykes, where the borehole section was almost circular), but controlled by the orientation of the horizontal stress field. Thus, the orientation observed correspond to a northeast southwest direction of the maximum horizontal stress (azimuth 190-205°). The borehole sections generally stabilized 22-24 hours after the onset of the break-out process.

Hydrofracturing tests were made at the interval 3721-3820 m. The maximum and minimum horizontal stress components were 89 MPa and 31 MPa respectively. The calculated, effective vertical stress (lithostatic) was 60.2 MPa.

The tensile strength of the rock varied from 3.1 MPa to 105 MPa, and the uniaxial compressive strength ranged between 61.2 MPa and 250 MPa.

At a depth of 600 m, the open porosity decreases, VSP velocities increase (Fig. 5-5) and the content of petrogenic oxides changes (Fig. 5-6). In the interval 1600-2300 m the open porosity and VSP velocities increase, and the fracture frequency drops considerably.

5.2.4 Hydrogeology, groundwater chemistry and gases

The Tyrnauz borehole is contained within an hydrogeological domain defined by the Eldjurtinsky granite massif. The Paleozoic rock hosting the granite forms another hydrogeological domain. The groundwater in the rock is essentially carried in fractures and veins.

The middle Paleozoic, metamorphic rock is hydraulically connected to the Pshekish-Tyrnauz zone. Faults and fracture zones form flow paths in a system of deep circulation, often involving considerable water flows. Large quantities of water are stored under pressure (3-4 MPa) in fractures and cavities. Inflows into mine workings reach 400 l/s (mine No 16, Dec, 1967). In the carbonate rock, the hydraulic zonation is vertical. In the upper part of the mine (+2600 m absolute level), the water contains hydrocarbonate-sulphate and calcium magnesium; on intermediate levels (+2300 m) sulphate-hydrocarbonate, and on deep levels it contains chloride-hydrocarbonate and sodium-calcium.

The Eldjurtinsky granite massif is characterized by a mountain relief causing rapid hydrogeological processes, with active drainage of water-bearing zones and aquifers. Over the drilled section of the granite, three systems of discharge were defined; a local subsurface flow, a regional subsoil run-off, and a deep flow system [3:6]. The two shallow systems are formed in surface and diluvial deposits in slopes and in the

weathered zone of the bedrock. They are controlled by seasonal variations. The deep flow system is formed at depths of several hundreds of metres, and incorporates the upper few kilometres. It is connected to regional and local fracture zones. Hydrochemical zonation within the massif has not been thoroughly investigated. In brief, zones of fresh water, salt water and brines have been distinguished (Fig. 5-8).

The water of Quarternary alluvial, diluvial and proluvial deposits in the Eldjurtinsky massif contains hydrocarbonate calcium-magnesium and magnesium-calcium at concentrations of 0.1-0.2 g/l.

In the shallow rock, the existing, extensive fracture network in the granite is affected by weathering, resulting in widening of the fractures. This facilitates penetration of surface water into the bedrock. Fracture zones are generally hydraulically interconnected, and thus an integrated discharge system is formed. The water contains chloride-hydrocarbonate and calcium-magnesium.

In the zone of active drainage, no emission of gas was observed in the boreholes down to 750 m (anomaly factor $K\alpha < 1$). The first gas entrance was encountered in borehole No 104 at a depth of 751.8 where the fluid pressure exceeded the theoretical hydrostatic pressure, due to gas saturation of the groundwater. The yield of gaswater mixture from the borehole was 0.08-0.1 l/s under its own pressure. The gas was mostly carbonic acid (Table 5-5). Systematic observations indicate carbonmonoxide water in isolated fracture zones within the Eldjurtinsky granite.

In the Tyrnauz borehole, a drill-stem test (KII-2M-146 tester) was carried out to investigate three intervals; 602-706 m, 751-916 m and 1149-1230 m. Results are given in Tables 5-4 and 5-5. Differential pressures within the tested intervals varied from 4 MPa to 6.9 MPa. There was no inflow into the uppermost interval, but the other two yielded gas and mineralized water. The waters were blackish, sulphide-hydrocarbonate-chloride sodium, lime, neutral and very hot. By its isotopic content, ($\delta^{18}O$ -10.3 per mille; δD -90 to 100 per mille) the water corresponds to a meteoric type of glacial origin.

In borehole No 1500 (a pilot hole) measurements were made using SHCHP and RETS-2 flow meters. Measurement intervals were 10-20 m, except in sections showing inflow, where 1 m intervals were used. Large inflows into the borehole were recorded. The first occurred at a depth of 80 m, where the inflow was 0.8 l/s. At 130 m, the rate of inflow rose to 0.9 l/s. The interval 530-550 m involved drill string retrieval. At depths of 820-840 m and 860-900 m, minor inflows were again observed. Furthermore, groundwater sampling (wireline, PD-3m sampler with volume capacity 750 cm^3) and pressure recordings were made at depths 900, 1140, 1290, 1310 and 1800 m in borehole1500. Results of the hydrochemical analyses are presented in Table 5-4.

The information obtained consistently shows that the water is sulphate-hydrocarbonate-chloride, mostly sodium, neutral and blackish. Hydrochemical zonation at depth is poorly developed; Over the depth interval investigated, there is active drainage and uniform mineralization of the water from the host rock. This is further verified by the stable content of microcomponents. The water temperature increases distinctly with depth. Over the interval 900-1500 m, the thermal gradient averages 49 K/km.

There is no regularity of changes in the anomaly factor with depth, which might be explained by different levels of gas saturation of the groundwater. Thus, the value of the gas factor accounts for 4.47 dm^3/dm^3 at 900 m, 4.37 dm^3/dm^3 at 1140 m and 6.99 dm^3/dm^3 at 1300 m. The total gas pressures are 9.87 MPa, 7.2 MPa and 7.78 MPa respectively, and 0.62 MPa at 1500 m (Table 5-6).

The zonation is characterized by nitric oxygen water in the upper parts, which is then replaced by nitric and nitric methane water.

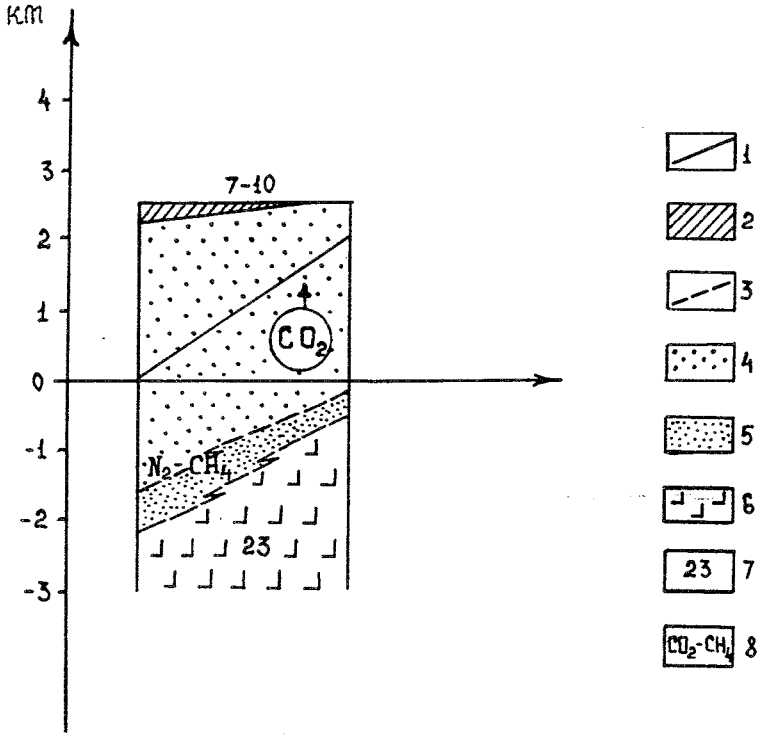

Fig. 5-8. Schematic illustation of hydrochemical zonality of the Caucasian folded region.

Legend

(1) Location of regional drainage basis (2) Permafrost zone (3) Boundary between hydrochemical zones (4) Fresh water (5) Salt water (6) Brines (7) Mineralization of salt water, g/l (8) Water gas content

Table 5-4. Results from water chemical analyses

No.	Borehole	Sampling interval, (m)	Unit	Cations								Anions			Compounds		Total mineral amount	Dry residue	pH	CO		Hardness	
				Na	K	Na+K	Ca	Mg	NH	Fe^{2+}	Fe^{3+}	HCO_3	Cl	SO_4	H_4SiO_4	$Fe(OH)_3$				Agres.	Free	Total	Reducible
1	1500	900	mg/l	1850.0	125.0	-	92.8	59.9	15.0	75.0	-	1928.2	2045.5	293.8	98.4	8.6	6592.5	5790	6.6	-	-	-	-
2	1500	900	-"-	1940.0	125.5	-	96.8	25.2	1.5	5.0	-	1940.0	1969.4	372.8	148.8	14.3	6639.7	5996	6.5	6.9	6.9	-	-
3	1500	1258	-"-	2357.5	157.4	-	85.2	24.1	5.0	N.d.	-	2452.2	2258.1	442.8	299.2	N.d.	8081.5	6920	7.6	6.23	6.23	-	-
4	1500	1356	-"-	2523.6	161.5	-	59.2	33.5	N.d.	N.d.	-	1330.2	2942.9	423.0	38.8	N.d.	7512.7	6960	7.4	-	-	5.74	5.71
5	T-1	1149-1230	-"-	2740	165.0	-	117.0	54.2	5.0	-	55.8	3160.7	2483.5	470.7	120.0	8.5	9380.4	7400	7.0	-	-	10.3	10.3
6	104	756.8-872.4	-"-	-	-	3380	155.5	48.0	-	-	178.5	3451.2	4933.8	440.3	154.4	-	13142.2	12432	Eh +260	-	1793	-	-

	Microcomponents, mg/l																					
No	Mn	Mo	As	HBO	Br	J	Li	Rb	Cs	Sr	Cu	Cr	Zn	Pb	Ag	F	B	Be	Se	Hg	U	Ra
1	0.8	0.004	0.01	-	-	-	16.7	-	-	2.2	-	<0.004	<0.005	<0.005	-	1.9	0.01	<0.0002	<0.00001	<0.002	2.5×10^{-4}	0.04×10^{-7}
2	0.9	0.01	0.008	-	-	-	17.8	-	-	2.3	-	<0.004	<0.005	<0.005	-	1.0	0.005	<0.0002	<0.0001	<0.002	9.5×10^{-4}	0.06×10^{-7}
3	0.2	0.0006	0.5	-	-	-	20.6	-	-	3.0	0.002	<0.004	<0.005	<0.005	-	5.1	-	0.005	<0.001	0.004	$<2.5 \times 10^{-4}$	0.75×10^{-7}
4	1.2	0.006	0.08	-	-	-	20.9	-	-	2.6	-	<0.004	0.8	<0.005	-	5.0	0.6	<0.0002	<0.001	0.005	$<2.5 \times 10^{-4}$	$<0.01 \times 10^{-7}$
5	-	0.018	0.06	1246.1	6.3	8.8	20.7	0.8	0.7	4.6	<0.002	-	-	<0.005	0.001	2.3	-	-	-	-	-	-
6	2.4	-	-	84.9	16.98	7.96	280.8	-	-	2.2	0.052	-	-	-	-	4.95	-	-	-	-	-	-

N. d.: Not detectable
-: Not evaluated

Table 5-5. Results from packer tests in the Tyrnauz borehole

No.	Interval, m	Trip	Average inflow m^3/h	Average differential pressure DP_0 MPa	Hydraulic conductivity	Formation pressure MPa	Actual productivity, $\frac{m^3}{day\ MPa}$	Potential productivity, $\frac{m^3}{day\ MPa}$
1	602-760	I	No water seepage					
2	751-916	I	13.2	5.27	3.2	8.34	2.5	-
		II	4.1	5.35	-	-	0.77	6.6
3	1149-1230.5	I	61.4	9.38	2.2	12.17	6.5	1.9

The mineralized water discovered in the Tyrnauz borehole differs widely from the background hydrocarbonate fresh water. The increased hydrothermal gradient near the intervals tested indicates the inflow of meteoric water conveyed from deeper levels by upwards flow through fracture zones. These zones are probably hydraulically connected to a groundwater recharge area. From this area, the meteoric water flows downward through fracture zones, is heated, causes dissolution of the rock along its way, and finally discharges on surfaces as mineralized solutions. At the same time large tectonic crush zones are characterized by considerable, negative values of the geothermal gradient ($\Delta T > 0.4°$), as shown in Fig. 5-9. This indicates downward flow detected to a depth of 3780-3800 in the Tyrnauz hole.

In summary, active circulation probably prevails down to a depth of 1500-1750 m from the roof of the granite. Down to this depth, hydrocarbonate calcium-magnesium and magnesium-calcium water is found. In the uppermost part, down to a depth of 300-500 m, the water is fresh with a mineralization of 0.1-0.4 g/l. Below this level, sodium hydrocarbonate concentration increases. The increase in the degree of mineralization is irregular, and the water is hundreds of years old or more. The total porosity as obtained from neutron-neutron logging is 4-6%. From core samples, the open porosity was determined at 1.5-1.75 % and permeability at 0.04-$0.37 \cdot 10^{-15}$ m^2.

Table 5-6. Groundwater gas saturation and gas composition.

No	Borehole No: 1500	Gas factor l/l	Dry residue g/l g/mole/l	Gas components																
				N_2			CH_4			CO_2			He			H_2			O_2	Total gas
				%	Coefficient of solubility ml/l	Elasticity	%	Coefficient of solubility ml/l	Elasticity	%	Coefficient of solubility ml/l	Elasticity	%	Coefficient of solubility ml/l	Elasticity	%	Coefficient of solubility ml/l	Elasticity	%	pressure kgs/sm² MPa
1	Spontaneous inflow, Q=0.8-1 l/s depth 900 m	4.47	8.348 0.14	18.08	9.9	85.64 8.56	1.42	18	3.52/ 0.35	79.55	380	9.35 0.94	0.035	7.8	0.2 0.02	0.006	15.8	0.02 0.002	0.47	98.73 9.87
2	Spontaneous inflow Q=0.8-1 l/s depth 1140 m	4.37	7.636/0.13	12.99	9.7	58.56 5.86	1.36	17.3	3.44 0.34	85.63	380	9.85 0.99	0.022	7.9	0.12 0.012	-	-	-	0.22	71.97 7.2
3	Spontaneous inflow Q=0.8-1 l/s depth 1300 m	6.99	8.780 0.15	7.75	9.5	57.00 5.7	0.94	17.1	3.86 0.33	91.29	380	16.79 1.68	0.011	7.7	0.1 0.01	0.003	15.8	0.01 0.001	0.25	77.76 7.78

Below 1750 m and down to the bottom of the hole, there is a zone of obstructed groundwater circulation. The water is sulphate-hydrocarbonate-chlorite, mostly sodium, with a total mineralization of 6-13 g/l or more. The low permeability of the rock (K_{int} = 0.19 $\cdot 10^{-15}$ m^2 within the interval 3721-3820 m) inhibits circulation, implying long residence times. Total porosity (neutron-neutron logging) is 2-6 % and open porosity (core samples) is 1.3-2.6 %. A zone of chloride water is predicted below the borehole bottom, i.e. at depths exceeding 5500 m from the roof of the granite massif. This zone is connected with direct evolution and diffusion of water from the magmatogenic host rock [3:6].

Hydrochemical zonation is disturbed in fracture zones, where the permeability is an order of magnitude higher than in the undisturbed rock. Mineralization is usually enhanced, and the mineral distribution does not correspond to the sampling depth. This suggests the formation of water at depths differing from that of its present location, as sampled in the Tyrnauz borehole.

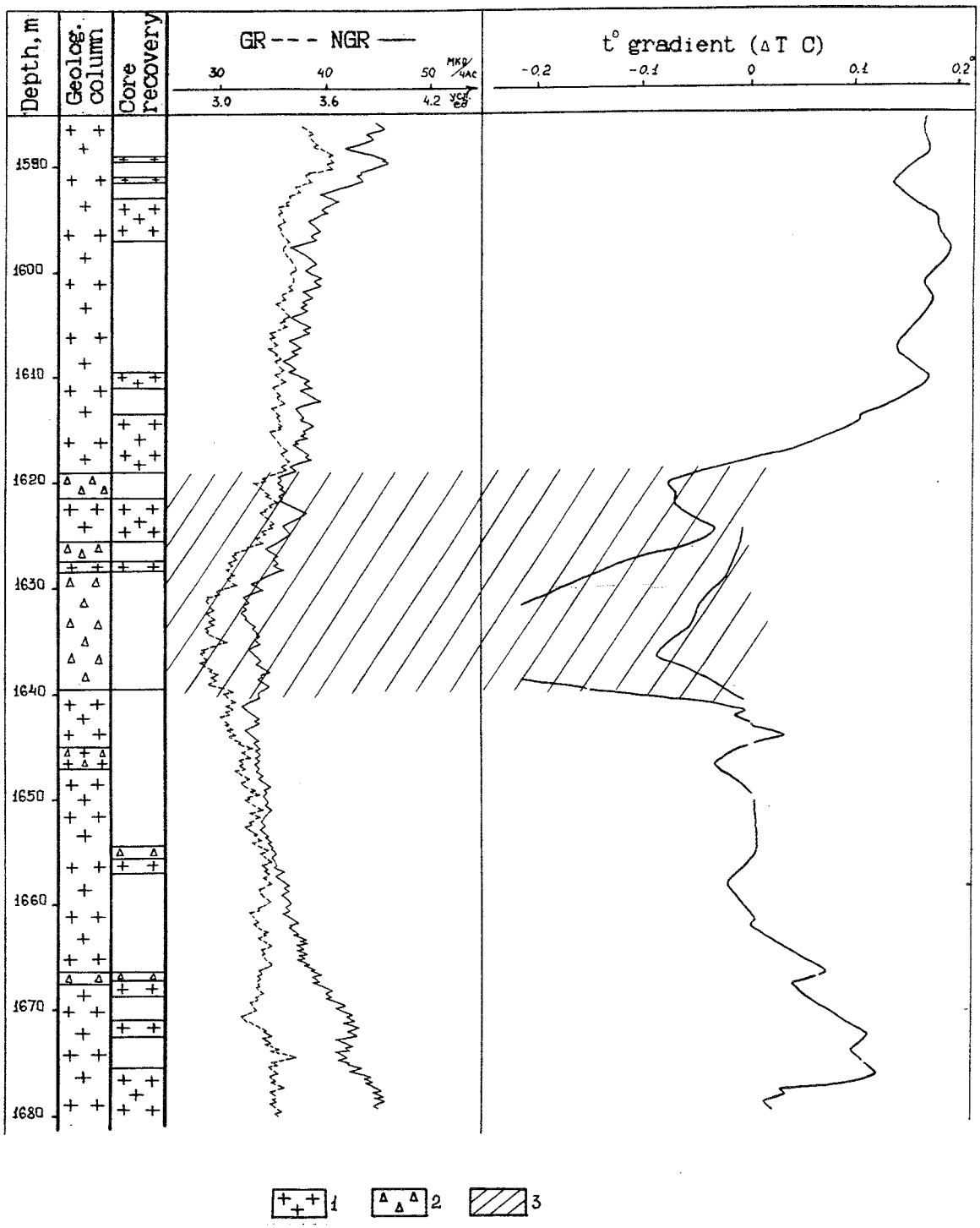

Fig. 5-9. Characteristics of a fracture zone in the interval between 1620 and 1647 m in the Tyrnauz borehole

Legend

1 Granite
2 Tektonite
3 Zone of downward filtration
GR = Gamma Ray
NGR = Neutron Gamma Ray

5.2.5 Thermal conditions

The Tyrnauz borehole is located within a thermally strongly anomalous zone [3:9]. Temperature measurements were made at 100 m intervals in the borehole, using a TR-7 thermometer with an accuracy of ±0.5°C. Prior to measurements, conditions were allowed to stabilize for periods varying from several hours up to a month. The hole collar temperature was +18°C and the hole bottom temperature (4001 m) was +223.5°C. Within this interval, data indicated the following thermal zones:

1)	Seasonal variations	from 0 m to 50 m
2)	High gradients	from 50 m to 220 m
3)	Inconsistent gradients	from 220 m to 3835 m
4)	High gradients	from 3835 m to 4000 m

A temperature increase was observed in the uppermost 100 m of the bedrock. This was due to the presence of a finely dispersed pelitic material with low thermal conductivity in the Quarternary deposits of the area.

In the zone with inconsistent gradients (both positive and negative), low gradients coincide with crush zones and boundaries between tectonic blocks. Other factors that might contribute to the decrease in thermal gradient include hydrothermal alterations of the granite (2500-2700 m, 3000-3100 m), ore mineralization, etc.

An abrupt change in the thermal gradient is observed at 3835 m, below which the gradient increased. This increase corresponds to the petrographic change from grey granite to leucocratic granite, prevailing below 3835 m. There is no corresponding change in the thermal conductivity, and the increase in the thermal gradient may be due to heat convection by discharge of thermal water.

Measurements of thermal properties were made on core samples, using JT-S-400 and TT-λ-400 devices and "λ-profile" scanner (942 samples). Measurement errors were ±10, 5 and 8 % respectively (Table 5-2, 5-7; Fig. 5-5) [3:10]. The thermal properties within the Eldjurtinsky massif were found to be homogeneous, both vertically and laterally. The vertical average of the thermal conductivity is λ=2.29 W/mK, varying from 1.52 to 3.09 W/mK. Defining the coefficient of thermal inhomogeneity, β as: $\beta=\lambda_{max}-\lambda_{min}/\lambda_{aver}$, this coefficient assumes values of 0.17-0.25. The relatively high values reflects the porphyrid texture of the rock.

Samples displaying chloritization and quartzitization are characterized by high thermal conductivity (2.9-3.0 W/mK). Highly fractured intervals and crushed zones correspond to low values (1.8-2.0 W/mK).

In brief, the area can be divided into two large petrothermal zones. The lower zone, characterized as relatively homogeneous with low thermal conductivity (λ_a=2.30

W/mK; std.dev. 0.39 W/mK) is the Eldjurtinsky massif. The upper zone, which is thermally inhomogeneous and shows high conductivity, is the host rock. The upper extreme conductivity values in this zone are characteristic of terrigenous rock of the Mukulansky suite (λ_a=3.29 W/mK; std.dev. 0.56 W/mK).

Investigations of core samples from the interval with "grey" granite (715-3835 m) showed that the open porosity increases from 1.32-1.42 % to 2.58 % in the interval 2850-3000 m, and then decreases to 2.1-2.28 % (Table 5-2, Fig 5-5). The density remains practically unchanged (2.68-2.69 g/cm^3).

In the central part of the granite, there are sections with high porosity and high permeability of the rock matrix (permeability coefficient increases from 4-6 to 24-60$\cdot 10^{-15}$ m^2), low bulk density and low acidity (SiO_2 content decreases from 71.56-71.84 to 69.02 %).

Table 5-7. *Range of variation of the thermal conductivity in different boreholes within the Eldjurtinsky massif.*

Borehole:	S-1501	S-600	S-104	S-1393
Min	2.12	2.14	1.99	2.05
Max	2.51	2.44	2.48	2.62
Average	2.30	2.29	2.21	2.30

The given materials and special thermobaro geochemical investigations of melt (MI) and associated fluid inclusions (AFI) in faulty nuclei of quartz intrusions of the Eldjurtinsky massif (Table 5-8) suggested centripetal crystallization of melts into the massif with formation of a nucleation site of highly-flooded residue melt [3:12]. The granite crystallized from it is characterized by anomalous porosity and infiltration properties.

Table 5-9 compares the thermal conductivity of Eldjurtinsky granite with values for ancient granites, having almost identical density and very similar mineral composition. Despite these similarities, the conductivity of the Eldjurtinsky granite is found to be lower than that of the other granites. In the Eldjurtinsky granite, potassium feldspar is represented by anorthoclase, whereas in the ancient granites, it is represented by microcline. Evidently, these differences cause the discrepancy in thermal conductivity. Heat flow was calculated for the Tyrnauz borehole and also for holes S-1500 and S-1501. This was done using values of the geothermal gradient representing the depths 300 m and 500 m. Thus, avoiding the influence of the shallow zone with extreme thermal gradients.

Table 5-8. *Results of investigations of melt and associate fluid inclusions in faulty nuclei of quartz intrusions of granite in the Eldjurtinsky massif.*

No.	Absolute level of sampling, m	Depth from the roof of the massif, m	AFI presence	H_2O content, weight %	MI homogenization T°C
1	+2102	0.4	-	2.6±0.8/1/	895±9/64/
2	+2102	0.5	-	3.1±0.6/3/	
3	+1062	1040	+	3.8±0.5/5/	825±15/16/
4	+1027	1075	+	no data	no data
5	-202	2304	+	4.7±0.9(3)	760±5(61)
6	-238	2340	+	4.9±1.1(2)	
7	-1027	3129	+	5.5±1.0(3)	740±10(13)
8	-1321	3423	+	5.8±1.0(4)	740±10(42)
9	-1682	3784	+	7.6±1.7(2)	700(50)
10	-2181	4283	+	4.8±1.1(2) 7.0±2.20(1) 9.3±2.9(1)	720±10(42)
11	-2428	4530	+	9.8±2.2(2)	690±5(73)
12	-2681	4783	+	7.0±0.9(6)	720±10(11)

Notes: In No 10 the H_2O content was evaluated on the different intrusions. The numbers within brackets gives the number of inclusions investigated.

Gradient values derived were as follows:

Tyrnauz borehole:	300 m	47 K/km
	500 m	46 K/km
Borehole S-1500:	300 m-	47 K/km
	500 m	43 K/km
Borehole S-1501:	300 m	58 K/km
	500 m	57 K/km

This yielded the following heat flow values:

Tyrnauz borehole:	114±5 mW/m^2
Borehole S-1500:	109 mW/m^2
Borehole S-1501:	131 mW/m^2

The total heat flow measured near the surface is composed of [3:13]:

1) Radiogenic heat generated in the Earth's crust

2) Heat transferred from the mantle

3) Heat related to relatively short-term energy processes which are followed by redistribution of thermal energy.

In Prielbrusie (the Northern Caucasus) the radiogenic component of heat flow is 41 mW/m^2, which allows estimation of the mantle component to 70 mW/m^2 in the Tyrnauz area.

Table 5-9. *Thermal conductivity of granite from different regions in the USSR.*

No.	Rock charcterization	Age	Locality	Thermal conductivity, W/mK	Dispersion, W/mK	Number of tests
1	Granite porphyroid	AR	Ukrainian Shield	2.75	0.51	65
	Medium-grained granite	-"-	-"-	2.95	0.38	95
2	Granite	-"-	Baltic Shield	3.01	0.20	40
3	Medium and coarse crystalline granite	PZ_3	Northern Caucasus	2.91	0.20	136
4	Porphyroid (Eldjurtinsky granite)		-"-	2.30	0.15	455

6 A GENERALIZED MODEL OF THE THREE BOREHOLES

6.1 INTRODUCTION

In previous chapters, the upper 5 km of the Earth's crust, at the locations of the three boreholes, was characterized. The holes are located several hundreds of kilometres apart and represent different geological and tectonic environments. Thus, the Kola and Krivoy Rog boreholes penetrate ancient (2.3 billion years) low Proterozoic and Archaean complexes, and are located within the Baltic and Ukrainian crystalline shields of the Eastern-European platform. The Tyrnauz hole is located in a junction zone of a young (Cenozoic) Caucasian fold belt and the ancient Skif-Turansky plate.

The boreholes penetrate sections of different rock composition: Proterozoic volcanogenic-sedimentary deposits in the Kola borehole, Proterozoic metasedimentary complexes, Archaean granitoids in the Krivoy Rog hole and the young (2 million years) Eldjurtinsky granite in the Tyrnauz hole. In terms of silica content, the approximate figures are 50% in the Kola hole, 65-67 % in the Krivoy Rog hole and 70-72 % in the Tyrnauz hole. Thus, the formations penetrated ranges from basic to essentially acidic rocks.

The geothermal characteristics of the three areas are also different. Thus, in the Kola and Krivoy Rog holes the temperature at 4000 m depth does not exceed 70°C, whereas the temperature in the Tyrnauz hole at the same depth is 230°C. The thermal conductivity in the Kola and Krivoy Rog holes reaches 3.5-4.5 W/mK, but does not exceed 2.5 W/mK in the Tyrnauz borehole. Total heat flow is 100-120 mW/m^2 in the Tyrnauz area and 40-45 mW/m^2 in Krivoy Rog. These values are typical for young folded belts and ancient shields respectively. In the Kola area, the heat flow is to a considerable extent influenced by radiogenic heat transfer, and amounts to 65-70 mW/m^2 at 4000-5000 m depth.

Major differences are observed in the rock stress conditions prevailing in the three areas. The Tyrnauz borehole is located in a zone of active horizontal stresses related to the subduction of the Skifsky plate beneath the Eurasian plate. Fracture zones detected over the drilled interval dip steeply. High horizontal stresses initiated intense core discing throughout the borehole. The Kola and Krivoy Rog holes are located in areas of horizontal stress relief (maybe even slight tension) and the stress field is mainly governed by gravitational forces and metamorphism. In each borehole, at the interval 3800-4800 m, a zone can be distinguished that is characterized by reduced dip angles of fracture zones (to 20-30°) and severe borehole caving resulting in elliptical borehole cross sections.

Further differences between the three boreholes are observed as regards, for example, origin and chemistry of groundwater, mineral chemistry and physical rock properties. However, there are also a number of important common features related

to the structural, hydrogeological, hydrochemical and geothermal conditions that allows data to be compiled into generalized models. These aspects are further discussed below.

6.2 STRUCTURAL CONDITIONS

Firstly, it should be emphasized that fractures and fracture zones are abundant in all the areas investigated. Fracturing, in the form of random fractures or fracture systems is a common feature of all formations and boreholes investigated to depths of 1-2 km. There is practically no rock, accessed by outcrops or excavations, in which fractures are absent. Actual characteristics of fracturing under natural conditions at great depths were obtained by means of drilling the superdeep boreholes. As presented in previous chapters, the sections penetrated by all the boreholes display at least three categories of fracture: diagenetic (or endogenic), tectonic (or exogenic) and stress-relief fractures. The latter category may be referred to as "technogenic" or artifical, since they are not natural, but occur as a result of excavation or drilling. The in-situ, structural conditions at depth are determined by diagenetic and tectonic fracturing, of which the tectonic category dominates.

Diagenetic fracturing is in most cases associated with a specific stratum, sharply terminated at boundaries with other strata, and oriented parallel or at an angle to the stratification. Diagenetic fractures are developed in the process of lithification, change of volume, temperature etc. Sometimes, cleavage and fracturing connected with intrusion of dykes are referred to these categories. Characteristic features are the close connection with the matter composition of the rock, and fracture filling minerals that are dependent on the composition of the initial rock. Fractures associated with metamorphic processes were found in the Kola borehole. As a rule, fractures associated with progressive metamorphism are filled with material of similar composition to the host rock, whilst fractures formed later related to regressive metamorphism show a wider range of filling minerals. Tectonic fractures are associated with plicative and many disjunctive disturbances, and their spatial positions are concordant with the position of the disturbance. Tectonic fracturing includes tension fractures and shear fractures. Tearing-off fractures generally have insignificant extension and are rarely planar. Shear fractures are characterized by traces of sliding on the fracture walls, considerable extent and typically cut stratigraphic boundaries without changing orientation. Tectonic fractures are filled with various veinstone and ore-mineral associates.

The main fracture parameters (bedding elements, fracturing intensity, extent, mineral filling, etc) are dependent on a number of factors, including initial rock composition, degree of metamorphism, genesis of fractures, current and past stress fields, etc. In the Kola borehole, a relationship between fracturing intensity and rock type was established. Intensity was found to decrease from metamorphosed sedimentary rock to ultrabasites, tuffes of basic composition and basic intrusive

rocks. A similar reduction in fracture widths was also noted. Neither fracture frequency, nor the width of fracture zones depends significantly on depth. In all boreholes, the fracture frequency is 10-40 fractures/m throughout the investigated horizons. This excludes fracture zones, where the frequency increases by a factor of 5-10. Usually, the width of the individual fractures also increases within fracture zones. A more distinct depth dependency is noted in the relative proportions of shear versus tension fractures.

In the Kola borehole, shear fractures account for 10-30% of the total fracture count in the interval 0-3200 m. This figure increases up to 90% in the interval 3500-6700 m. The dip angles of fracture zones are also found be depth dependent. This is particularly well documented in the Krivoy Rog borehole, where dip angles of fracture zones decrease from 60-70° in the upper parts to 20-30° at a depth of 4000-5000 m. Subhorizontal fractures also occur at depth in the Kola borehole.

The width of individual fractures rarely exceeds 10 mm, and the width of fracture zones ranges from some metres to 50-80 m. More extensive fracture zones are disjunctive and tectonic. On the basis of geophysical investigations fracture zones are found to extend up to 10 km. Such, extensive zones identified on the surface were penetrated by the boreholes at depths of 4000-5000 m and more.

Most fractures are filled with fracture filling. Regardless of rock type, quartz, calcite and chlorite are found in practically all fractures. Minerals belonging to veinstones associated with the composition of the host rock include serpentinite, talc, chrysotile - asbestos, albite, epidote, actinolite, hematite and magnetite.

Common to almost all fracture zones is the fact that porosity and permeability is enhanced by more than one order of magnitude compared with the host rock. The geophysical characteristics (acoustic velocity, density, resistivity, etc.) change accordingly.

Altogether, the information available suggests that the depth interval within which fracturing, crush zones and zones of wide-temperature hydrothermal mineralization occur in crystalline basement extends down to 15 km [1:12].

Thus, a generalized structural model of the environment of a deep hole in such formations should include a system of fracturing and fracture zones comprising the entire depth interval considered. The major fracture zones involves tectonic (disjunctive and cleavage) fractures and diagenetic fractures with mineral infillings. At a depth of 3-4 km, subhorizontal or gently dipping fracture zones would be expected. More evenly distributed fracturing, involving fracture widths up to 1.5 mm, would be encountered over the entire section. Furthermore, relatively wide fracture zones (widths up to a few metres) are almost invariably found in the uppermost few hundreds of metres.

The spatial orientation of tectonic fractures is mainly governed by the orientation of a system of tensile and plicative structures, or to the stress field, including its variation during phases of geological evolution of the area. Diagenetic fractures are distributed in accordance with the lithologic-petrographic structure of the section or the directions of metamorphism.

Fracture zones at depths less than 1-2 km would be expected to exhibit considerably greater permeability, due to the stress conditions prevailing within this interval and to hypogenic processes.

6.3 GEOTHERMAL AND HYDROGEOLOGICAL CONDITIONS

The geothermal gradient varies very distinctly with depth. In all three boreholes it increases with depth. Neglecting local fluctuations related to fracture zones, specific intervals of the thermal gradient may be distinguished. For the Kola and Krivoy Rog boreholes these intervals coincide; A geothermal gradient less than 10 K/km corresponds to depths less than 1000-1200 m. From this depth and down to 2500-3000 m, the value is 10-15 K/km. Down to 4000 m it is 17 K/km, and below 4000 m it again increases to 20 K/km. In the Tyrnauz borehole two distinct intervals are distinguished with respect to the geothermal gradient; above 2800 m and below 2800 m. In the upper interval the value is 40 K/km and in the lower it goes up to 60 K/km.

Another feature common to all boreholes is the vertical hydrogeological zonation. Thus, three major hydrogeological zones are distinguished:

1) A zone of free circulation, characterized by fresh or slightly mineralized meteoric water (up to 50-60 g/l) in fractures.

2) A zone of obstructed circulation, characterized by weak or medium brines with a mineralization up to 200 g/l.

3) A zone of deep water, characterized by strong brines of juvenile or metamorphogenic water with mineralization up to 350 g/l.

The presence of the first two zones was observed in all three boreholes. The third zone was investigated in the Kola borehole, where chlorine-calcium water with a mineralization of 200-300 g/l was discovered at a depth of 4500 m. Similar chlorine-calcium brines with a mineralization of 390-300 g/l were encountered at 4703-5089 m depth in the Minibaev borehole, which is located in Archaean formations of the Russian plate. The uppermost part of the first hydrogeological zone is characterized by active and rapid (tens of thousands of years) water circulation. This part is intensely fractured and exhibits high porosity and water conductivity.

Although the existence of the two first zones is well verified, determination of their boundaries is difficult. In the Kola and Krivoy Rog boreholes, the transition from the first to the second zone is at 800-1200 m depth. The water in the first zone is hydrocarbonate-calcium or sulphate-chloride-sodium. It should be noted that the geothermal gradient in these holes also changes (increases) at a similar depth, i.e.1200 m. In the Tyrnauz borehole, the only thoroughly analysed water sample was obtained at a depth of 1149-1230 m. The water (mineralization 8.6 g/l) is chloride-hydrocarbonate-sulphate and sodium-calcium, and corresponds to glacial water. Carbonate filling of fractures down to a depth of 2000-2500 m supports the hypothesis that the first hydrogeological zone extends to this depth. Again, the estimated boundary corresponds roughly to an observed increase of the geothermal gradient.

It is thus concluded that the lower boundary of the zone of free circulation (zone 1) is defined by the depth where hydrocarbonate and sulphate water are replaced by highly chloride water with a mineralization exceeding 50-60 g/l. The location of this boundary can be discerned from observed changes in the geothermal gradient.

In the Kola borehole, the boundary between the second and third hydrogeological zones is located at a depth of 4500 m, which again coincides with an increase in the geothermal gradient. Considering the similarities in geothermal gradients between the Kola and Krivoy Rog boreholes, it is believed that the hydrogeological boundary is located at the same depth in the Krivoy Rog hole. In the Minibaev borehole, the boundary is above 4700 m. Within the interval comprising the second zone, two levels of the geothermal gradient were discerned in the Kola and Krivoy Rog boreholes. The transition depth is 2800-3200 m (Krivoy Rog). Deep hydrogen and helium occurrences are associated with the interval 3200-3500 m. In the Kola borehole, these gases were observed at larger depths (4400 m).

In terms of a generalized model, the second hydrogeological zone thus comprises the interval from 1000-2500 m to 4500-5000 m. It is characterized by chlorine-calcium, chlorine-sodium or chloride-sulphate-sodium brines with mineralization 50-200 g/l. Within the zone, water circulation is assumed to take place between the upper (meteoric) and lower (juvenile or metamorphogenic) water. The data available suggests that circulation rates should not be less than several tens of thousands of years or hundreds of thousands of years. As a rule, the porosity is low (0.5-1.5 %) and permeability does not exceed the mD range. Relatively thick, impermeable intervals are located within the zone. The diabase of the Zapolyarninsky suite in the interval 2900-4300 m in the Kola borehole is an example of such a formation. Excluding the Tyrnauz borehole, the temperature within the second zone does not exceed 70°C.

Considering the genetic background of the third hydrogeological zone, some further comments may be given as to the location of its upper boundary. In the Kola and Krivoy Rog boreholes, from a depth of 4500 m and 3600 m respectively, specific

borehole deformations occurred and the dip angle of fracture zones decreased considerably. A. V. Kremenetsky discerned a zone of hydrogenic-metamorphogenic unconsolidated rock and generation of deep water in the interval 4500-5000 m in the Kola borehole.

With average rock densities of 3.0 g/cm^3 in the Kola borehole and 2.8 g/cm^3 in the Krivoy Rog borehole, the lithostatic pressure at the depths indicated above must be 135 MPa and 98 MPa respectively. Within the intervals in question, the compressive strength of the rock is between 100 MPa and 160 MPa, and thus conditions would allow rock failure. If ductile rock is over- and underlying the interval under failure, the volume of which increases due to water rejection, then excess pressure and corresponding tensile stress must be generated. This, in turn, may initiate subhorizontal fracturing. Typical for both boreholes is the drop in acoustic velocity within the intervals in question. Thus, it appears that the upper boundary of the third zone will depend on the ratio between the lithostatic pressure and rock strength. On this basis,the boundary may be expected to occur at a depth of 5000 m in the Tyrnauz borehole.

The third hydrogeological zone is characterized by chlorine-calcium or chlorine-sodium brines of juvenile or metamorphic water in fractures, disconnected from meteoric water. Water circulation times are hundreds of thousands of years. The zone is characterized by high thermal gradients related to the large depths.

Attempting to condense the observed hydrogeological and geothermal characteristics in crystalline rock formations into a generalized model, it appears that the section from the surface and down to 5 km depth can be envisaged as a three-layer medium, reflecting the vertical hydrogeological and geothermal zonation:

- The first, upper layer encompasses the interval down to 1-2 km depth. It is characterized by active water circulation, minimum geothermal gradients, intense exogenic fracturing and fresh meteoric water under continuous circulation with the atmosphere.

- The third, lowermost layer has its upper boundary at a depth of 4.0-5.0 km, corresponding to the occurrence of deep chloride brines which are hydraulically essentially disconnected from the upper layer. The depth to the boundary is larger in young folded belts than in ancient structures. The thermal gradient is essentially stable within the interval.

- The second layer forms an intermediate zone of obstructed circulation, between the upper and lower layers. Within this zone, the mineralization of the groundwater and the geothermal gradient changes with depth. The upper parts of the zone are considered to have hydraulic communication with the upper layer of active groundwater circulation. The lower parts appears to be slightly connected to the lower layer of deep water (very low rate of circulation).

7. REFERENCES

1 KOLA BOREHOLE

1:1. Abdrakhimov, M.Z., 1987: PT influence on the strength of the silicate rock which have contacts with surfactants. (In Russian).

1:2 Berezin, V.V. & Popov, A., 1986: Heat flow of the Pechenga structure. (In Russian).

1:3 Berezin, V.V. et. al., 1988: Geothermal section of the Pechenga structure. (In Russian).

1:4 The Eastern part of the Baltic Shield, geology and deep structure: 1975 (In Russian).

1:5 Galdin, N.E., 1981: About the Earth's crust sections of high velocity in the Eastern part of the Baltic Shield. (In Russian).

1:6 Geology of the USSR, Vol.27 1958 (In Russian).

1:7 Duk, G.G., 1977: Structural - metamorphic history of the rock of the Pechenga complex. (In Russian).

1:8 Zagorodny, V.G. et. al., 1964: Geological structure of the Pechenga sedimentary- volcanogenic series. (In Russian).

1:9 Kazansky, V.I., 1987: Objectives and methods of specialized studies of the core from deep and superdeep boreholes in the ore-bearing areas. (In Russian).

1:10 Kremenetsky, A.A. & Ovchinnikov, L.N., 1986: Geochemistry of deep rock. (In Russian).

1:11 Kremenetsky, A.A. et. al., 1990: Geological and geochemical methods of deep prognosis for mineral resources. (In Russian).

1:12 The Kola superdeep borehole: 1984 (In Russian).

1:13 Kropotkin, P.H. et. al., 1987: Stress of the Earth's crust and geodynamics. (In Russian).

1:14 Kuznetsov, O.L. et. al., 1987: Problems of geological and geophysical investigations in deep and superdeep boreholes and in a near borehole environment. (In Russian).

1:15 Litvinenko, I.V., et. al., 1989: Superdeep drilling and regional seismic investigations of the eastern Baltic shield. (In Russian).

1:16 Nalivkina, E.B., et. al., 1989: Deep structure of low Precambrian continental crust. (In Russian).

1:17 Patalakha, E.I., 1989: Some tectonic facial data on the Kola superdeep borehole. (In Russian).

1:18 Predovsky, A.A. et. al., 1974: Geochemistry of the Pechenga complex. (In Russian).

1:19 Rusanov, M.S., 1981: Tholeiite-comatite formation of the Pechenga complex. (In Russian).

1:20 Smyslov, A.A. et al: 1989: Composition and petrophysical characterization of the Earth's crust from the results of superdeep drilling. (In Russian).

1:21 Turchaninov, I.A. et. al., 1975: Tectonic stress in the Earth's crust and stability of workings. (In Russian).

1:22 Haimson, B.C. & Herrick, C.G., 1985: In - situ stress evaluation from borehole breakouts. Experimental studies. In: Research and engineering applications in rock mechanics. Vol.2 Balkeme, Rotterdam, p 1207-1218.

1:23 Zoback, M.D., Moos D. & Masoin, L., 1985: Well bore breakouts and in-situ stress. //J.Geophys. Res. 90,B7, p 5523-5530.

1:24 Slunda, R., Norman, P. & Glass, A.C., 1984: Baltic Shield seismicity, the results of a regional network. //Geophys. Res.Lett; 11-12, p 1247-1250.

2 KRIVOY ROG BOREHOLE

2:1 Belevtsev, Ya.N., Belevtsev, R.Ya. et. al., 1981: Geological structure and iron ore of the Krivoy Rog basin. (In Russian).

2:2 Belevtsev, R.Ya., 1975: Problems of Precambrian metamorphic zonality. (In Russian).

2:3 Tolstoy, M.I. et. al., 1989: Matter and physical peculiarities of granitoids in the Krivoy Rog borehole and its environment //Geological magazine, No 2. (In Russian).

2:4 Galetsky, L.S., 1984: Precambrian geology and metallogeny of the Ukrainian shield. (In Russian).

2:5 Belevtsev, R.Ya. et. al., 1989: Geodynamic models of Precambrian metamorphic iron formations (geodynamic model of Precambrian iron formations of the Krivoy Rog type). (In Russian).

2:6 Semenenko, N.P. et. al., 1959: Geology of iron formations of the Ukraine. (In Russian).

2:7 Chekunov, A.V. et. al., 1989: Geodynamic model of the central part of the Ukrainian Shield and the Krivoy Rog superdeep borehole. No. 4. (In Russian).

2:8 Galetsky, L.S. et. al., 1989: Deep structure of the Krivoy Rog iron ore basin. (In Russian).

2:9 Belevtsev, R. Ya, Belevtsev, Ya., Kurlov, N.S. et. al., 1990: Deep geological structure and vertical metamorphic zonation of the Krivoy Rog ore basin on data of superdeep drilling //Geological Journal, 90,2.

2:10 Kremenetsky, A.A. et. al., 1986: Geochemistry of deep water. (In Russian).

2:11 Lebedev, T.S., Korchin, V.A. et. al., 1988: Petrophysical investigations under high PT-parameters and their geophysical applications. (In Russian).

2:12 Malakhov, G.M. et. al., 1983: Mining of magnetite quartzite in the Krivoy Rog basin. (In Russian).

2:13 Belevtsev, R.Ya. et. al., 1989: Mineral paragenesis and PT conditions of metamorphism of Precambrian iron formations (mineralogic and petrographic data obtained from the Krivoy Rog superdeep borehole). (In Russian).

2:14 Nevsky, V.A., 1979: Fracture tectonics of ore fields and deposits. (In Russian).

2:15 Neishtadt, L.I., Pirogov, L.A., 1969. Engineering and geological studies of rock fracturing. (In Russian).

2:16 Tokhtuev, G.V. et. al., 1962: Physical-mechanical properties of Krivbass rock. (In Russian).

3 TYRNAUZ BOREHOLE

3:1 Adamia, Sh.A., 1989: Characteristic features of the tectonics of the Caucasus. (In Russian).

3:2 Adamia, Sh.A., Shavishvily, L.D., 1982: About the root zone of Hercynian ophiolite covers of the Western Caucasus. (In Russian).

3:3 Baranov, G.I., Kropachyov, S.M., 1976: Stratigraphy, magnetism and tectonics of the Great Caucasus at Precambrian and Paleozoic stages of evolution. (In Russian).

3:4 Belov, A.A. & Omelchenko, V.L., 1976: Ophiolite in the structure of the Marukhansky cover and some problems of stratigraphy and magmatism of the Paleozoic of the Forward Range of the Northern Caucasus. (In Russian).

3:5 Zaitsev, I.K. & Tolstikhin, N.L., 1963: The principles for determining structural and hydrogeological regions in the USSR. (In Russian).

3:6 Kirukhin, V.A. et. al., 1989: Hydrogeochemistry of folded belts. (In Russian).

3:7 Lyakhovich, V.V., 1976: Connection between ore formation and magmatism (Tyrnauz). (In Russian).

3:8 Milanovsky, E.E., 1968: Update tectonics of the Caucasus (In Russian).

3:9 Moiseyenko, U.I. & Smyslov, A.A., 1986: Temperature of the Earth's Interior. (In Russian).

3:10 Popov, U.A. et. al. Methods and equipment for contact-free determination of thermal conductivity. (In Russian).

3:11 Rastsvetaev, L.M., 1987: Tectodynamic conditions of formation of the structure of the Great Caucasus. (In Russian).

3:12 Smyslov, A.A. et. al., 1979: Thermal regimes and the radioactivity of the Earth. (In Russian).

3:13 Khain, E.V., 1984: Ophilite and Hercynian cover structure of the advanced ridge of the Northern Caucasus. (In Russian).

List of SKB reports

Annual Reports

1977-78
TR 121
KBS Technical Reports 1 – 120
Summaries
Stockholm, May 1979

1979
TR 79-28
The KBS Annual Report 1979
KBS Technical Reports 79-01 – 79-27
Summaries
Stockholm, March 1980

1980
TR 80-26
The KBS Annual Report 1980
KBS Technical Reports 80-01 – 80-25
Summaries
Stockholm, March 1981

1981
TR 81-17
The KBS Annual Report 1981
KBS Technical Reports 81-01 – 81-16
Summaries
Stockholm, April 1982

1982
TR 82-28
The KBS Annual Report 1982
KBS Technical Reports 82-01 – 82-27
Summaries
Stockholm, July 1983

1983
TR 83-77
The KBS Annual Report 1983
KBS Technical Reports 83-01 – 83-76
Summaries
Stockholm, June 1984

1984
TR 85-01
Annual Research and Development Report 1984
Including Summaries of Technical Reports Issued during 1984. (Technical Reports 84-01 – 84-19)
Stockholm, June 1985

1985
TR 85-20
Annual Research and Development Report 1985
Including Summaries of Technical Reports Issued during 1985. (Technical Reports 85-01 – 85-19)
Stockholm, May 1986

1986
TR 86-31
SKB Annual Report 1986
Including Summaries of Technical Reports Issued during 1986
Stockholm, May 1987

1987
TR 87-33
SKB Annual Report 1987
Including Summaries of Technical Reports Issued during 1987
Stockholm, May 1988

1988
TR 88-32
SKB Annual Report 1988
Including Summaries of Technical Reports Issued during 1988
Stockholm, May 1989

1989
TR 89-40
SKB Annual Report 1989
Including Summaries of Technical Reports Issued during 1989
Stockholm, May 1990

1990
TR 90-46
SKB Annual Report 1990
Including Summaries of Technical Reports Issued during 1990
Stockholm, May 1991

1991
TR 91-64
SKB Annual Report 1991
Including Summaries of Technical Reports Issued during 1991
Stockholm, April 1992

Technical Reports

List of SKB Technical Reports 1992

TR 92-01
GEOTAB. Overview
Ebbe Eriksson[1], Bertil Johansson[2], Margareta Gerlach[3], Stefan Magnusson[2], Ann-Chatrin Nilsson[4], Stefan Sehlstedt[3], Tomas Stark[1]
[1]SGAB, [2]ERGODATA AB, [3]MRM Konsult AB
[4]KTH
January 1992

TR 92-02
Sternö study site. Scope of activities and main results
Kaj Ahlbom[1], Jan-Erik Andersson[2], Rune Nordqvist[2], Christer Ljunggren[3], Sven Tirén[2], Clifford Voss[4]
[1]Conterra AB, [2]Geosigma AB, [3]Renco AB, [4]U.S. Geological Survey
January 1992

TR 92-03
Numerical groundwater flow calculations at the Finnsjön study site – extended regional area
Björn Lindbom, Anders Boghammar
Kemakta Consultants Co, Stockholm
March 1992

TR 92-04
Low temperature creep of copper intended for nuclear waste containers
P J Henderson, J-O Österberg, B Ivarsson
Swedish Institute for Metals Research, Stockholm
March 1992

TR 92-05
Boyancy flow in fractured rock with a salt gradient in the groundwater – An initital study
Johan Claesson
Department of Building Physics, Lund University, Sweden
February 1992

TR 92-06
Characterization of nearfield rock – A basis for comparison of repository concepts
Roland Pusch, Harald Hökmark
Clay Technology AB and Lund University of Technology
December 1991

TR 92-07
Discrete fracture modelling of the Finnsjön rock mass: Phase 2
J E Geier, C-L Axelsson, L Hässler, A Benabderrahmane
Golden Geosystem AB, Uppsala, Sweden
April 1992

TR 92-08
Statistical inference and comparison of stochastic models for the hydraulic conductivity at the Finnsjön site
Sven Norman
Starprog AB
April 1992

TR 92-09
Description of the transport mechanisms and pathways in the far field of a KBS-3 type repository
Mark Elert[1], Ivars Neretnieks[2], Nils Kjellbert[3], Anders Ström[3]
[1]Kemakta Konsult AB
[2]Royal Institute of Technology
[3]Swedish Nuclear Fuel and Waste Management Co
April 1992

TR 92-10
Description of groundwater chemical data in the SKB database GEOTAB prior to 1990
Sif Laurent[1], Stefan Magnusson[2], Ann-Chatrin Nilsson[3]
[1]IVL, Stockholm
[2]Ergodata AB, Göteborg
[3]Dept. of Inorg. Chemistry, KTH, Stockholm
April 1992

TR 92-11
Numerical groundwater flow calculations at the Finnsjön study site – the influence of the regional gradient
Björn Lindbom, Anders Boghammar
Kemakta Consultants Co., Stockholm, Sweden
April 1992

TR 92-12
HYDRASTAR – a code for stochastic simulation of groundwater flow
Sven Norman
Abraxas Konsult
May 1992

TR 92-13
Radionuclide solubilities to be used in SKB 91
Jordi Bruno[1], Patrik Sellin[2]
[1]MBT, Barcelona Spain
[2]SKB, Stockholm, Sweden
June 1992

TR 92-14
Numerical calculations on heterogeneity of groundwater flow
Sven Follin
Department of Land and Water Resources, Royal Institute of Technology
June 1992

TR 92-15
Kamlunge study site.
Scope of activities and main results
Kaj Ahlbom[1], Jan-Erik Andersson[2],
Peter Andersson[2], Thomas Ittner[2],
Christer Ljunggren[3], Sven Tirén[2]
[1]Conterra AB
[2]Geosigma AB
[3]Renco AB
May 1992

TR 92-16
Equipment for deployment of canisters with spent nuclear fuel and bentonite buffer in horisontal holes
Vesa Henttonen, Miko Suikki
JP-Engineering Oy, Raisio, Finland
June 1992

TR 92-17
The implication of fractal dimension in hydrogeology and rock mechanics. Version 1.1
W Dershowitz[1], K Redus[1], P Wallmann[1],
P LaPointe[1], C-L Axelsson[2]
[1]Golder Associates Inc., Seattle, Washington, USA
[2]Golder Associates Geosystem AB, Uppsala, Sweden
February 1992

TR 92-18
Stochastic continuum simulation of mass arrival using a synthetic data set. The effect of hard and soft conditioning
Kung Chen Shan[1], Wen Xian Huan[1], Vladimir Cvetkovic[1], Anders Winberg[2]
[1] Royal Institute of Technology, Stockholm
[2] Conterra AB, Gothenburg
June 1992

TR 92-19
Partitioning and transmutation.
A review of the current state of the art
Mats Skålberg, Jan-Olov Liljenzin
Department of Nuclear Chemistry,
Chalmers University of Technology
October 1992

TR 92-20
SKB 91
Final disposal of spent nuclear fuel. Importance of the bedrock for safety.
SKB
May 1992

TR 92-21
The Protogine Zone.
Geology and mobility during the last 1.5 Ga
Per-Gunnar Andréasson, Agnes Rodhe
September 1992

TR 92-22
Klipperås study site.
Scope of activities and main results
Kaj Ahlbom[1], Jan-Erik Andersson[2],
Peter Andersson[2], Tomas Ittner[2],
Christer Ljunggren[3], Sven Tirén[2]
[1]Conterra AB
[2]Geosigma AB
[3]Renco AB
September 1992

TR 92-23
Bedrock stability in Southeastern Sweden. Evidence from fracturing in the Ordovician limestones of Northern Öland
Alan Geoffrey Milnes[1], David G Gee[2]
[1]Geological and Environmental Assessments (GEA), Zürich, Switzerland
[2]Geologiska Institutionen, Lund, Sweden
September 1992

TR 92-24
Plan 92
Costs for management of the radioactive waste from nuclear power production
Swedish Nuclear Fuel and Waste Management Co
June 1992

TR 92-25
Gabbro as a host rock for a nuclear waste repository
Kaj Ahlbom[1], Bengt Leijon[1], Magnus Liedholm[2],
John Smellie[1]
[1]Conterra AB
[2]VBB VIAK
September 1992

TR 92-26
Copper canisters for nuclear high level waste disposal. Corrosion aspects
Lars Werme, Patrik Sellin, Nils Kjellbert
Swedish Nuclear Fuel and Waste Management Co, Stockholm, Sweden
October 1992

TR 92-27

Thermo-mechanical FE-analysis of butt-welding of a Cu-Fe canister for spent nuclear fuel

B L Josefson[1], L Karlsson[2], L-E Lindgren[2], M Jonsson[2]
[1]Chalmers University of Technology, Göteborg, Sweden
[2]Division of Computer Aided Design, Luleå University of Technology, Luleå, Sweden
October 1992

TR 92-28

A rock mechanics study of Fracture Zone 2 at the Finnsjön site

Bengt Leijon[1], Christer Ljunggren[2]
[1]Conterra AB
[2]Renco AB
January 1992

TR 92-29

Release calculations in a repository of the very long tunnel type

L Romero, L Moreno, I Neretnieks
Department of Chemical Engineering,
Royal Institute of Technology, Stockholm, Sweden
November 1992

TR 92-30

Interaction between rock, bentonite buffer and canister. FEM calculations of some mechanical effects on the canister in different disposal concepts

Lennart Börgesson
Clay Technology AB, Lund Sweden
July 1992

TR 92-31

The Äspö Hard Rock Laboratory: Final evaluation of the hydro-geochemical pre-investigations in relation to existing geologic and hydraulic conditions

John Smellie[1], Marcus Laaksoharju[2]
[1]Conterra AB, Uppsala, Sweden
[2]GeoPoint AB, Stockholm, Sweden
November 1992

TR 92-32

Äspö Hard Rock Laboratory: Evaluation of the combined longterm pumping and tracer test (LPT2) in borehole KAS06

Ingvar Rhén[1] (ed.), Urban Svensson[2] (ed.), Jan-Erik Andersson[3], Peter Andersson[3], Carl-Olof Eriksson[3], Erik Gustafsson[3], Thomas Ittner[3], Rune Nordqvist[3]
[1]VBB VIAK AB
[2]Computer-aided Fluid Engineering
[3]Geosigma AB
November 1992

TR 92-33

Finnsjö Study site. Scope of activities and main results

Kaj Ahlbom[1], Jan-Erik Andersson[2], Peter Andersson[2], Thomas Ittner[2], Christer Ljunggren[3], Sven Tirén[2]
[1]Conterra AB
[2]Geosigma AB
[3]Renco AB
December 1992

TR 92-34

Sensitivity study of rock mass response to glaciation at Finnsjön, Central Sweden

Jan Israelsson[1], Lars Rosengren[1], Ove Stephansson[2]
[1]Itasca Geomekanik AB, Falun, Sweden
[2]Royal Institute of Technology, Dept. of Engineering Geology, Stockholm, Sweden
November 1992

TR 92-35

Calibration and validation of a stochastic continuum model using the Finnsjön Dipole Tracer Test. A contribution to INTRAVAL Phase 2

Kung Chen Shan[1], Vladimir Cvetkovic[1], Anders Winberg[2]
[1]Royal Institute of Technology, Stockholm
[2]Conterra AB, Göteborg
December 1992

TR 92-36

Numerical simulation of double-packer tests in heterogeneous media: Numerical simulations using the stochastic continuum analogue

Sven Follin
Department of Engineering Geology, Lund University, Lund, Sweden
December 1992

TR 92-37

Thermodynamic modelling of bentonite-groundwater interaction and implications for near field chemistry in a repository for spent fuel

Hans Wanner, Paul Wersin, Nicolas Sierro
MBT Umwelttechnik AG, Zürich, Switzerland
November 1992

TR 92-38

Climatic changes and uplift patterns – past, present and future

S Björck, N-O Svensson
Department of Quaternary Geology,
University of Lund
November 1992